ABSTRACT

BODDA, SARAN SRIKANTH. Risk Informed Validation Framework Using Bayesian Approach. (Under the direction of Dr. Abhinav Gupta.)

Safety of nuclear plants against external flooding has gained significant attention following the accident at Fukushima Daiichi nuclear power station. In United States, Oyster Creek nuclear plant was safely shutdown when high storm surge during hurricane Sandy caused a potential flooding threat. Subsequently, the nuclear energy industry experienced a significant activity in Probabilistic Risk Assessment (PRA) for external flooding. Increasingly, methods of computational fluid dynamics including advanced simulation codes are being considered to evaluate the sequence of events during different scenarios of flooding at a plant. One of the key limitations in the use of advanced codes for external flooding is related to a lack of validation (credibility) of such simulations. This dissertation develops a formal validation approach that provides a basis to quantify credibility of risk assessments that are based on advanced simulation codes. The efficiency of the risk informed validation approach lies in the identification of critical structures, systems and components (SSCs) that contribute to the system-level risk using Bayesian statistics. The validation methodology employs a data-driven approach to quantify the quality of data that is used to evaluate experimental fragilities for flooding failures. As the fragility assessment of a flooding scenario suffers from large epistemic uncertainties, the credibility of system-level validation is expressed using probabilistic distribution and maturity levels. To ensure that the system-level validation is complete and consistent, an additional validation metric called consistency index is introduced. The risk informed validation approach is integrated with USNRC's Evaluation Model Development and Assessment Process (EMDAP) framework for a complete and wider applicability of the framework.

© Copyright 2020 by Saran Srikanth Bodda

All Rights Reserved

Risk Informed Validation Framework Using Bayesian Approach

by
Saran Srikanth Bodda

A dissertation submitted to the Graduate Faculty of
North Carolina State University
in partial fulfillment of the
requirements for the Degree of
Doctor of Philosophy

Civil Engineering

Raleigh, North Carolina

2020

APPROVED BY:

Dr. Kumar Mahinthakumar	Dr. Brian Reich
Dr. Kevin Han	Dr. Abhinav Gupta Chair of Advisory Committee

DEDICATION

To *Life Itself*

BIOGRAPHY

Saran Srikanth Bodda was born and brought up in the city of Vizag in India. He joined the undergraduate program in Civil Engineering at Indian Institute of Technology, Guwahati, India in 2010 and received the Bachelors of Technology degree in July, 2014. He joined North Carolina State University in Spring 2015 to pursue his Master of Science in Civil Engineering. After his M.S., he continued to pursue his doctoral degree in Structural Engineering and Mechanics and minor in Statistics at North Carolina State University.

Saran is a member of two honor societies, Tau Beta Pi and Chi Epsilon at NC State University. He also interned at Idaho National Laboratory in the summer of 2017. He has received the Paul Zia graduate fellowship award for Structural Engineering from the department of CCEE at NC State University in 2019. The work presented in Part II of this dissertation got him recognized as one of the three winners of the Shibata Early Career Award at SMiRT 25 Conference, 2019.

Apart from research, he has served as a Teaching Assistant for both undergraduate and graduate courses in Structural Engineering and Mechanics at NC State University. Saran's research interests include Bayesian Approaches for Validation, Nuclear Safety, Seismic and Flooding PRA, Fragility Assessment of flood defense structures subjected to seismic and flooding, Coupled Analysis of Primary-Secondary Systems, Software Development for PRA, Machine Learning, and Statistical modeling.

ACKNOWLEDGEMENTS

Firstly, I would like to express my sincere gratitude to my advisor, Dr. Abhinav Gupta, for giving me the opportunity to pursue my graduate studies at NCSU. His patience, motivation, immense knowledge and constant guidance helped me during the entire research work and in writing this dissertation. I would also like to thank Dr. Nam Dinh, Dr. Kumar Mahinthakumar, Dr. Brian Reich, and Dr. Kevin Han for graciously agreeing to serve on my advisory committee and for their valuable suggestions.

I am always grateful to my undergrad advisor, Dr. Hrishikesh Sharma, for enlightening me with the first glance of research. I am extremely grateful to Dr. Shinyoung Kwag, Dr. Paridhi Athe, and Dr. Linyu Lin for their input and feedback without which this research could not have been possible. I am always thankful to Ankit Dubey, a valued friend, without whom it would be impossible to imagine PhD life. A very special thanks to Harleen and Pragya, for giving me happiness, strength and keeping me in high spirits when I felt troubled. I thank my colleagues and friends – Krishna, Uday, Akshay, Payel, Sugandha, Nick, Sangwoo, Parth, Alexis, Jimmy, Abraham, Revanth, Ankith, Arpit, STP, Sheik, Raj, and Abhinab for their precious support and for the wonderful time I spent with them during my stay in Raleigh.

I express a profound gratitude to my parents and to my brother ("Dr." Sriram) for providing me with constant support and continuous encouragement throughout my life in general. This accomplishment would not have been possible without them.

Finally, the research was supported by the Center for Nuclear Energy Facilities and Structures (CNEFS) at North Carolina State University. I am greatly indebted to the center for providing me with all the facilities and support throughout my graduate school. I would also like to thank all the staff members of the Civil Engineering department for their help and support extended over the years.

TABLE OF CONTENTS

LIST OF TABLES

LIST OF FIGURES

PART I

Introduction

I.1 Introduction

In recent years, safety of nuclear facilities against external hazards has gained significant importance. Fukushima Daiichi nuclear disaster occurred due to tsunami induced flooding [1]. In United States, the South Texas Project nuclear plant was shut down when floods due to hurricane Harvey threatened the nuclear plant [2]. Several nuclear power plants (Oyster Creek, Indian Point, Nine Mile Point, and Salem) in the US were shut down due to flooding from hurricane Sandy [3]. Subsequently, the nuclear industry has led the development of risk-informed design and decision making approaches for the safety assessment of nuclear power plants against external flooding hazard. This requires appropriate characterization of uncertainties in the understanding of physical phenomenon and in the advanced simulation models that are used to represent them. This research develops a robust risk informed framework for validation of advanced simulation codes with a probabilistic criterion for adequate level of validation.

I.2 Background

Probabilistic risk assessment for external flooding hazard typically involves three technical elements: (i) probabilistic flood hazard assessment (PFHA), (ii) performance based flooding fragility curves, and (iii) fault tree/event tree model of the plant response to an external flooding event [4]. The reliability of fragility curves that are generated by high-fidelity simulation codes is assessed primarily by validation process.

The formal definition of Verification and Validation (V&V) is [5, 6, 7]:

- Verification – "The process of determining that a computational model accurately

represents the underlying mathematical model and its solution."

- Validation – "The process of determining the degree to which a model is an accurate representation of the real world from the perspective of the intended uses of the model."

Loosely speaking, verification deals with the problem "are we solving the equations right"? and validation deals with "are we solving the right equations"? [8].

A validation framework should be able to capture all sources of uncertainty due to incomplete knowledge and inherent randomness in the performance of the system as well as in the characterization of the external hazard. The range of applicability of a computational tool is assessed by the physics and the models it contains. Verification, Validation, and Uncertainty Quantification (VVUQ) methodology helps to assess the adequacy of simulation codes in predicting the credibility of risk assessments and the uncertainty associated with those predictions.

Fields such as computational fluid dynamics and heat transfer, computational solid mechanics, and computational integrated system thermal fluids behavior have developed their own set of guidelines for V&V in modeling and simulation. The widely used frameworks for VVUQ in nuclear power plant safety applications are:

(1) ***Code Scaling, Applicability, and Uncertainty methodology (CSAU)***

In 1996, U.S. Nuclear Regulatory Commission (NRC) approved CSAU methodology that can be used to identify and estimate uncertainties in a nuclear reactor. Prior to this time, a deterministic approach with conservative assumptions was employed to address uncertainties. The CSAU methodology is described by three major elements as described below [9]:

- *Requirements and Code Capabilities* – It includes various components such as identification of the accident scenario and nuclear power plant to be analyzed, establishment of phenomena resolution using PIRT process, and specification of frozen simulation code with complete documentation.
- *Assessment and Ranging of Parameters* – This element focuses on validation by establishment of an experimental database which consists of relevant separate effect tests (SETs) and integral effect tests (IETs). An assessment matrix is created based on SETs and IETs for all the phenomena identified in element 1. Scaling effects of the code are determined by performing simulations of different reduced scale test facilities. Bias and uncertainty are estimated for all the evaluated quantities.
- *Sensitivity and Uncertainty Analysis* – The final element performs sensitivity analysis and UQ by combining the biases and uncertainties due to all the sources. Response surface method is used to evaluate the effect of uncertainty from the range of input parameters.

(2) *Evaluation Model Development and Assessment Process (EMDAP)*

In 2005, USNRC Regulatory Guide 1.203 introduced EMDAP which is a systematic process to confirm the adequacy of a particular code to analyze transient and accident behavior that is within the design basis of a nuclear power plant. The key steps involved in the EMDAP process are listed below [10]:

- Identification of analysis purpose, figures of merit (FOM), mathematical modeling methods, components, phenomena, and physical processes.
- Hierarchical breakdown of systems, phenomena and process.
- Development of an experimental database comprising of SETs and IETs. Scaling and applicability analysis of test facilities and models.

- Development of evaluation model (EM) with state-of-the-art modeling tools and algorithms.
- Assessment of EM models adequacy using a two-tier review process (top-down and bottom-up). The bottom-up approach focuses on the fundamental building blocks of the code in which closure and correlation models are evaluated by considering their fidelity to fundamental or SET data, and scalability. The top-down approach focuses on capabilities and performance of the EM in which field equations and numeric solutions are evaluated by considering their fidelity to component or IET data, and scalability.
- Characterization of EM bases and uncertainties.

(3) ***Predictive Capability Maturity Model (PCMM)***

Sandia National Laboratories (SNL) developed PCMM to assess the maturity of modeling and simulation tools for nuclear weapon applications. However, the elements of PCMM can be applied to broad range of engineering applications. PCMM is a model which assesses the confidence one should place in computational tools by evaluating the maturity level of the following six fundamental attributes [11]:

- *Representation and geometric fidelity* – level of detail specified in physical modeling of the system (spatial and temporal). Ranging from simple model relying on expert judgment to CAD modeling of the real system.
- *Physics and material model fidelity* – the degree that models are physics based and how much they are calibrated. Models typically range from fully empirical to complete physics based.
- *Code Verification* – correctness of source code and numerical algorithms that are used in implementing the mathematical models (PDE equations). Ranging from

no formal verification testing to rigorous benchmark solutions testing.

- *Solution Verification* – assessment of numerical solution errors and confidence in the computational results. Ranging from no formal assessment to error estimation of all system response quantities (SRQs) by performing quantitative error estimation methods.
- *Model Validation* – assessment of physical accuracy of the computational model by comparing with experimental measurements, and relevancy of the experimental conditions. Ranging from no comparison with experimental data to comparison of computational results with an extensive database of both SET and IET experiments.
- *Uncertainty quantification and sensitivity analysis* – identification of sources of uncertainty, the effect of uncertainty on computational results, and the determining the critical parameters that contribute to uncertainty in system responses. For high maturity levels, aleatory and epistemic uncertainties are comprehensively treated.

(4) ***Predictive Capability Maturity Quantification (PCMQ)***

CSAU, EMDAP, and PCMM are all expert elicitation methodologies and these frameworks does not give any guidance on quantification methods for making decision on reliability of a simulation tool. PCMQ framework addresses this issue by formalizing the validation process as structured knowledge representation, information abstraction, multilevel evidence incorporation, which is further quantified as a decision-making process for nuclear reactor engineering or safety application [12].

(5) ***PRA based model validation method using Bayesian network***

Kwag et al. [13] proposed a risk consistent approach for validation particularly in

the context of external hazard PRA. This methodology employs a probabilistic index to quantify the degree of validation within the context of uncertainty. In this approach, logic trees for system level performance are mapped into a Bayesian Network (BN) that allows formal propagation of uncertainty at component-level validation to assess the degree of validation at system-level. It uses Bayesian inference for identifying the risk-consistent events along a critical path and evaluates the need for additional validation that may be required. Identification of critical path from a validation standpoint within a risk-informed framework in this approach provides a basis for improving the overall validation through identification of specific events along the critical path. The overall validation can be improved either by enhancing the simulation models of components along the critical path or by collecting additional validation data until the adequacy of the system level validation is satisfied. Application of the framework proposed by Kwag et al. [13] was illustrated for two case studies related to the performance of structure, system, or component (SSCs) subjected to earthquake hazard.

I.3 Research Objectives

The primary objective of this research is to develop a framework for system-level validation based on a risk consistent approach against external flooding hazard. The key objectives of the proposed research are outlined as follows:

- Formally include the quality of experimental data in a quantitative assessment through validation uncertainty quantification (VUQ).
- Employ a probabilistic metric to quantify the degree of validation within the context of uncertainty.

- Identify the critical events which are consistent with both simulation and data-driven models.
- Assess the maturity of the adequacy of a simulation tool for an intended application.
- Update the evaluation (simulation or data-driven) models to obtain a desirable acceptance criterion using Bayesian inference.
- Integrate risk informed validation methodology into EMDAP framework for a wider applicability of the framework.
- Illustrate the effectiveness of the proposed framework to a synthetic example and a realistic example based on NRC working example.

I.4 Proposed Research

The following tasks are needed to accomplish the objectives mentioned in this research:

I.4.1 Risk Informed Validation Framework for External Flooding Scenario

In this research, we illustrate the application of performance based risk-informed validation framework proposed by Kwag et al. [13] to an external flooding event. However, it is determined that a direct application of this approach to flooding is restricted due to a lack of relevant data to evaluate experimental fragilities for flooding failures. Therefore, we take a simple synthetic example to evaluate the applicability of the proposed framework to validation of flooding PRA scenario and update the proposed framework as needed. The specific tasks undertaken to conduct this research are:

- Develop an event tree to represent all possible accident scenarios resulting from an initiating external flood hazard. Construct required fault trees to obtain the failure

probability of top events in the event tree.

- Develop an assessment base which consists of experimental data at component level and subsystem level. Grade the quality of available experimental data and introduce the concept of data-driven fragility.
- Develop performance-based simulation and data-driven fragility curves.
- Develop a mapping algorithm for the transformation of an Event tree into a Bayesian network. Map the event tree and the corresponding fault trees into the Bayesian network.
- Propagate fragilities from basic events to intermediate-level events and ultimately to system-level event through the Bayesian network.
- Identify the critical events based on simulation models or data-driven models.
- Use Overlapping coefficient (OC) as the validation index to quantify the degree of validation within the context of uncertainty.
- Calculate OCs in component-level using simulation and data-driven fragility curves.
- Evaluate system-level OC and improve it by enhancing the simulation model or collecting additional experimental/field data for the critical events if required.

I.4.2 Enhancement of Existing Risk Informed Validation Framework

This research enhances the existing risk informed validation methodology presented in section I.4.1. The proposed risk-informed validation framework by Kwag et al. [13] and Bodda et al. [14] have two key limitations: (a) the system-level validation maybe incomplete if the set of critical events for simulation-based fragility differs from the set of critical events for data-driven fragility. (b) the methodologies do not represent the confidence in adequacy of system-level validation in terms of different maturity levels. In this research, additional attributes and a new set of validation metrics are developed

for a complete and wider applicability of the framework. The specific tasks required to achieve the objectives of this research is summarized below:

- Identify the critical path that leads to system-level failure by using the concept of importance measures.
- Introduce the concept of Consistency Index which ensures that the simulation and data-driven fragilities correspond to the same set of critical events.
- Incorporate and interpret the consistency index in the risk informed validation framework through various case studies.
- Assess the decision regarding the adequacy of a simulation code for an intended application using the concept of maturity level.
- Develop an additional attribute Code Adequacy (CA) in terms of Validation Result (VR) and Data Applicability (DA) attributes for validation assessment.
- Label maturity levels as very low, low, medium, and high (increasing order of value).
- Compare the validation results for two types of validation metric: Overlapping coefficient and Kullback-Leibler divergence.
- Illustrate the effectiveness of the enhanced methodology for a simple example of flooding risk assessment.

I.4.3 Assessment of Risk Informed Validation Framework to a Real Life Like Application – Sunny Day Dam Failure

In this research, we propose to evaluate the applicability of risk informed validation framework to a more complex flooding scenario that corresponds to real life like application of sunny day dam failure. This research combines the work presented in section I.4.1 and I.4.2 of this proposal. In addition, such an application would require

integration of the proposed risk informed methodology into Evaluation Model Development and Assessment Process (EMDAP) framework. The specific tasks undertaken to conduct this research are:

- Integrate risk informed validation methodology into EMDAP framework.
- Develop event tree and the corresponding fault trees for the realistic flooding scenario of the Sunny Day Dam failure.
- Identify non-physical events that are not sensitive to hydrodynamic and fragility modeling.
- Handle the non-physical events by treating them as either completely safe or fail.
- Illustrate the integrated framework to the realistic flooding scenario.

I.5 Organization

This dissertation primarily consists of five parts. Part I gives an introduction to the problem being studied followed by a discussion of the objective of the research. The second Part of the dissertation presents risk informed validation framework for external flooding scenario. The third Part focuses on the enhancement of existing risk informed validation framework to assess the system-level validation. In the fourth Part, risk informed methodology is integrated with EMDAP framework and illustrated for a realistic flooding scenario. Finally, the fifth Part of this dissertation presents a summary and conclusions of the work that has been discussed in Part II, Part III, and Part IV. It also proposes recommendations for future work.

PART II

Risk Informed Validation Framework for External Flooding Scenario

II.1 Introduction

In recent years, flooding at nuclear power plants (NPP) has increased emphasis on considering advanced simulation codes to evaluate the vulnerability of nuclear plants. Absence of a complete and sufficient verification and validation (V&V) of advanced simulation codes results in adoption of greater uncertainty by experts in risk informed evaluations which in turn leads to conservative assumptions. Past experience has shown that such conservative assumptions in the context of safety assessment for other external hazards such as seismic have resulted in highly over-designed nuclear power plant systems and excessively high costs. Therefore, it is quite important that various uncertainties in this process are appropriately identified and included through formal uncertainty quantification (UQ). A robust framework for verification and validation is needed to not only include uncertainties but also to formalize the confidence in predictions of PRA studies that are based on advanced simulations.

The concept of developing formal strategies for verification, validation, and uncertainty quantification (VVUQ) is not new in nuclear power plant safety applications and a few different frameworks already exist. The widely used frameworks are (i) Code Scaling, Applicability, and Uncertainty methodology [9], (ii) Evaluation Model Development and Assessment Process [10], (iii) Predictive Capability Maturity Model [11], and (iv) Predictive Capability Maturity Quantification [12]. Each of these methodologies have certain specific aspects that are quite powerful and yet none of them can be directly extended to a risk consistent approach for validation particularly in the context of flooding PRA. Recently, Kwag et al. [13] proposed a performance-based probabilistic risk assessment (PRA) based approach to VVUQ.

In this manuscript, a synthetic flooding scenario is used as case study to allow a preliminary interrogation of the proposed framework. It is determined that a direct application of Kwag et al. [13] approach to flooding is restricted due to a lack of relevant data to evaluate experimental fragilities for flooding failures. As experimental data is scarce and expensive, modification to the existing framework is needed in order to utilize the data from existing, somewhat related, and diverse experimental studies for validation of certain aspects. To be more precise, a modification is needed to formally include the quality of experimental data in a quantitative assessment through what is often termed as validation uncertainty quantification (VUQ). Furthermore, the available experimental data is not directly related to the failure of SSCs for flooding conditions. Instead, the data typically relates to the various parameters of a hydrodynamic and fluid flow simulations which is related to fragility assessment only indirectly. In fact, one may use a historically well-established empirical model based on many years of research and laboratory studies to determine fluid flow conditions. Consequently, it is proposed to replace "experimental fragility" in the existing framework by "data-driven fragility."

In the proposed modification, we incorporate a data-driven approach used by Athe [12] to grade the quality of data used for generating data-driven fragility curves in terms of three attributes: Relevance, Scaling, and Data Uncertainty. "Relevance (R)" reflects the degree of applicability of experimental data from a historic study to a completely independent application. In many cases, the available data for a flooding analysis is from scaled laboratory experiments. Therefore, when the same data is used for different but larger scale applications, "Scaling (S)" of uncertainty needs to be incorporated. "Data uncertainty (U)" in this context refers to the uncertainty (epistemic) in the measured data which may exist due to a variety of sources including but not limited to instrument

errors. The proposed modification grades the R/S/U attributes based on their VUQ quality and incorporates each of them quantitatively in the data-driven fragility analysis.

Existing framework proposed by Kwag et al. [13] uses a mean fragility curve that results in a point estimate for the validation index. However, fragility assessment of a flooding related event suffers from large epistemic uncertainty making a point estimate for validation index less meaningful. Therefore, we propose a modification to the existing framework which considers multiple fragility curves using different confidence levels instead of just the mean fragility curve. Based on these multiple curves, the validation metric changes from a point estimate to a distribution.

In summary, this manuscript proposes three major modifications to the existing framework proposed by Kwag et al. [13]. First, a data-driven approach is adopted to quantify the quality of experimental data used for generating data-driven fragility curves. Next, the credibility of the overall validation is expressed by using probabilistic distribution rather than a point estimate. Finally, the framework is extended to a systems level analysis by considering both the event trees and the corresponding fault trees. The framework utilizes the power of Bayesian network for propagating uncertainties in a system-level model and for predicting confidence in system-level validation of flooding risk. Bayesian inference is used for updating the validation metric when additional experiment or simulation data becomes available. The proposed methodology serves as a vehicle to enable clarity, consistency, and completeness of the risk informed validation framework for external flooding.

II.2 Summary of Risk Informed Validation Framework by Kwag et al. [13]

The existing framework of Kwag et al. [13] employs two key stages that are described below. The complete framework is illustrated through the flowchart in Figure II.1.

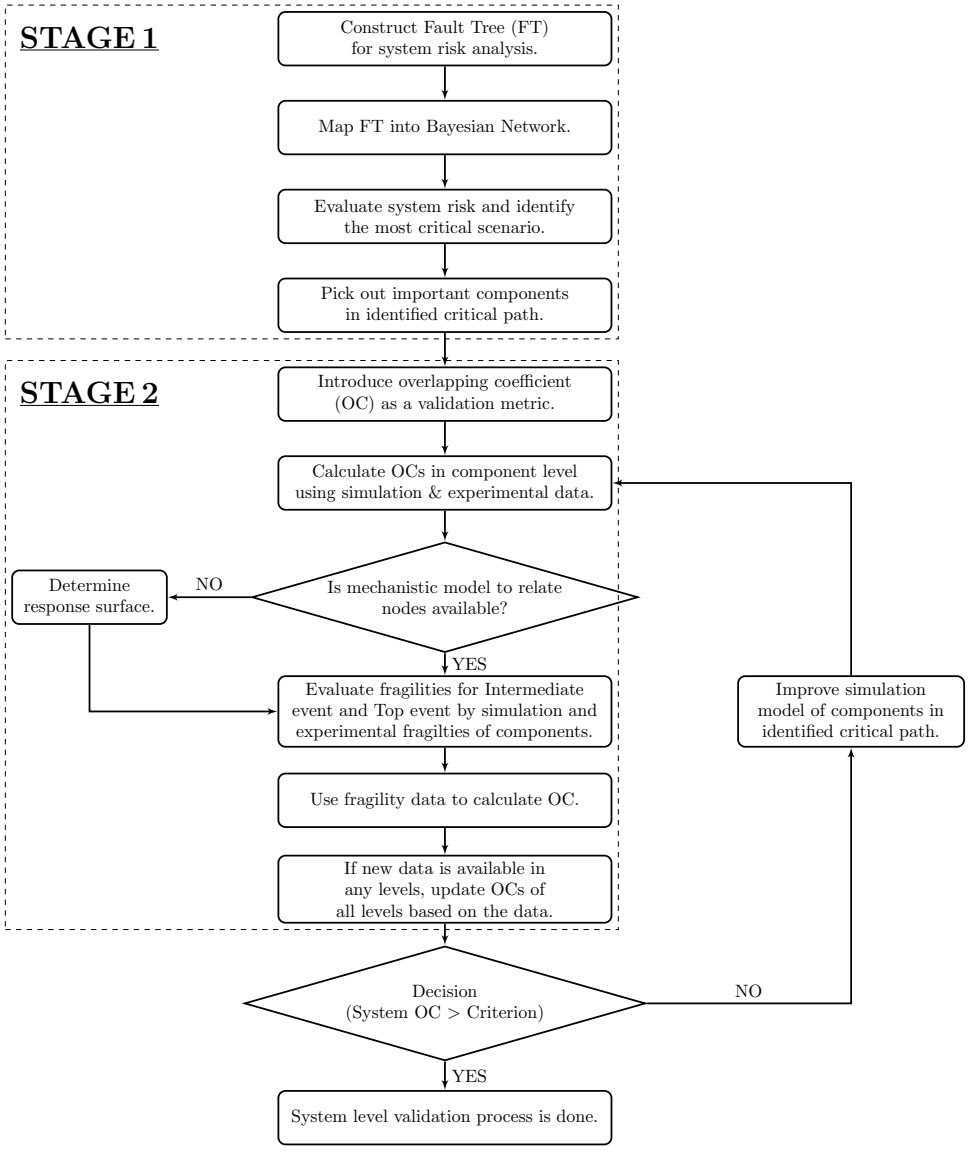

Figure II.1: Flowchart of proposed model validation method (Kwag et al. [13])

Stage 1:

The initial step involves development of a fault tree for the given scenario. The risk of basic events is calculated by convoluting the hazard curve under consideration with the corresponding fragility curve using Eq. (II.1).

$$P_f = \int P_{f|\lambda}(\lambda) \left| \frac{dH(\lambda)}{d\lambda} \right| d\lambda \tag{II.1}$$

where, λ is the hazard intensity measure. $H(\lambda)$ is the hazard curve, representing annual exceedance frequency for λ. $P_{f|\lambda}$ is the fragility curve which represents the conditional probability of failure given λ.

The fault tree is mapped into a Bayesian network in order to account for non-binary and statistical relationships between events. Then, a system analysis is carried out to identify the important events along the critical path with respect to the overall system-level risk. The entire framework is based on the definition of an overlapping coefficient that is used as the validation index to quantify the degree of validation within the context of uncertainty.

Definition of Overlapping Coefficient

Overlapping coefficient (OC) is simply defined as the percentage of overlapping area between two probability density curves (Figure II.2) and is given by Eq. (II.2). OC ranges from 0 to 1. A value of equal to zero represents complete disagreement between the probabilistic distributions of any quantity as calculated from the simulation and the experiments. On the contrary, a value of 1 represents a perfect agreement within the context of uncertainty.

$$OC = \int_{R_n} \min(f_1(x), f_2(x))dx \tag{II.2}$$

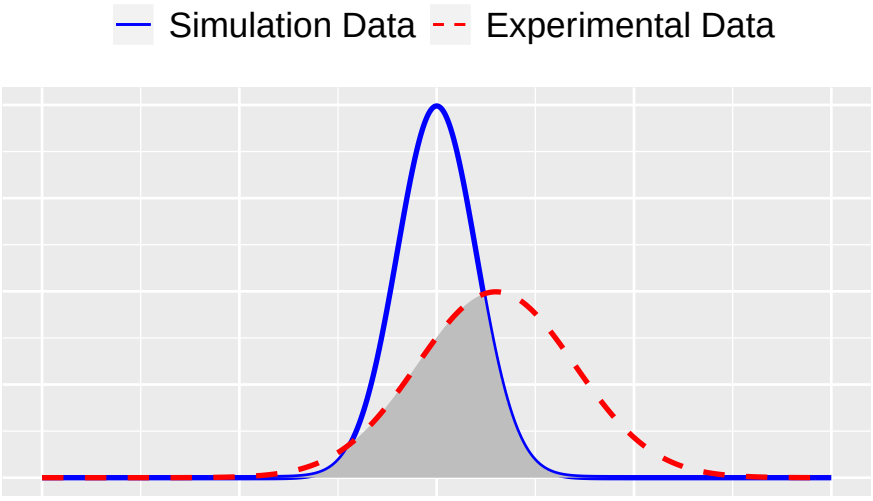

Figure II.2: Overlapping Coefficient

Stage 2:

In Stage 2, Overlapping coefficients are calculated for all the basic events based on the corresponding simulation and experimental (or data-driven) fragility curves. The fragility curves are propagated from basic events to intermediate-level events and ultimately to system-level events through the BN using either mechanistic relationships or response surfaces between the component-level and upper-level nodes. Then, the overlapping coefficients are evaluated for all the nodes using the fragility information. At this stage, if new information becomes available then the *OCs* are updated.

Finally, the system-level *OC* is compared with a pre-defined acceptance criterion for adequacy check. If the system-level *OC* doesn't meet the requirements, the overall

validation can be improved either by enhancing the simulation models of components along the critical path or by collecting additional validation data until the adequacy of the system level validation is satisfied.

II.3 Consideration of Event Trees in the Proposed Framework

The framework by Kwag et al. [13] was based on using Fault trees for risk assessment and it did not consider Event tree for representing the event failure against a seismic hazard. In general, a complete risk assessment requires a combination of fault trees and event tree that are connected together. Specifically, in a flooding scenario it is important to evaluate the sequence of events through an event tree and each top event in the event tree can have its own fault tree. Therefore, in this manuscript we extend the existing framework to include both the event tree and the corresponding fault trees.

However, in a risk informed validation approach, the use of Event and Fault trees can have limitations in certain applications such as: (1) statistical correlations between basic events, (2) non-binary or distributional relationship between intermediate and basic events, (3) more than one initiating event, (4) little or no experimental data available for some events, (5) treatment of uncertainty quantification, and (6) incorporation of additional data. A Bayesian Network based approach has been successful in addressing these issues through a unified single formulation. The mapping algorithm for transforming a fault tree into a Bayesian network is described in detail in Kwag et al. [13, 15] but not for an Event tree. Therefore, we introduce the mapping algorithm for the transformation of an Event tree into a Bayesian network which is quite important for a flooding scenario.

II.3.1 Event tree analysis

Event trees are widely used to analyze accident scenarios in PRA. Event tree analysis uses a (Boolean) logical modeling technique that shows all possible outcomes arising from a single accident event by taking into account multiple safeguards or barriers which are placed as protective features to deal with the accidental event. While the methodology presented in this manuscript is quite generic and can incorporate dynamic nature of events, only static event trees are considered for simplicity of illustrating the methodology.

An Event tree starts with an initiating (accident) event, such as an external/internal hazard. The failure or success consequences (outcomes) of the initiating event are followed through a series of possible branches or paths. The frequencies of various possible outcomes are calculated by assigning a conditional probability of occurrence for each branch and a frequency for the initiating event. Figure II.3 shows a generic example of how an event tree can be drawn. The green lines show the success paths and the red lines show the failure paths. Usually, the failure probabilities (P_f) of intermediate events are calculated from a fault tree analysis and the success probabilities (P_s) of the events are calculated as: $P_s = 1 - P_f$. The overall (end state) frequency of occurrence of a path is calculated by multiplication rule i.e. multiplying all the conditional probabilities of events in that specific path with the frequency of the initiating event. The end state frequency of path A as shown in Figure II.3 is given by Eq. (II.3).

$$\begin{aligned} F_A &= P\left(IE.1s.2s.3s.4s_1\right) \\ &= F\left(IE\right) P\left(1s|IE\right) P\left(2s|1s.IE\right) P\left(3s|2s.1s.IE\right) P(4s_1|3s.2s.1s.IE) \end{aligned} \tag{II.3}$$

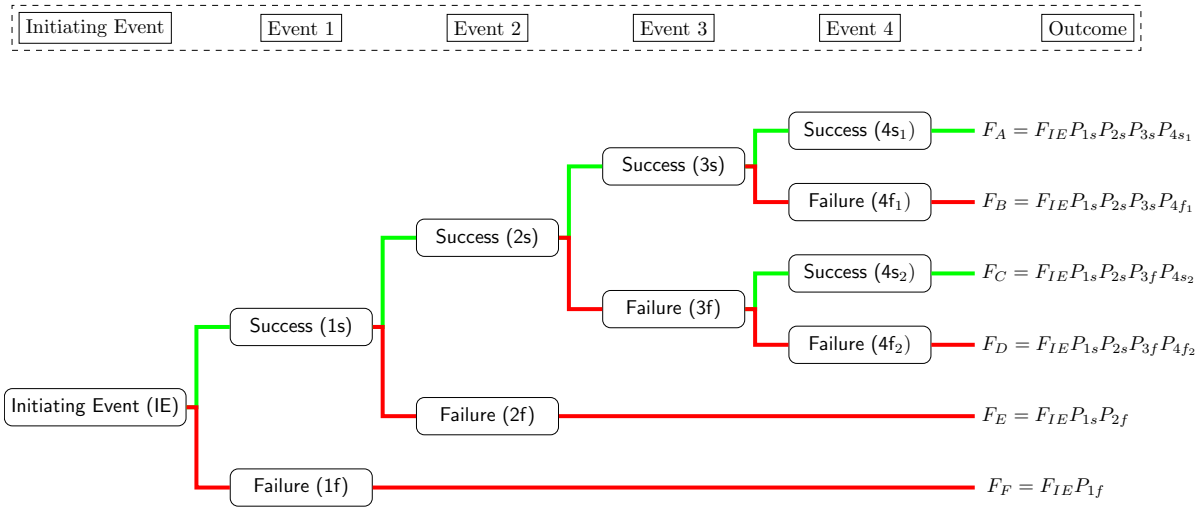

Figure II.3: Generic Event tree

II.3.2 Mapping Algorithm

Accident sequences are first created using an Event tree (ET) due to its simplistic representation. The transformation of an event tree into a Bayesian network (BN) is done in three steps [16]:

1. convert branching points or events in ET into nodes in BN.
2. convert branches or paths in ET into corresponding directional arcs between nodes in BN.
3. convert conditional probabilities in ET into conditional probability tables (CPT) in BN.

Figure II.4 shows the compact BN representation of the generic event tree in Figure II.3. Even though the network looks similar to an event tree with a single sequence of events, but all the possible outcomes are represented by the node states in the BN. Figure II.5 shows the BN representation of the generic event tree with the total success and failure probabilities for each top event in the event tree. The CPTs of all the nodes in

the compact BN are shown in Table II.1. When mapping an Event tree into a Bayesian network, the initiating event is represented as either occurred (True) or not occurred (False) rather than frequency due to conditional probability representation of nodes in a BN. Therefore, the outcome of all the end states is represented by probability. The frequency of end states can be obtained by simply multiplying the probability with the frequency of the initiating event. CPT of Event 2 has a third state $E1_{1f}$ in addition to the states $E2_{1s}$ and $E2_{1f}$, which is due to the branch coming out of Event 1 failure state. Node Event 4 is the last event in the BN, and it contains all the outcomes. An outcome node can also be created with total sum of failure (True) and success (False) state probabilities as shown in Figure II.4.

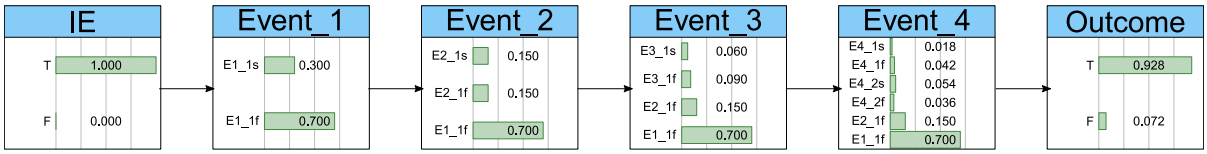

Figure II.4: Compact Bayesian Network representation of Generic Event tree

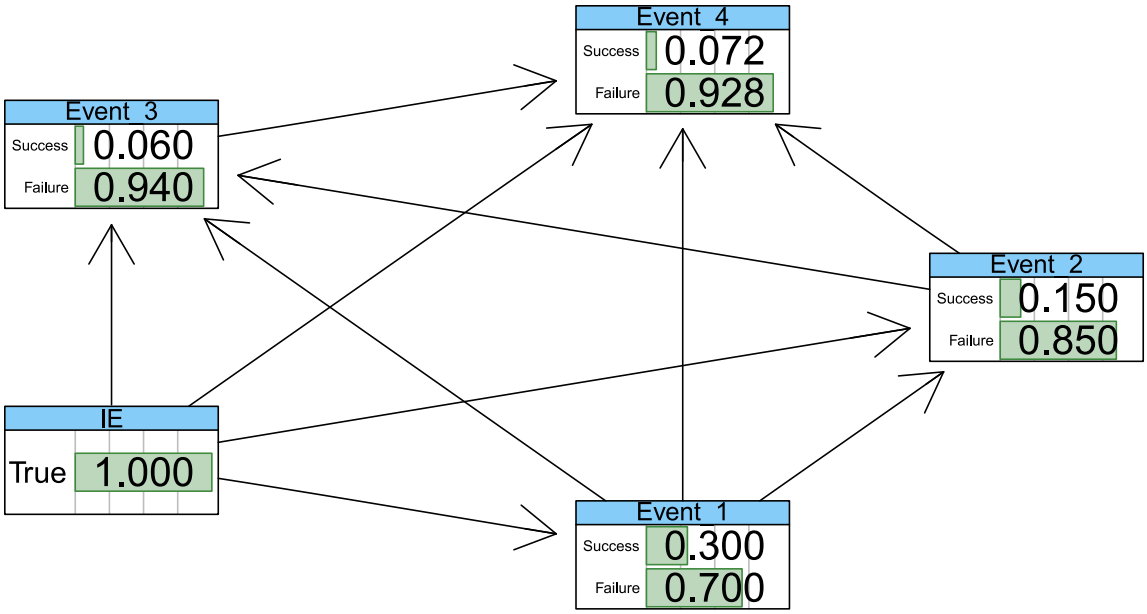

Figure II.5: Bayesian Network representation of Generic Event tree

Table II.1: CPTs of all the nodes in the Compact Bayesian network

(a) CPT of IE

States	
T (True)	P_{IE}
F (False)	$1 - P_{IE}$

(b) CPT of Event 1

States	$IE = T$	$IE = F$
$E1_{1s}$	P_{1s}	0
$E1_{1f}$	P_{1f}	1

(c) CPT of Event 2

States	$E1 = E1_{1s}$	$E1 = E1_{1f}$
$E2_{1s}$	P_{2s}	0
$E2_{1f}$	P_{2f}	0
$E1_{1f}$	0	1

Table II.1: Continued

(d) CPT of Event 3

States	$E2 = E2_{1s}$	$E2 = E2_{1f}$	$E2 = E1_{1f}$
$E3_{1s}$	P_{3s}	0	0
$E3_{1f}$	P_{3f}	0	0
$E2_{1f}$	0	1	0
$E1_{1f}$	0	0	1

(e) CPT of Event 4

States	$E3 = E3_{1s}$	$E3 = E3_{1f}$	$E3 = E2_{1f}$	$E3 = E1_{1f}$
$E4_{1s}$	P_{4s_1}	0	0	0
$E4_{1f}$	P_{4f_1}	0	0	0
$E4_{2s}$	0	P_{4s_2}	0	0
$E4_{2f}$	0	P_{4f_2}	0	0
$E2_{1f}$	0	0	1	0
$E1_{1f}$	0	0	0	1

II.4 Data Applicability in Data-Driven Fragility

II.4.1 Fragility

Fragility curves are essential for assessing the vulnerability of an event, and offer a means of communicating the probability of damage over a range of potential hazard intensity measure levels. A fragility assessment requires characterization of failure in terms of a performance function, Z. The performance function defines the governing limit-state to evaluate the probabilities of failure. Fragility of systems, structures, and components (SSCs) is defined as the conditional probability of failure, $P_{f|\lambda}$, to exceed the defined performance function at a given measure of intensity parameter λ. Some of the commonly used Intensity measures (IM) are Flood height, Surge height, Peak ground acceleration (PGA), etc.

$$\begin{aligned} Z &= Capacity - Demand \\ P_{f|\lambda}(Z) &= P(Z < 0|\lambda) \end{aligned} \tag{II.4}$$

Fragility analysis should account for all possible uncertainties in the SSCs. In the nuclear safety community, these uncertainties are broadly divided into two types [17, 18]:

1. *Aleatory uncertainty* – inherent randomness in the system's performance as well as in the characterization of external hazard. This uncertainty is often irreducible and refer to as variability. Some of the sources of aleatory uncertainty are model parameters having random variability such as geometric dimensions, initial conditions, boundary conditions, or excitation load.
2. *Epistemic uncertainty* – uncertainty due to lack of knowledge. This uncertainty is reducible and is often refer to simply as uncertainty. Some of the sources of epistemic uncertainty are numerical error, human error, or instrumentation error.

In practice, it might become blurry to distinguish between randomness and uncertainty.

The most common form of a fragility function is the log-normal cumulative distribution function (CDF) [19, 20].

$$\begin{aligned} \lambda &= \hat{\lambda}\varepsilon_{EU}\varepsilon_{AU} \\ P_f\left(Z|\lambda=\lambda^*\right) &= \Phi\left[\frac{\ln\left(\lambda^*/\hat{\lambda}\right)+\beta_{EU}\Phi^{-1}\left(Q\right)}{\beta_{AU}}\right] \\ P_{f,mean}\left(Z|\lambda=\lambda^*\right) &= \Phi\left[\frac{\ln\left(\lambda^*/\hat{\lambda}\right)}{\beta_{mean}}\right] \end{aligned} \tag{II.5}$$

where, λ^* corresponds to a particular value of the hazard intensity measure, λ. $\hat{\lambda}$ is the median capacity of resistance of SSCs against the hazard. ε_{EU} and ε_{AU} are variables representing epistemic and aleatory uncertainties about the median value. These variables are usually taken to be lognormal with unit median and logarithmic standard deviations of β_{EU} and β_{AU}, respectively. Q represents the confidence level in the estimated median capacity, $\hat{\lambda}$. $\beta_{mean} = \sqrt{{\beta_{EU}}^2 + {\beta_{AU}}^2}$ represents the combined uncertainty. Φ is the standard Gaussian cumulative distribution.

II.4.2 Data Applicability

As experimental data is scarce and expensive, data from existing experimental studies can be utilized in the validation of a simulation even if the experimental setup may not directly relate to the application of simulation tool in the PRA study. Such utilization of existing experimental studies in validation would require some modification of the validation approach as it is important to characterize the quality of experimental data

used in Validation Uncertainty Quantification (VUQ). In this study, we incorporate a data-driven approach proposed by Athe [12] to quantify the quality of data used for generating data-driven fragility curves in terms of three attributes:

a. *Relevance (R)*: Relevance reflects the degree of applicability of experimental data from an existing database to the current application "based on the preconceived view of phenomenology/process."
b. *Scaling (S)*: In many cases, the validation data for a flooding analysis is taken from scaled laboratory experiments. Therefore, when the same data is used for different larger scale applications, geometric scaling uncertainty should be incorporated to assess the similarity between reduced scale experiment and the full-scale application. Similarly, physics scaling uncertainty captures the degree of phenomena similarity between the applications. E.g. range of Reynolds number used in the prototype and full-scale application.
c. *Data Uncertainty (U)*: Data uncertainty refers to the uncertainty (epistemic) in the measured data which arises due to sources such as instrument errors – accuracy and precision (resolution) of measuring instruments, data acquisition, and data processing.

Four grades ranging from 1 to 4 (increasing order of value) are assigned to the R/S/U attributes based on their VUQ quality as shown in Table II.2 [21]. The emphasis in Dinh [21] is on characterizing R/S/U attributes qualitatively that are subjective, potentially biased, and uncertain. In this paper, we make an attempt to include the effect of these attributes quantitatively. The different grades that are based on expert opinion is quantified (Table II.3) by adopting similar approaches based on belief theory [12, 22, 23]. Next, the epistemic uncertainty in the data-driven fragility

analysis for different grade levels is quantified based on the following procedure.

1. For the data-driven fragility, with the perfect knowledge, the probability of failure is 0.5 at the median capacity. When epistemic uncertainty β_{EU} is included, the fragility at median capacity becomes an uncertain variable.
2. If the grade level is high, then there is more confidence in the data. Therefore, there is very less uncertainty in the available experimental data for the intended application. This is quantified by varying the median fragility (= 0.5) with a uniform width of 0.1 ranging from -0.05 to 0.05.

$$\beta_{high} = 0.5 + runif(-0.05, 0.05) \tag{II.6}$$

   where, $runif(a, b)$ generates a uniform random number from the interval (a, b)
3. Similarly, the epistemic uncertainty corresponding to a different grade level is quantified using step (2) and Table II.3.
4. Then, the combined uncertainty of R/S/U is characterized by their weighted average:

$$\beta_{EU} = w_R\beta_R + w_S\beta_S + w_U\beta_U \tag{II.7}$$

   In this study, the weights are considered to be equal for all the three attributes.
5. The new median capacity, $\hat{\lambda}^*$ is calculated by incorporating the epistemic uncertainty due to R/S/U using the following expression:

$$\hat{\lambda}^* = \hat{\lambda}/\exp(qnorm(\beta_{EU}) \times \beta_{AU}) \tag{II.8}$$

   where, $qnorm(p)$ is the Z-score of the p^{th} quantile of the normal distribution

6. Figure II.6 shows the uncertainty variation in data-driven fragility curves for different grade levels.

Table II.2: Description of VUQ Quality grade for different Data Applicability attributes

Attributes	**VUQ Quality – Grade**			
	4	**3**	**2**	**1**
Relevance [R]	Very High (direct)	High	Medium	Low
Scaling [S]	Prototypic (full-scale)	Adequately scaled	Medium	Inadequately scaled
Uncertainty [U]	Well-Characterized	Characterized	Medium	Poorly-Characterized

Table II.3: Quantification of Maturity level for Data Applicability

Grade	**Range of Uncertainty,** β
Very Low (1)	$[-0.50 \quad 0.50]$
Low (2)	$[-0.35 \quad 0.35]$
Medium (3)	$[-0.20 \quad 0.20]$
High (4)	$[-0.05 \quad 0.05]$

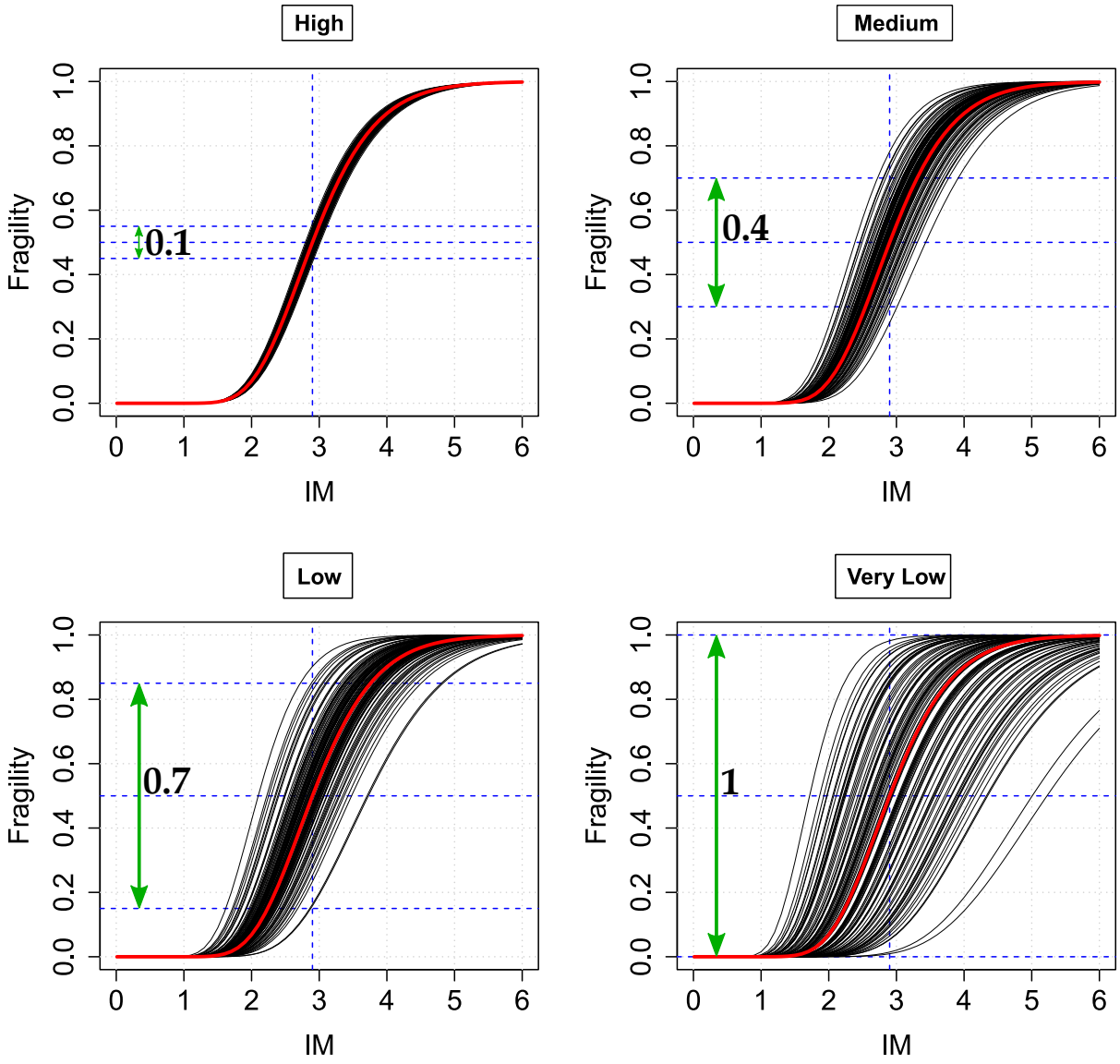

Figure II.6: Family of Data-driven fragility curves corresponding to different maturity levels of Data Applicability (IM – Intensity Measure)

II.5 Modified Risk Informed Validation Framework

As mentioned earlier in this manuscript, a modified framework is needed to enhance the originally proposed framework by Kwag et al. [13] due to three specific reasons:

1. For a systems level analysis, an event tree is necessary to represent the failure sequence of events resulting from an initiating flooding hazard. The framework is extended to include both the event trees and the corresponding fault trees for the representation of all possible accident scenarios and system-level performance.
2. When data from existing and related studies is utilized to evaluate experimental fragilities for flooding failures, a formal approach is needed to include quality of experimental data. The framework is modified to incorporate the quality of experimental data quantitatively by adopting a data-driven approach.
3. In general, fragility assessment of a flooding related event suffers from large epistemic uncertainty. Therefore, for credibility of overall validation, probabilistic distribution of validation metric (overlapping coefficient) is required rather than a point estimate.

The modified framework employs three key stages that are described below. The complete framework is illustrated through the flowchart in Figure II.7.

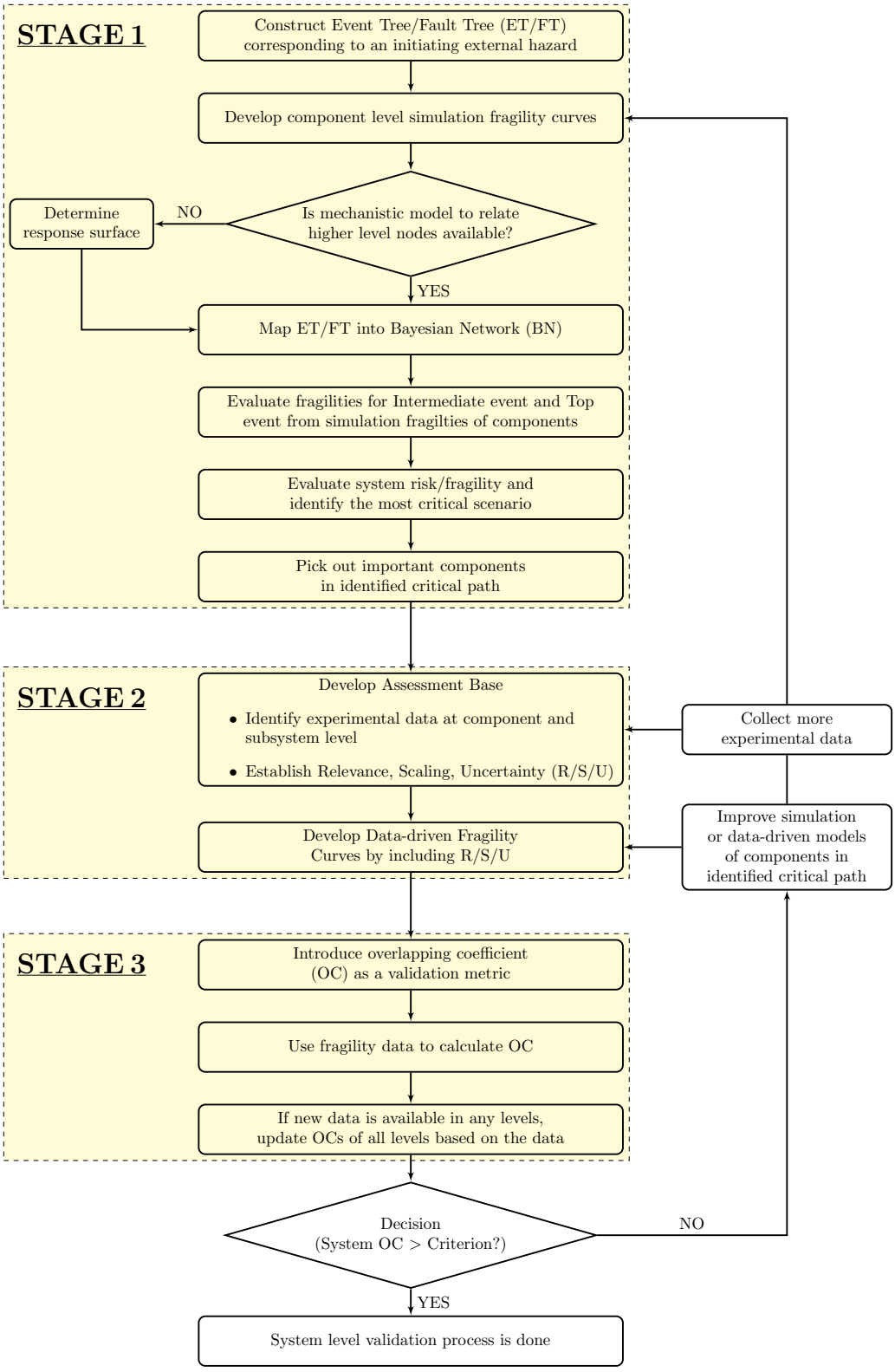

Figure II.7: Flowchart of Proposed Framework with Data Applicability

STAGE 1

- Develop an event tree to represent all possible accident scenarios resulting from an initiating external flood hazard.
- Construct required fault trees to obtain the failure probability of top events in the event tree.
- Develop simulation fragility curves for all the basic events. In general, fragility assessment requires use of a Monte Carlo approach to include uncertainties from various sources. However, if sufficient knowledge base has been developed then one can make use of the standard lognormal fragility parameters.
- Develop response surfaces between the basic events and intermediate events especially if a mechanistic relationship is not directly known.
- Map the event tree and fault trees into a Bayesian network.
- Evaluate system fragility by propagating the simulation fragility information from basic events through the Bayesian network.
- Identify critical events with respect to system vulnerability.

STAGE 2

- Develop an assessment base which consists of experimental data at component level and subsystem level.
- Establish Relevance, Scaling, and Data uncertainty (R/S/U) for the available experimental data using expert judgment.
- Generate data-driven fragility curves by including R/S/U as described in subsection II.4.2 Data Applicability.
- Similar to stage 1 process, evaluate system level fragility based on data-driven

fragility information.

STAGE 3

- Calculate overlapping coefficient based on simulation and data-driven fragility curves.
- At this stage if new data becomes available, update overlapping coefficients.

DECISION

- Compare system level overlapping coefficient with a predefined acceptance criterion.
- If the adequacy of system level validation is not satisfied collect more experimental data or improve simulation models of the identified critical events.

II.6 Illustration of Flooding Case Study

In this section, we illustrate the application of the proposed framework to a synthetic example of a simplistic flooding scenario. The synthetic example is shown in Figure II.8 and the scenario begins with an external flooding event caused by a storm surge. The floodwall protecting the plant can either fail or be overtopped due to the storm surge. In either case, it leads to flooding at the plant. This is known as Landscape flooding. When the landscape starts overflowing, the vent at the diesel generator (DG) room can break and be overtopped. Failure of vent will eventually lead to flooding of the DG room and failure of the DG. For simplicity, we consider the accident sequence up to the DG failure. Next, we connect the individually validated events through the PRA informed validation framework proposed in this study.

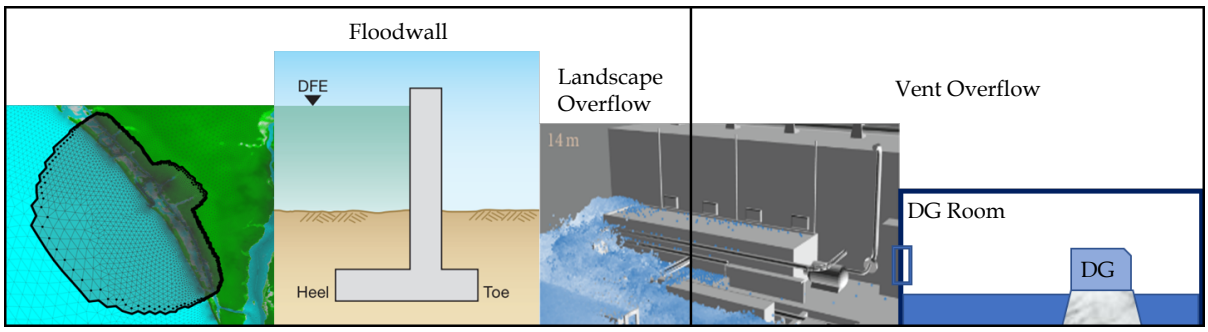

Figure II.8: Accident sequence layout of Synthetic Example

II.6.1 Event Tree / Fault Tree Logic

The event tree resulting from this synthetic example is shown in Figure II.9, and includes the following top events:

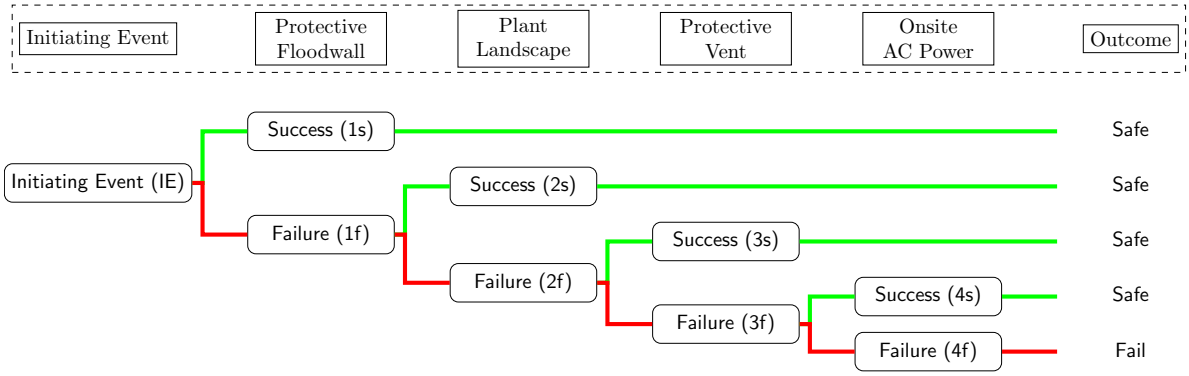

Figure II.9: Event Tree logic for the synthetic example

IE – Initiating Event

The initiating event is an external flooding event due to a storm surge and it has the hazard information. Probabilistic Flood Hazard Assessment (PFHA) provides the annual frequency of flood hazard over a wide range of intensity measure levels, with estimates of uncertainty. For a storm surge, the annual rates of exceedance are plotted against storm surge height. Due to uncertainties in a PFHA model, there are a set of flood hazard curves with respect to different confidence levels. In this study, we use the

weighted mean probabilistic storm hazard information from Dababneh and Weglian [24] shown in Figure II.10 for the risk calculation. In practice, the PFHA model should be developed for the site of interest.

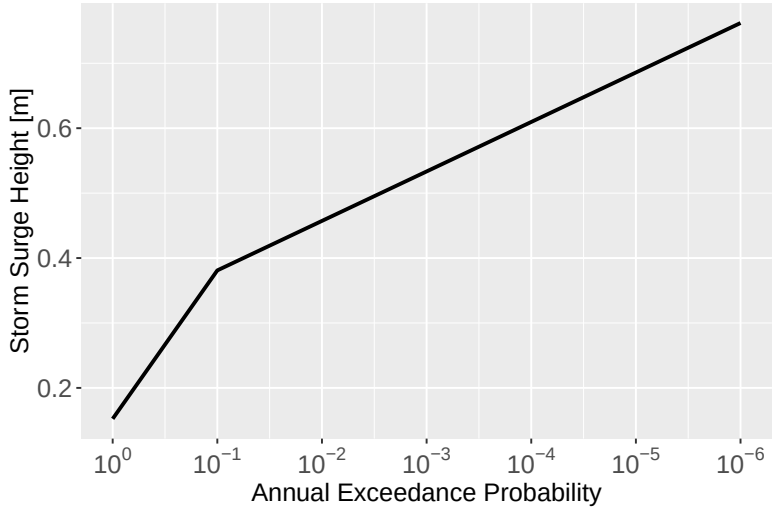

Figure II.10: Weighted Mean Storm Surge Hazard Curve

Protective Floodwall

The protective floodwall top event is further decomposed using a fault tree to obtain the failure probability of floodwall as shown in Figure II.11. Bodda [25] presents a methodology for developing the flooding fragility of a concrete floodwall by accounting for all the critical failure modes such as rigid body failure and foundation failure.

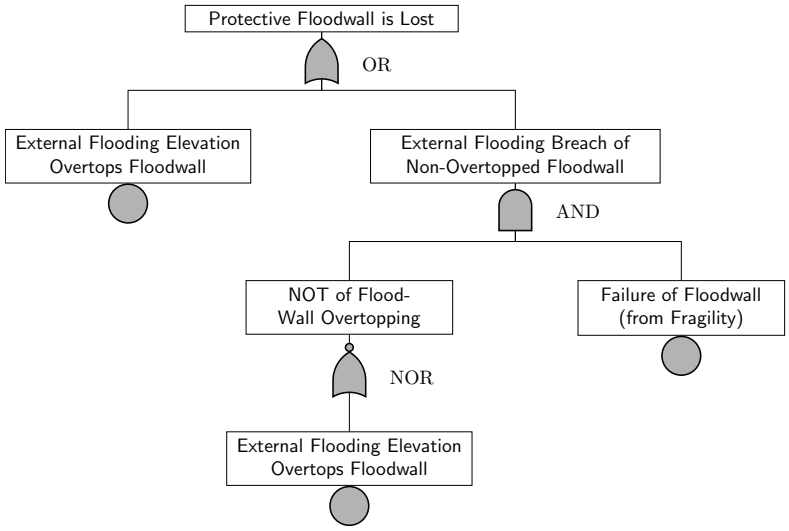

Figure II.11: Fault Tree of Protective Floodwall event

Plant Landscape

Plant landscape is used to describe the next top event in the event tree. This event is effective in preventing the flooding inundation ($h_{\text{landscape}}$) to exceed the height of the vent (H_{vent}). The performance function for plant landscape failure is characterized by following limit state:

$$Z_{\text{landscape}} = H_{\text{vent}} - h_{\text{landscape}} \tag{II.9}$$

And the conditional probability of landscape failure given storm surge height is expressed as:

$$P_f(\text{Landscape}|\text{surge height}) = P(Z_{\text{Landscape}} < 0) \tag{II.10}$$

Protective Vent

Protective vent describes the event in which the vent is successful in preventing the external flood due to landscape overflow to enter the DG room. The vent can break due to various loads such as wave impact, debris and sediment loads. Fragility analysis is carried

out for these loads individually and later combined to obtain the failure probability of vent using a fault tree.

Onsite AC Power

The last top event in the synthetic example is the onsite AC power. This event is necessary to be maintained until hot shutdown is achieved. For this event, the performance function characterizes failure as DG failure. Failure occurs when water level in the DG room, $h(t)$, due to vent overflow exceeds the height of the DG (H_{DG}). The performance function for DG failure is characterized by following limit state:

$$Z_{\mathrm{DG}} = H_{\mathrm{DG}} - h(t) \tag{II.11}$$

And the conditional probability of DG failure given storm surge height is expressed as:

$$P_f(DG|\text{surge height}) = P(Z_{\mathrm{DG}} < 0) \tag{II.12}$$

The formulation for calculating water level in the DG room, $h(t)$ is given by:

$$\begin{aligned} \frac{dh(t)}{dt} &= \frac{C_d Q(t)_{\mathrm{theoretical}}}{A} \\ Q(t)_{\mathrm{theoretical}} &= A_{\mathrm{vent}} V = W\sqrt{2g\Delta H} \end{aligned} \tag{II.13}$$

$C_d =$ Discharge Coefficient $\quad W =$ total height of vent opening

$Q(t) =$ Discharge Rate $\quad g =$ acc. due to gravity

$A_{\text{vent}} =$ Cross-Sectional Area $\quad \Delta H =$ water height above the vent opening

$V =$ Velocity

The discharge coefficient, C_d can exhibit uncertainty leading to change of water level in the DG room. The coefficient C_d can be calculated from experimental measured data (Reader-Harris and McNaught [26]) which is given by an empirical relationship, see Eq. (II.14), as well as formulated using a simulation model, see Eq. (II.15) [27]. The variation of C_d (probability density curves) for the experimental and simulation-based data is shown in Figure II.13. Now, we can estimate the water levels $h_{\text{vent, sim}}$ and $h_{\text{vent, exp}}$ in the DG room based on the simulation model of C_d and the experimental data of C_d. The simulation and data-driven (median) fragility curves for the DG failure can be generated based on $h_{\text{vent, sim}}$ and $h_{\text{vent, exp}}$ models, respectively.

$$C_{d,\text{exp}} = 0.5961 + 0.0261\beta^2 - 0.216\beta^8 + 0.000521\left(\frac{10^6\beta}{Re_D}\right)^{0.7} + \left[0.0188 + 0.0063\left(\frac{19000\beta}{Re_D}\right)^{0.8}\right]\beta^{3.5}\left(\frac{10^6}{Re_D}\right)^{0.3} + (0.043 + 0.08e^{-10L_1} - 0.123e^{-7L_1}) \times \left[1 - 0.11\left(\frac{19000\beta}{Re_D}\right)^{0.8}\right]\frac{\beta^4}{1-\beta^4} - 0.031\left[2L_2' - 0.8\left(\frac{L_2'}{1-\beta}\right)^{1.1}\right]\beta^{1.3} \tag{II.14}$$

$$C_{d,\text{sim}} = \alpha \text{Re}^{\beta} \tag{II.15}$$

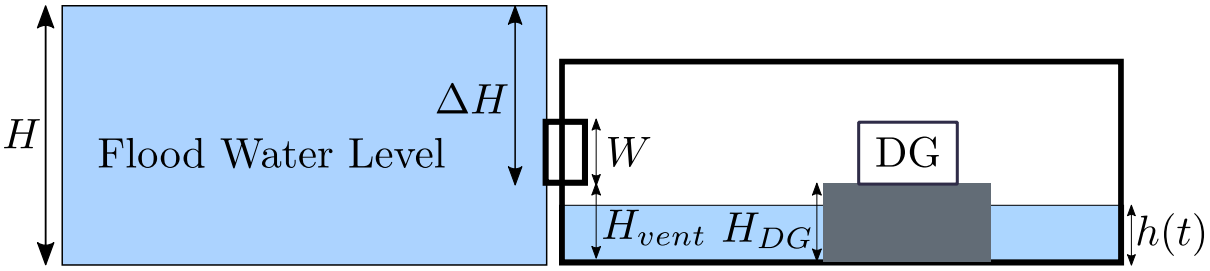

Figure II.12: Loss of Onsite AC Power Scenario

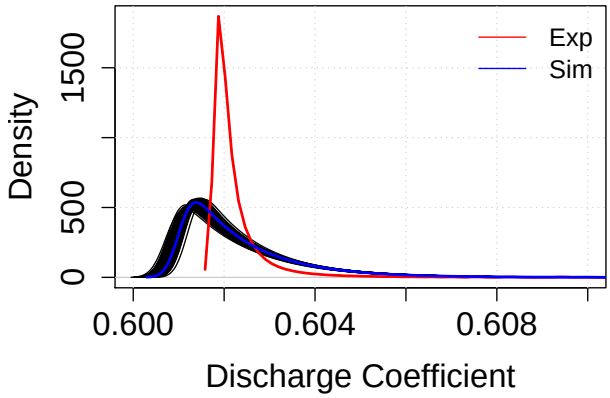

Figure II.13: Variation of Discharge Coefficient, C_d

II.6.2 Fragility Estimates and Data Applicability

Development of simulation-based fragility models for the events mentioned in section II.6.1 can be either a finite element (FE) or a smoothed-particle hydrodynamic (SPH) analysis [25, 27, 28, 29, 30]. In this study, the intensity measure for the initiating event is storm surge height. Therefore, all the fragility models need to be developed based on the surge height for risk calculation. Moreover, in a PRA informed validation framework as we propagate fragilities from basic events to intermediate-level events, the intensity measure must be same for all the events. However, the intensity measure for the flooding fragility analysis of individual events can be different. For example, the water level in the DG room depends on the flood elevation over the vent. Similarly, the landscape flooding

inundation depends on the height of the water over the floodwall which in turn depends on the surge height. In order to have same intensity measure for all the events, it requires interaction between different models, software, and domains.

In this study, we assume that the simulation and the data-driven fragility information for all the top events is directly available. Table II.4 gives the lognormal fragility parameters for all the events. In practice, the fragility parameters are developed based on actual analysis of the site specific plant SSCs. In addition to the data-driven fragility parameters, we also assume that the grade quality of experimental data for the top events is available as given in Table II.5.

Table II.4: Simulation and Data-driven fragility parameters

TOP EVENT	***Simulation Fragility***		***Data-driven Fragility***	
	Median, $\hat{\lambda}$ (ft.)	**SD**, β_{AU}	**Median**, $\hat{\lambda}$ (ft.)	**SD**, β_{AU}
1. Floodwall Failure	1.9	0.20	1.7	0.30
2. Landscape Flooding	2.0	0.20	1.6	0.35
3. Vent Overflow	2.2	0.15	2.3	0.25
4. DG Failure	3.9	0.20	3.1	0.35

Table II.5: Grade quality of Validating events

TOP EVENT	Relevance	Scaling	Uncertainty
1. Floodwall Failure	High	Medium	Medium
2. Landscape Flooding	Low	Medium	High
3. Vent Overflow	Medium	Low	Very Low
4. DG Failure	Medium	High	Very Low

II.6.3 System level Validation

Critical Events – Risk vs Fragility

In this study, the critical events are obtained based on simulation models. The risk of all the top events is calculated by convoluting the weighted-mean storm hazard curve (Figure II.10) with the corresponding median simulation fragility curve (Table II.4) using Eq. (II.1). As there is only one failure path in this synthetic example (Figure II.9), the risk of the end state event depends on the Vent overflow event due to its maximum contribution for the system level risk. However, when we propagate fragilities through the Bayesian network, the end state fragilities are governed by the DG failure event as shown in Figure II.14 and the reason is explained as follows. The end state fragility is simply obtained by multiplying all the top event fragilities. As seen in Figure II.14, the simulation fragility of DG failure event starts around a storm surge height of 2.5 ft and the rest of all events reach a failure probability of 1 around this surge height. Therefore, when the end state simulation fragility is computed, the DG failure event nullifies the

effect of all other events. For a PRA informed validation, the system level validation needs to be evaluated based on fragility estimates rather than risk estimates because the specific magnitude of intensity measure is unknown for future events.

The same process can be extended to data-driven models and it should yield the same critical events as the one obtained based on simulation models for the validation study. In this case, the data-driven end state fragility is dependent on the data-driven DG failure event.

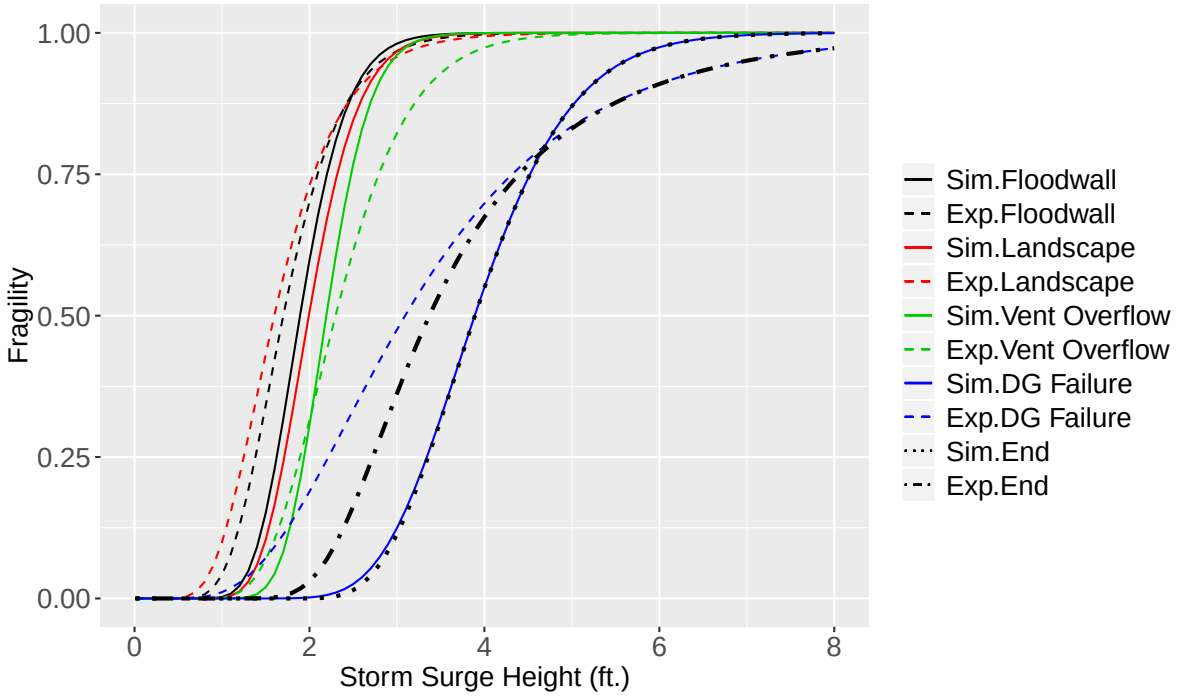

Figure II.14: Simulation and Data-driven (median) fragility curves

Validation Metric – Overlapping Coefficient

In the next step, multiple simulation fragility curves are generated by assuming a coefficient of variation of 0.1 for the simulation median capacity. Similarly, multiple data-driven fragility curves are generated by including data applicability as described in section II.4.2. Based on these multiple combinations of simulation and data-driven fragility curves, a histogram of overlapping coefficients is developed for all the top events as shown in Figure II.15. The OC for the system level has a mean of 0.59 which would be unacceptable if an acceptance criterion of 0.75 is adopted. Therefore, the overall validation has to be improved either by enhancing the simulation model or collecting additional experimental/field data for the DG failure event until the adequacy of the system level validation is satisfied.

Additional Data – Updating

In this study, we assume additional field data is collected for the DG failure event due to a larger uncertainty in the data-driven model compared to its simulation model. The additional data is given in terms of failure rate as shown in Table II.6. Based on this new information, the data-driven fragility curves and the subsequent OCs are updated using Bayesian inference [31]. The updated histogram of OCs is shown in Figure II.16. As seen in this figure, the validation of DG failure event has improved due to the additional data and thereby improving the overall system level validation. The uncertainty in the validation metric has also been reduced giving more confidence in the overall validation and satisfying the desired acceptance criterion.

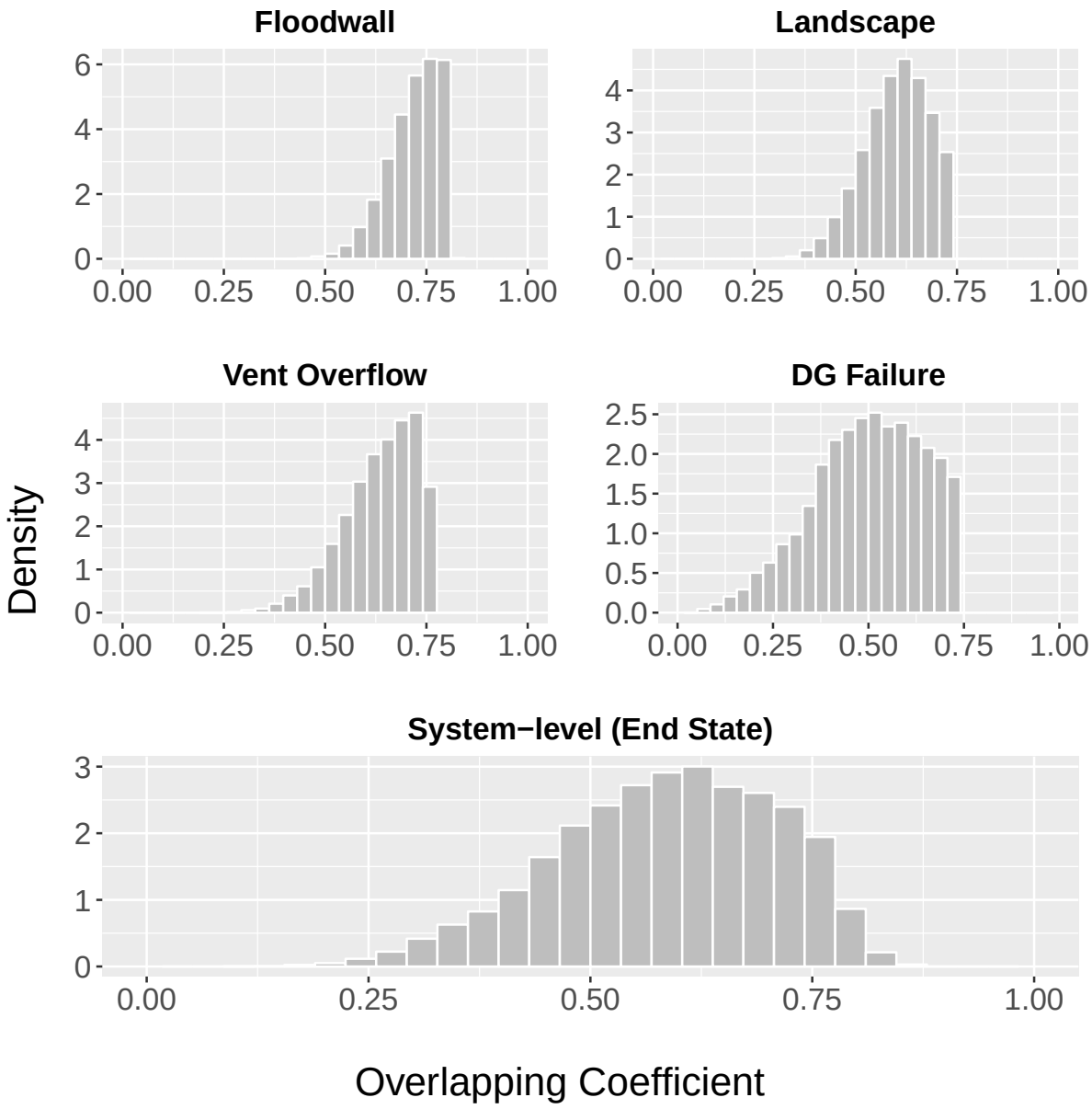

Figure II.15: Histogram of TOP events Overlapping Coefficients

Table II.6: Additional Failure data of DG Failure event

Surge Height (ft.)	No. of Failures	Total Test Cases
3	5	50
4	28	50
5	45	50
6	49	50

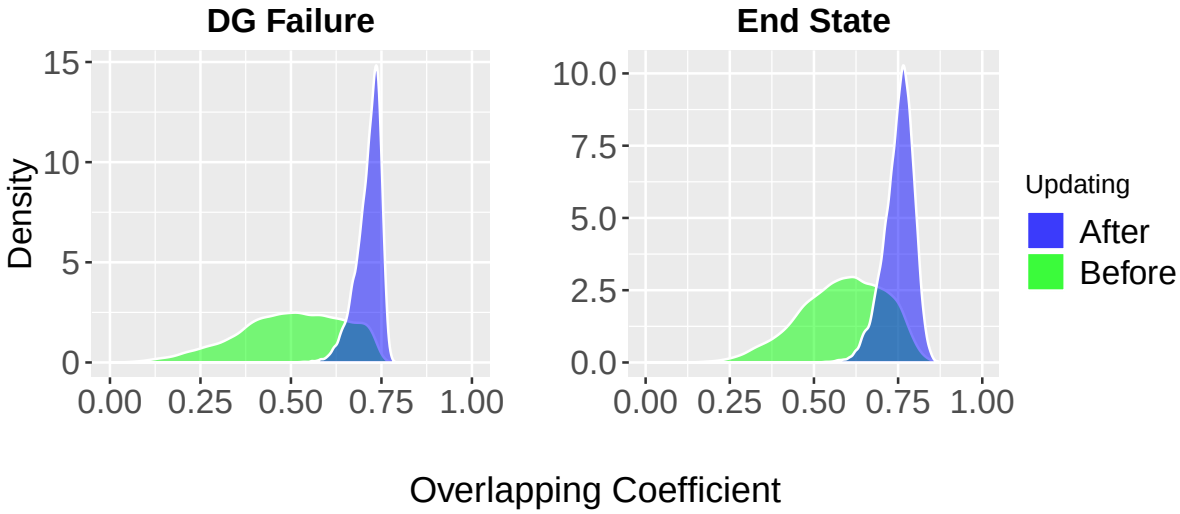

Figure II.16: OC Histogram of DG Failure and End state (System-level)

II.7 Summary and Conclusions

This paper presents a novel approach to quantitatively assess the system level validation by connecting individual validation events through a PRA informed validation framework. In this methodology, we include uncertainty in both simulation and data-driven models which gets reflected in the confidence levels of the overall validation. Event tree and fault trees are constructed for the system level performance, and they are mapped into a Bayesian network that allows propagation of fragility information from component level to system level. The uncertainty in the experimental data is represented in terms of three attributes: Relevance, Scaling, and Data Uncertainty. These attributes are graded based on their VUQ quality and are incorporated in the data-driven fragility analysis. In this study, the system level validation and the identification of critical events are evaluated based on fragility estimates. To improve the overall validation, we either enhance the simulation models of events along the critical path or collect additional field data until the adequacy of the system level validation is satisfied. This process helps in allocating the resources efficiently thereby reducing the effort to conduct high fidelity simulations and large-scale experiments. The proposed framework based on risk informed approach for system-level validation can be adopted by advanced flooding simulation codes such as Neutrino. The credibility of the Neutrino code for the intended application can be quantified similar to the synthetic example described in this manuscript.

The key conclusions of this study are summarized as follows:

- The quality of experimental data used in the validation study is quantified and incorporated in the data-driven fragility curves.

- The basic events that are critical in the perspective of system level validation are identified.
- Multiple fragility curves are evaluated using different confidence levels instead of just the mean fragility curves.
- The credibility of the overall validation is estimated which gives confidence in the decision making.
- The robustness of the modified framework is illustrated by enabling clarity, consistency, and completeness for a synthetic example of a simplistic flooding scenario.

PART III

Enhancement of Existing Risk Informed Validation Framework

III.1 Introduction

In recent years, USNRC [32] and IAEA [33] have developed methodologies to assess the vulnerabilities of nuclear plants against site specific extreme hazards following the Fukushima-Daiichi nuclear accident. In many cases, advanced simulation tools are being considered to simulate multi-hazard, multi-physics, multi-scale phenomena and to evaluate vulnerability of nuclear facilities [13, 14, 15, 25, 27, 28, 30]. A knowledge about the accuracy of simulation codes is essential so that they may be used with confidence for decision making. The credibility of advanced simulation tools is assessed based on a formal verification, validation, and uncertainty quantification procedure. One of the key limitations in validation is the lack of relevant experimental data at system and sub-system levels. This limitation leads to decrease in confidence in the prediction of system-level risk and excessive reliance on expert opinion. Therefore, a robust validation framework is needed to formalize the confidence in predictive capability of advanced simulation results particularly in the context of uncertainties from various different sources.

Probabilistic risk assessment (PRA) has been widely used to examine the risk posed by nuclear facilities and to identify the key components that have the most impact on safety [34]. PRA is a powerful tool due to its rigorous and systematic analysis, identification of major sources of uncertainty, provision for formal sensitivity analysis, and consideration of qualitative and quantitative decision-making measures. A traditional PRA approach has its limitations in the use of fault trees and event trees in certain applications such as: (a) non-binary or statistical relationship between intermediate and basic events, and (b) statistical correlations between basic events.

However, these limitations can be addressed by implementing Bayesian network representation of PRA [13, 14, 15]. Only a few structures, systems and components (SSCs) at a nuclear plant are critical from a perspective of system-level safety or performance. Therefore, a validation framework that is based on a PRA informed approach is quite powerful by identifying the critical SSCs for validation and formalizing the confidence in prediction of system-level validation that are based on component level data.

Experts in the areas of computational solid mechanics, computational fluid dynamics and heat transfer, and computational integrated system thermal fluids behavior have developed formal guidelines for verification and validation (V&V) in modeling and simulation. The widely used frameworks for verification, validation, and uncertainty quantification (VVUQ) in nuclear power plant safety applications are (i) Code Scaling, Applicability, and Uncertainty methodology (CSAU) [9] (ii) Evaluation Model Development and Assessment Process (EMDAP) [10] (iii) Predictive Capability Maturity Model (PCMM) [11], and (iv) Predictive Capability Maturity Quantification (PCMQ) [12]. CSAU, EMDAP, and PCMM are all expert elicitation methodologies and these frameworks do not give any guidance on quantification methods for making decision on reliability of a simulation tool. PCMQ framework [12] addresses this issue by formalizing the validation process as structured knowledge representation, information abstraction, and multilevel evidence incorporation, which is further quantified as a decision-making process for nuclear reactor engineering or safety application. Each of these methodologies (CSAU, EMDAP, PCMM, and PCMQ) have certain specific aspects that are quite powerful and yet none of them can be directly extended to a risk consistent approach for validation particularly in the context of PRA

for external hazards.

Recently, Kwag et al. [13] and Bodda et al. [14] proposed a PRA informed methodology for system-level validation within the context of uncertainty. In these methodologies, a Bayesian approach is used to assess the credibility of system-level estimates. Kwag et al. [13] used a seismic case study and Bodda et al. [14] a flooding case study to illustrate the application of the methodology. In these studies, the validation process is performed by creating a Bayesian network model to represent the system-level failure against an external hazard. Then, simulation based fragilities and data-driven fragilities (from experimental or high fidelity simulation data) are propagated in the Bayesian network model separately to evaluate the system-level fragility. The adequacy of the system-level validation is evaluated by comparing its simulation based and data-driven fragilities using a validation metric which is defined in terms of an overlapping coefficient. The validation process is carried out until the adequacy of system-level validation is satisfied against an acceptance criterion. However, the proposed risk-informed validation framework by [13] and Bodda et al. [14] have two key limitations:

(1) In the validation framework, the system-level fragility is obtained by propagating fragilities from basic events. Then, the validation metric is computed by comparing the simulation and data-driven fragilities. However, the system-level validation may actually give incorrect results if the set of critical events for simulation-based fragility differs from the set of critical events for data-driven fragility.
(2) The methodologies cannot evaluate the confidence in adequacy of system-level validation based on different maturity levels of the data used.

In this manuscript, we propose major enhancements to the existing framework for the assessment of decision regarding the adequacy of advanced simulation tools for system-level validation. Improvement in the PRA informed validation methodology requires development of additional attributes and a new set of validation metrics for a complete and wider applicability of the framework. The advantage of the proposed enhancements are illustrated in the context of the same examples as those used by Kwag et al. [13] in order to clearly delineate the proposed enhancements.

III.2 Summary of existing Risk Informed Validation framework by Kwag et al. [13] and Bodda et al. [14]

The existing framework of Kwag et al. [13] and Bodda et al. [14] employs three key stages that are described below. The complete framework is illustrated through the flowchart shown in Figure III.1.

Stage 1:

The initial step involves development of an event tree and the required fault trees to represent accident scenarios resulting from an initiating external hazard. Then, simulation based fragility curves for all the basic events are developed. Next, the event tree and the corresponding fault trees are mapped into a Bayesian network. The system-level and intermediate-level simulation based fragilities are obtained by propagating fragilities from basic events through the Bayesian network.

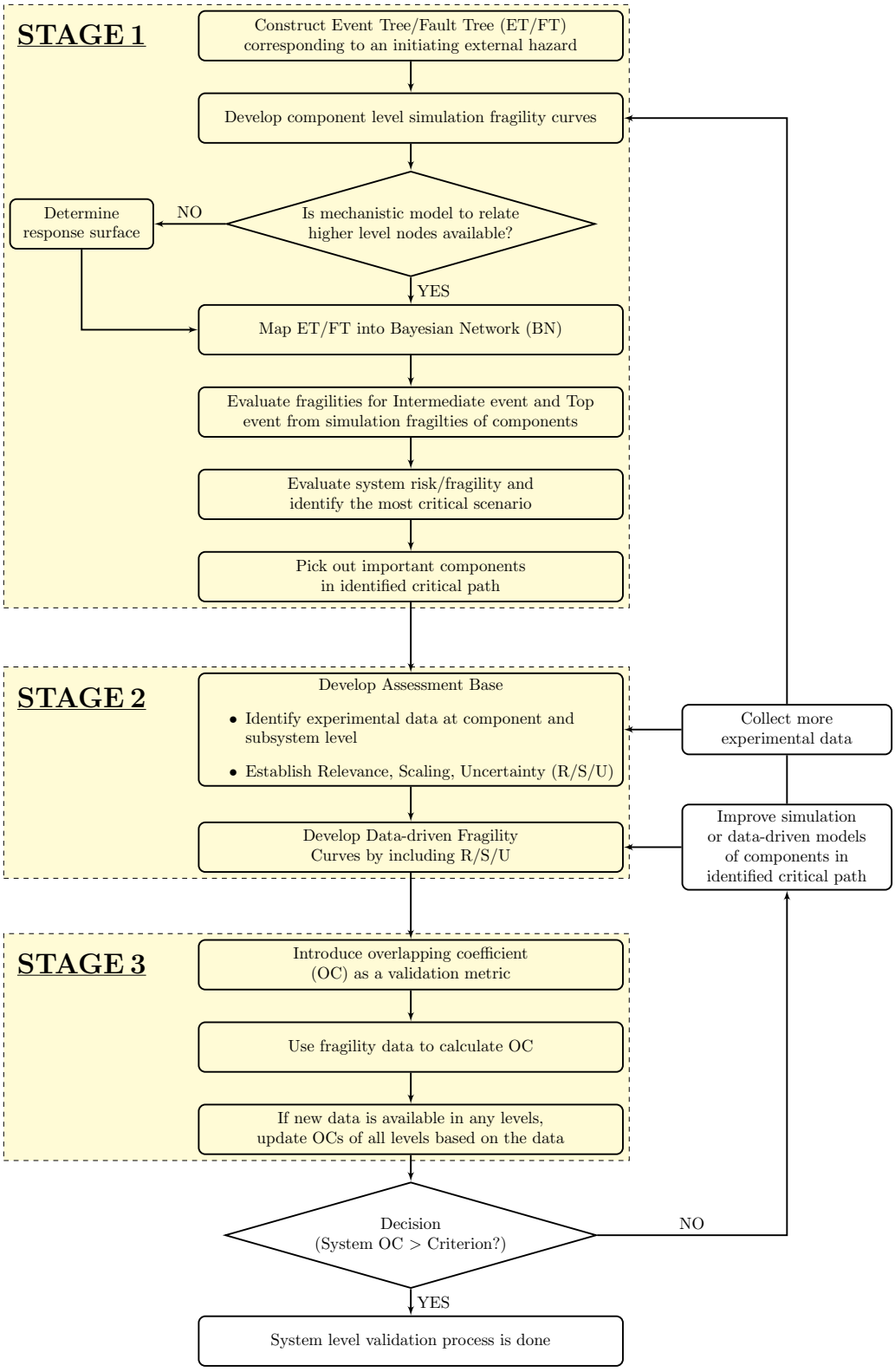

Figure III.1: Flowchart of risk informed validation framework [14]

Stage 2:

In Stage 2, an assessment base is developed which consists of experimental data at component and subsystem level. Next, a data-driven approach is adopted to quantify the quality of experimental data used for generating data-driven fragility curves. Similar to stage 1, system-level data-driven fragility curve is obtained by propagating data-driven fragilities from basic events through the Bayesian network.

Stage 3 and Decision:

In this framework, overlapping coefficient (OC) is used as the validation index to quantify the degree of validation within the context of uncertainty. OC is calculated by evaluating the percentage of overlapping area between two probability density curves and is given by Eq. (III.1). Numerically, OC ranges between 0 and 1. If $OC = 0$, then the distributions do not overlap with each other thereby indicating a complete disagreement and if $OC = 1$, then the distributions are identical thereby indicating a perfect validation within the context of uncertainty.

$$OC = \int_{-\infty}^{\infty} \min(f_{sim}(y), f_{exp}(y))dy \tag{III.1}$$

For each event, based on the simulation and data-driven fragility curves, OC is calculated. Finally, the system-level OC is compared with a predefined acceptance criterion for validation.

III.2.1 Information needed to implement Risk Informed Validation Framework for an external hazard scenario

The specific information required to carry out the validation of advanced simulation codes using the proposed validation framework is listed below:

- Develop event tree and its corresponding fault trees for the given external hazard scenario.
- For all the basic events or components, develop fragilities based on both simulation models and experimental or data-driven models. Establish the grade levels for Relevance, Scaling, and Data Uncertainty (R/S/U) for the available experimental data. The fragilities for each event can be developed based on individual simulation codes or an unified simulation code such as Neutrino can be used to evaluate fragilities for all the events at once.

  However, in the initial development of risk informed validation methodology, it is possible that the experimental fragilities might not be available for some events or all the events. This is similar to initial implementation of PRA in 1970s when there was not much information available on fragilities of components. The initial implementation of PRA relied significantly on expert opinion. Similar expert-based knowledge can be used for the initial implementation of the proposed risk informed methodology. The framework can be used to determine which specific information is more critical and then as more information becomes available either through high fidelity simulations or experiments, the complete validation process can be refined.
- Identify the critical events using the concept of importance measures as described in section III.3.

- If the data-driven fragilities are not available for the non-critical events, then it is assumed that the data-driven fragilities are same as the simulation-based fragilities.
- For comparing the accuracy between simulation fragilities and data-driven fragilities, select overlapping coefficient (OC) as the validation metric. Additional validation metrics such as KL Divergence, Mutual Information, and Bayes Factor can also be selected.
- Represent the adequacy of the code for the intended application in terms of maturity levels as described in section III.6.
- Define acceptance criterion for system-level validation using expert judgment.

III.3 Critical Path in a Bayesian Network

Typically, only a few components or events are critical for the system-level failure in a nuclear power plant. Therefore, it is necessary to identify the events along the critical path that leads to a system-level failure. For identifying critical events in a logic tree, we can use the concept of importance measures. The importance measure of a basic event provides information about its impact on the system. There are different types of importance measures such as Fussell-Vesely (FV) Importance, Risk Reduction Ratio/Interval, Risk Increase Ratio/Interval, Criticality, and Birnbaum Importance that are used in decision-making process [35, 36, 37, 38]. FV importance provides information about the relative degree to which the basic event is contributing to the system failure probability. The FV_i for an event i is defined as:

$$FV_i = \frac{P_i}{P_{sys}} \tag{III.2}$$

where P_i is the failure probability from all minimal cut sets which contains basic event i and P_{sys} is the system failure probability.

Traditionally, the importance measures are evaluated only for fault tree analysis. As mentioned earlier, due to limitations of fault tree analysis, Bayesian networks are used in the risk informed decision making. Therefore, we extend the concept of importance measures to a Bayesian network. In this study, Fussell-Vesely (FV) Importance is employed for identifying the critical path because the FV importance provides relative importance of all the nodes in the Bayesian network whereas other importance measures provide information only about the basic events or root nodes [39, 40].

The extended definition [39, 40] of FV importance for any node (x_i) in a Bayesian network can be obtained by evaluating the posterior failure probability of the node given that the system (ϕ) is failed, $P(x_i = 1|\phi = 1)$.

$$FV(x_i) = P(x_i = 1|\phi = 1) \tag{III.3}$$

III.3.1 Illustrative Case Study: Seismic Risk of Failure in Building-Piping System

Figure III.2 shows the fault tree for Building-Piping system failure subjected to seismic hazard [13]. The system comprises of a building structure, safety related equipment such as pump which is necessary to circulate the coolant, the piping system for circulating the coolant and pipe supports connecting the piping to the building. For simplicity and consistency with the current practice, we assume the fragility of all basic events to

follow lognormal distribution. The lognormal fragility parameters of all the basic events are shown in Table III.1 and the intensity measure is taken as peak ground acceleration (PGA). The fault tree is mapped into a Bayesian network using a mapping algorithm [15] and the corresponding mapped Bayesian network is shown in Figure III.3. The critical path is obtained for different values of intensity measures as the failure probability of an event depends on the intensity measure. The FV importance measure for all the events (nodes) in the Bayesian network is computed using Eq. (III.3) for various intensity measures of 0.5g, 1.5g, 2.5g, and 3.5g (Table III.2) The critical path is identified based on a top-down approach and utilizing the FV importance measures. The required steps for obtaining the critical path are described below:

- Start with the top node (TE) in the Bayesian network and identify its parent nodes, $Pa(TE) = IE1,\ IE2$.
- Compare the FV importance measures for all the parent nodes and obtain the parent node with largest value. ($IE1 = 0.999,\ IE2 = 0.056$)
- Next, identify the parent nodes of node $IE1$ and similarly, obtain the parent node with largest value. ($E1 = 0.997,\ E2 = 0.122$)
- Repeat the process until the root node (basic events) is reached.

The critical path and the corresponding critical events for the Building-Piping system failure is graphically illustrated by solid line in Figure III.3.

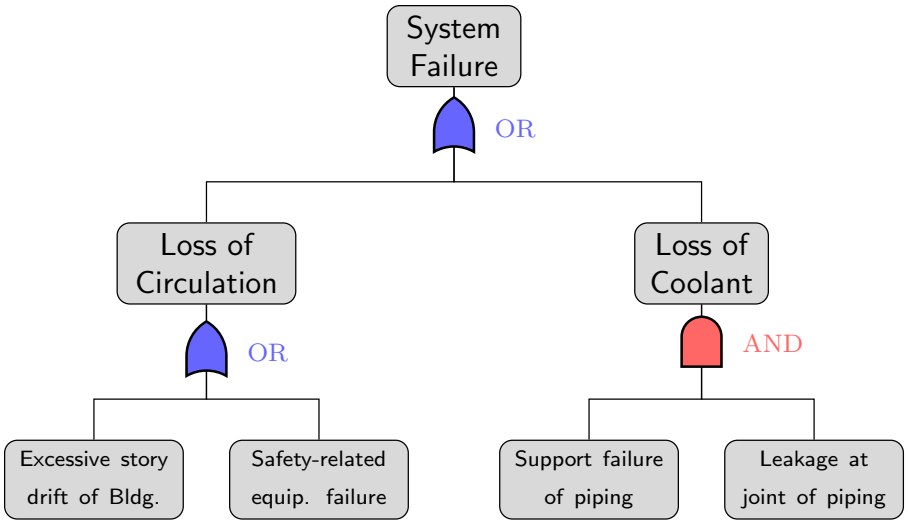

Figure III.2: Fault tree for Building-Piping System Failure

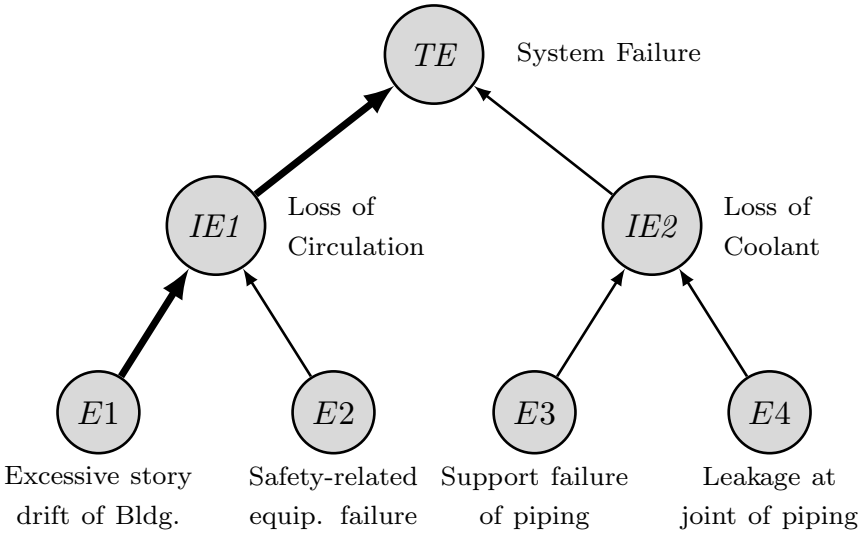

Figure III.3: Bayesian Network for Building-Piping System Failure

Table III.1: Lognormal Fragility parameters of basic events

BASIC EVENT	**Median**, $\hat{\lambda}$ (g)	**Log Standard Deviation**, β_{AU}
E1. Excessive story drift of Building	0.75	0.35
E2. Safety-related equipment failure	1.9	0.25
E3. Support failure of piping	2.5	0.29
E4. Leakage at joint of piping	1.2	0.33

Table III.2: Fussell-Vesely Importance measure for Building-Piping System Failure

Event	**0.5g**	**1.5g**	**2.5g**	**3.5g**
E1	1	0.997	1	1
E2	0	0.122	0.913	0.998
E3	0	0.077	0.506	0.833
E4	0	0.810	0.999	1
IE1	1	0.999	1	1
IE2	0	0.056	0.500	0.835
TE	1	1	1	1

III.4 Validation Path in a Bayesian Network

In the risk informed validation framework given by Bodda et al. [14], simulation and data-driven fragility curves for all the basic events in the fault tree and event tree are developed. Next, the fault trees and the corresponding event tree are mapped into a Bayesian network. The system-level fragilities are obtained by propagating fragilities from basic events through the Bayesian network. Based on the simulation and data-driven fragility curves, overlapping coefficient (OC) can be calculated for all the events. Then, the system-level OC is compared with a predefined acceptance criterion for validation. However, the validation may not be complete or consistent if the set of critical events for system-level simulation fragility differs from the corresponding set of critical events for system-level data-driven fragility. Therefore, in addition to OC, we employ Consistency Index (δ) in the validation metric in order to ensure that simulation and data-driven fragilities correspond to the same set of critical events.

III.4.1 Explanation of Consistency Index (δ)

In Figure III.4, the Bayesian networks represent the simulation (left) and the data-driven (right) models for the Building-Piping system failure, respectively. The fragilities of the basic events are propagated in both these models separately and the critical path is identified as describe in section III.3. If the critical path is same in both the models (Figure III.4), then $\delta = 1$. If the critical path is different in both the models as shown in Figure III.5, then $\delta = 0$. When the critical paths are different, the simulation model predicts the "Loss of Circulation" event as the critical event for the system failure whereas the data-driven model predicts the "Loss of Coolant" event as the critical event for the system failure. This shows there is inconsistency between the models, therefore the

consistency index, $\delta = 0$.

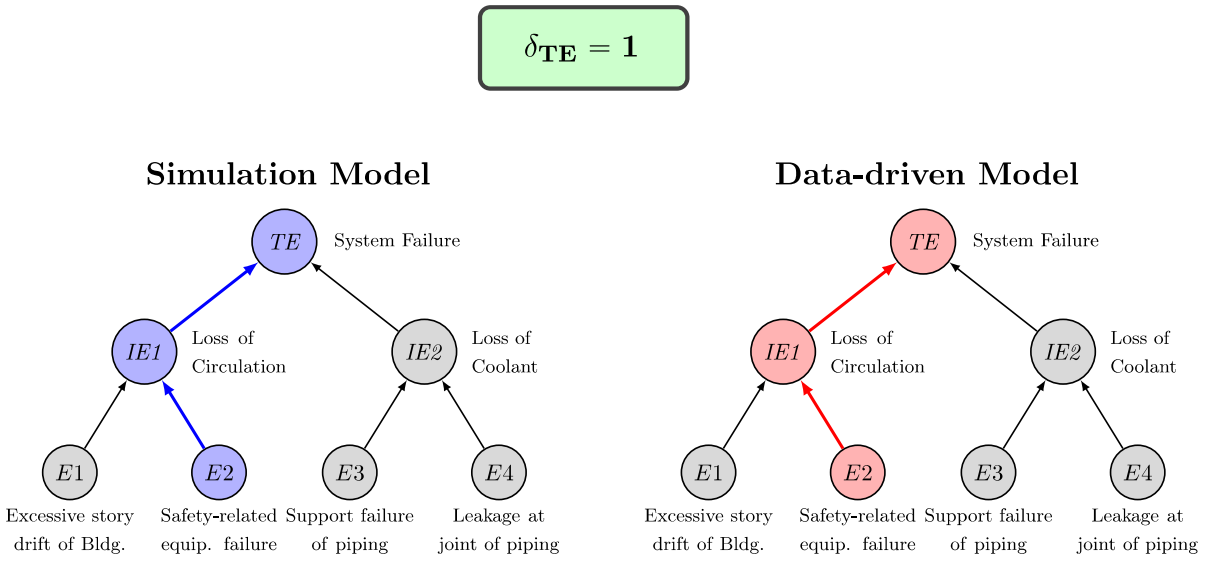

Figure III.4: Consistency Index, $\delta = 1$

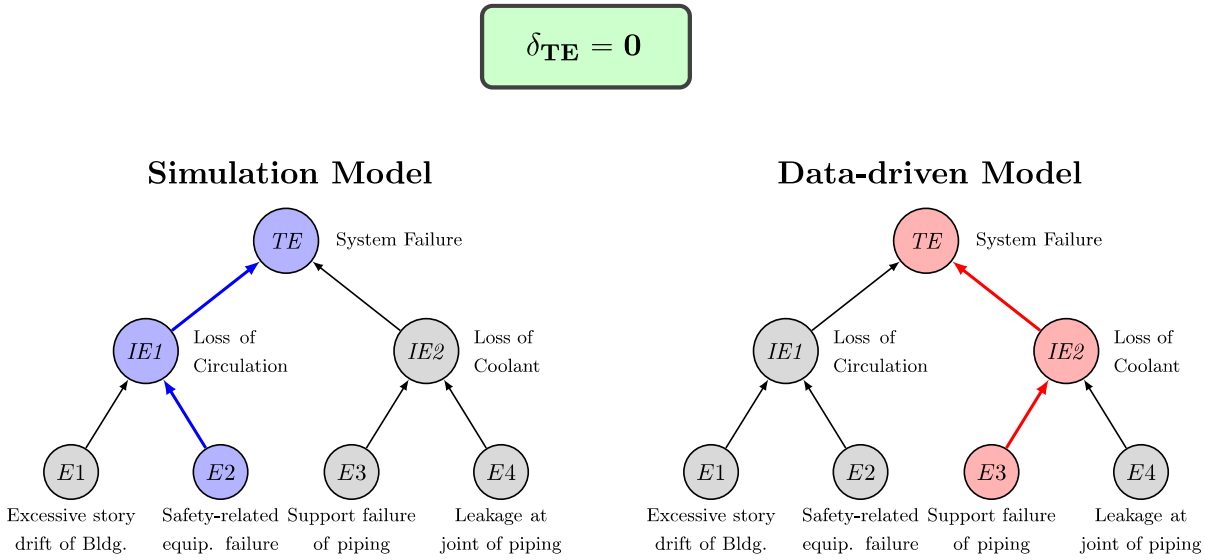

Figure III.5: Consistency Index, $\delta = 0$

III.5 Interpretation of Consistency Index

In this section, we illustrate the incorporation and interpretation of consistency index in the risk informed validation framework through the three cases described below. For all these cases, we consider the same Bayesian network for the building piping system failure as shown in Figure III.3 but with different lognormal fragility parameters for the basic events.

Case 1:

In Figure III.6, the basic events and are related to "Loss of Circulation" (*IE1*) event by OR logic. We obtain fragilities for *IE1* event by propagating fragilities of basic events $E1$ and $E2$. The critical events for both *IE1* simulation fragility and data-driven fragility come from the same event $E1$. Therefore, the consistency index is equal to 1 for event *IE1*. Then, we compute fragilities for event *IE2* which is connected to basic events $E3$ and $E4$ by AND logic. The consistency index is equal to 1 for event *IE2* as the critical event for both the models comes from the same event $E3$. Similarly, the "Top" event fragilities are computed from intermediate events (*IE1*, *IE2*) and the critical event is "Loss of Circulation" for both the models, making $\delta = 1$. As all the events on the critical path are consistent, we have confidence in the estimated overlapping coefficient of Top event which is shown in Table III.4.

Table III.3: Simulation and Data-driven fragility parameters (Case 1)

BASIC EVENT	***Simulation Fragility***		***Data-driven Fragility***	
	Median, $\hat{\lambda}$ (g)	**SD**, β_{AU}	**Median**, $\hat{\lambda}$ (g)	**SD**, β_{AU}
E1. Excessive story drift of Building	0.75	0.30	0.55	0.35
E2. Safety-related equipment failure	1.9	0.20	1.7	0.25
E3. Support failure of piping	2.5	0.35	2.2	0.29
E4. Leakage at joint of piping	1.2	0.25	1.0	0.33

Table III.4: Overlapping Coefficient of all the events (Case 1)

Event	**OC**	**Event**	**OC**
$E1$	0.65	*IE1*	0.65
$E2$	0.76	*IE2*	0.81
$E3$	0.80	*TE*	0.65
$E4$	0.73		

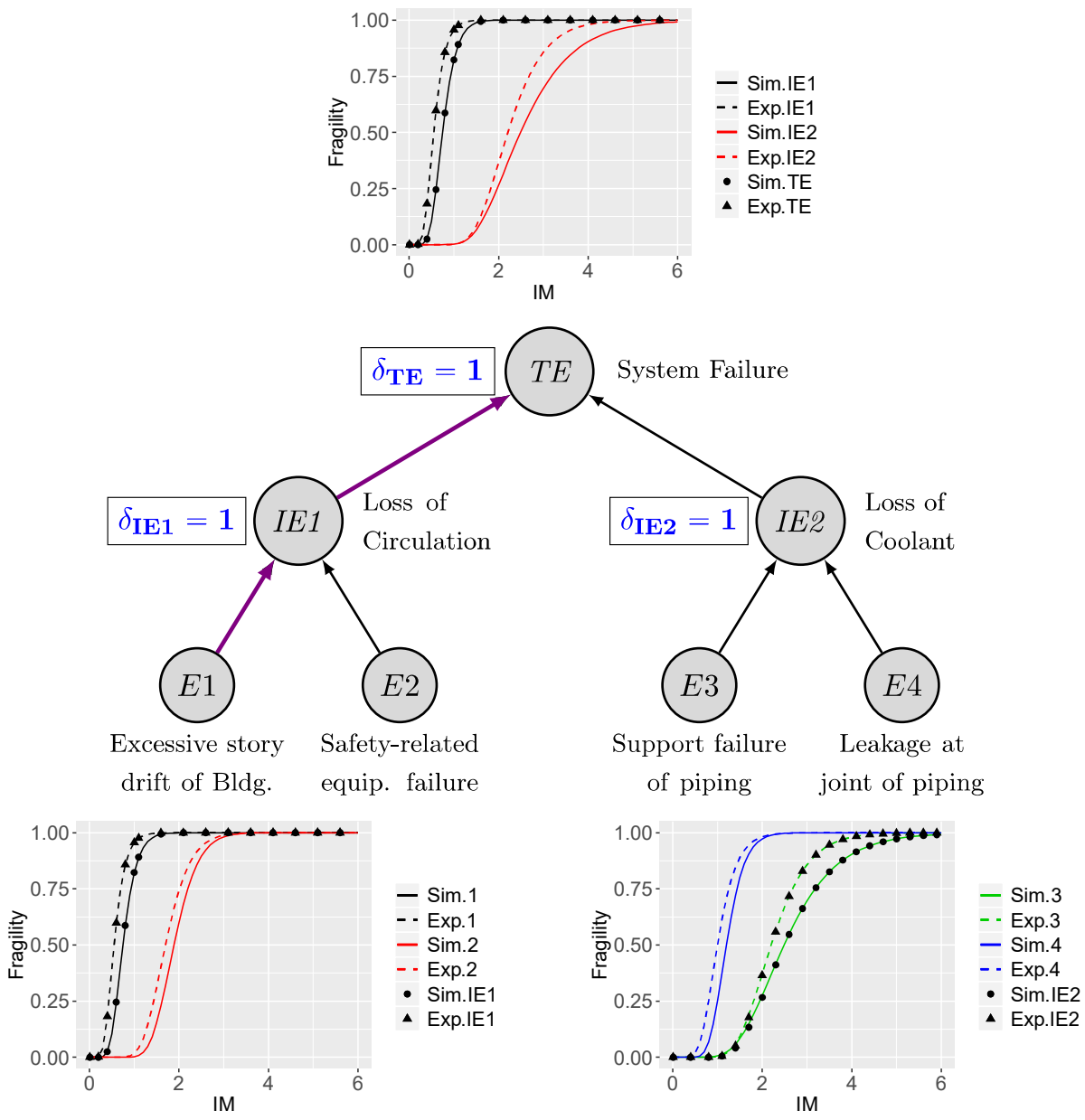

Figure III.6: Case 1

Case 2:

In this case, the lognormal fragility parameters for the basic events are given in Table III.5. The consistency index for "Loss of Circulation" event is equal to 1 which is same as Case 1. But for "Loss of Coolant" event, the consistency index is equal to 0 as the simulation fragility of *IE2* comes from event $E4$ and the data-driven fragility of *IE2* comes from event $E3$ as shown in Figure III.7. This is because the event *IE2* is connected to basic events $E3$ and $E4$ by AND logic. Therefore, the fragility of event *IE2* is obtained by multiplying the fragilities of basic events $E3$ and $E4$. As seen in Figure III.7 (left), the simulation fragility of event *IE2* is governed by the simulation fragility of event $E4$. Similarly, the data-driven fragility of event *IE2* is governed by the data-driven fragility of event $E3$ as shown in Figure III.7 (right).

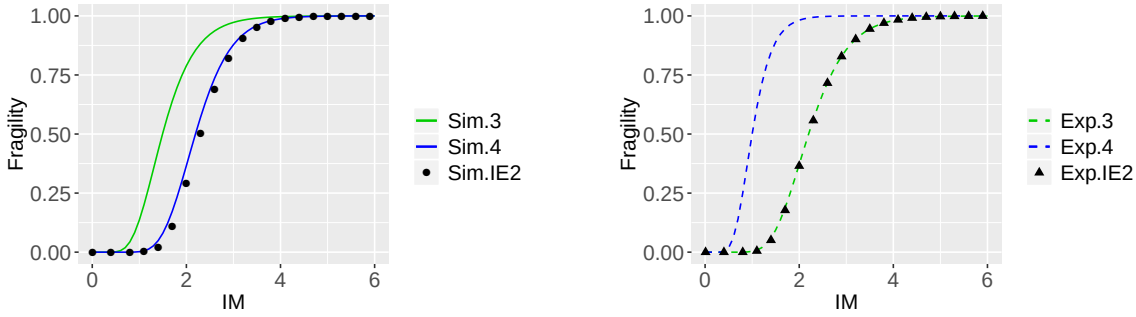

(a) (b)

Figure III.7: Consistency Index for Loss of Coolant Event ($\delta_{IE2} = 0$, Case 2)

Next, we calculate the consistency index for "Top" event which is equal to 1 as the critical event for both the simulation and data-driven models is "Loss of circulation" event. In this case, we still have confidence in the estimated validation metric of "Top" event as all the events on the critical path are consistent ($\delta_{TOP} = \delta_{IE1} = \delta_{E1} = 1$) as shown in Figure III.8.

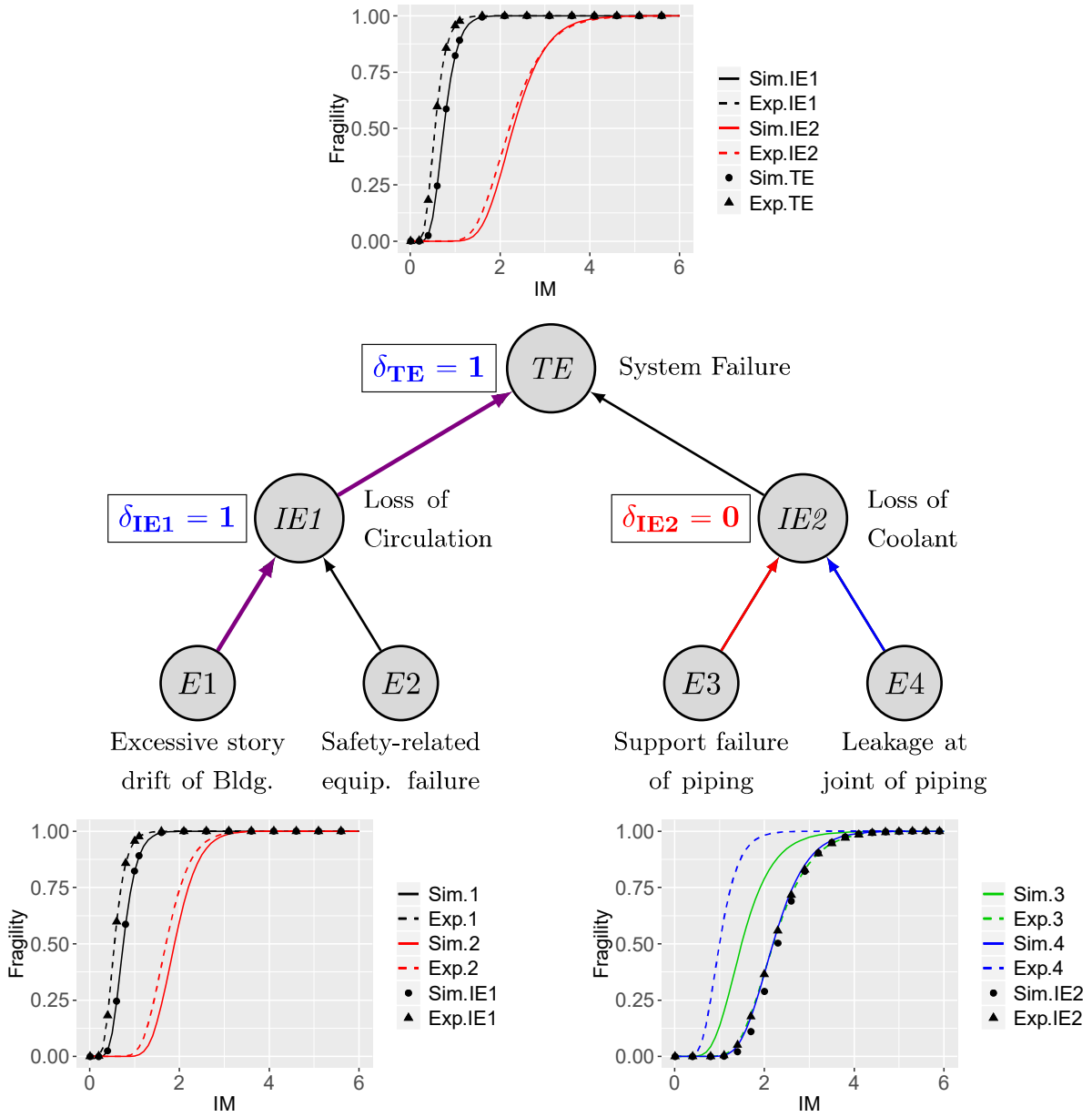

Figure III.8: Case 2

Table III.5: Simulation and Data-driven fragility parameters (Case 2)

BASIC EVENT	***Simulation Fragility***		***Data-driven Fragility***	
	Median, $\hat{\lambda}$ (g)	**SD**, β_{AU}	**Median**, $\hat{\lambda}$ (g)	**SD**, β_{AU}
E1. Excessive story drift of Building	0.75	0.30	0.55	0.35
E2. Safety-related equipment failure	1.9	0.20	1.7	0.25
E3. Support failure of piping	1.5	0.35	2.2	0.29
E4. Leakage at joint of piping	2.2	0.25	1.0	0.33

Case 3:

The lognormal fragility parameters for the basic events are given in Table III.6. In this case, the consistency index for the "Top" event is equal to 1. However, the consistency index for one of the events which lie on the critical path is equal to 0 (see Figure III.9). Therefore, in this case we do not have confidence in the estimated OC for overall validation even though the consistency index for "Top" event is equal to 1. In a risk informed validation framework, all the events on the critical path have to be consistent for obtaining an accurate estimate of overlapping coefficient for the system-level failure. Therefore, in order to make the "Loss of Circulation" event as consistent, we either enhance the simulation model or collect additional experimental/field data for events $E1$, $E2$ as "Loss of Circulation" event depends on $E1$, $E2$.

Next, we assume additional simulation data is collected for events $E1$, $E2$ due

to larger uncertainty in the simulation models compared to its data-driven models. The additional data is given in terms of failure rate as shown in III.7. Based on this new information, the fragility curves of basic events $E1$, $E2$ and the subsequent "Loss of Circulation" event are updated using Bayesian Inference (Bodda et al., 2019). As seen in Figure III.10, the consistency index of "Loss of Circulation" event has changed to 1 and therefore, the obtained OC for system-level is consistent.

Table III.6: Simulation and Data-driven fragility parameters (Case 3)

BASIC EVENT	***Simulation Fragility***		***Data-driven Fragility***	
	Median, $\hat{\lambda}$ (g)	**SD**, β_{AU}	**Median**, $\hat{\lambda}$ (g)	**SD**, β_{AU}
E1. Excessive story drift of Building	1.75	0.30	0.65	0.35
E2. Safety-related equipment failure	0.9	0.20	1.7	0.25
E3. Support failure of piping	2.5	0.35	2.2	0.29
E4. Leakage at joint of piping	1.2	0.25	1.0	0.33

Table III.7: Additional Failure data of events $E1$ and $E2$

(a) $E1$

Intensity measure (g)	**No. of Failures**	**Total Test Cases**
0.3	12	30
1.0	24	30

(b) $E2$

Intensity measure (g)	**No. of Failures**	**Total Test Cases**
1.5	9	30
2.0	21	30

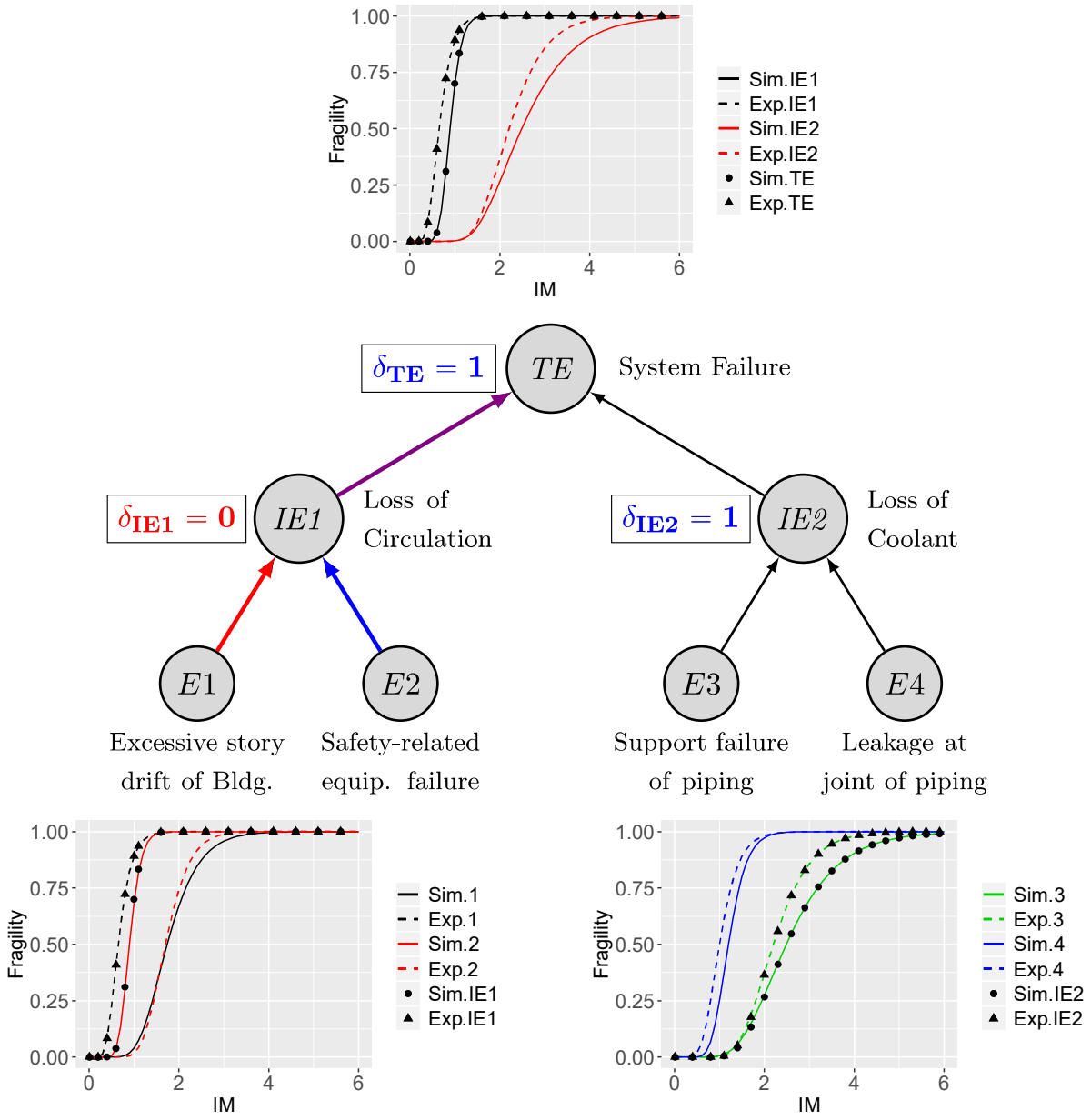

Figure III.9: Case 3

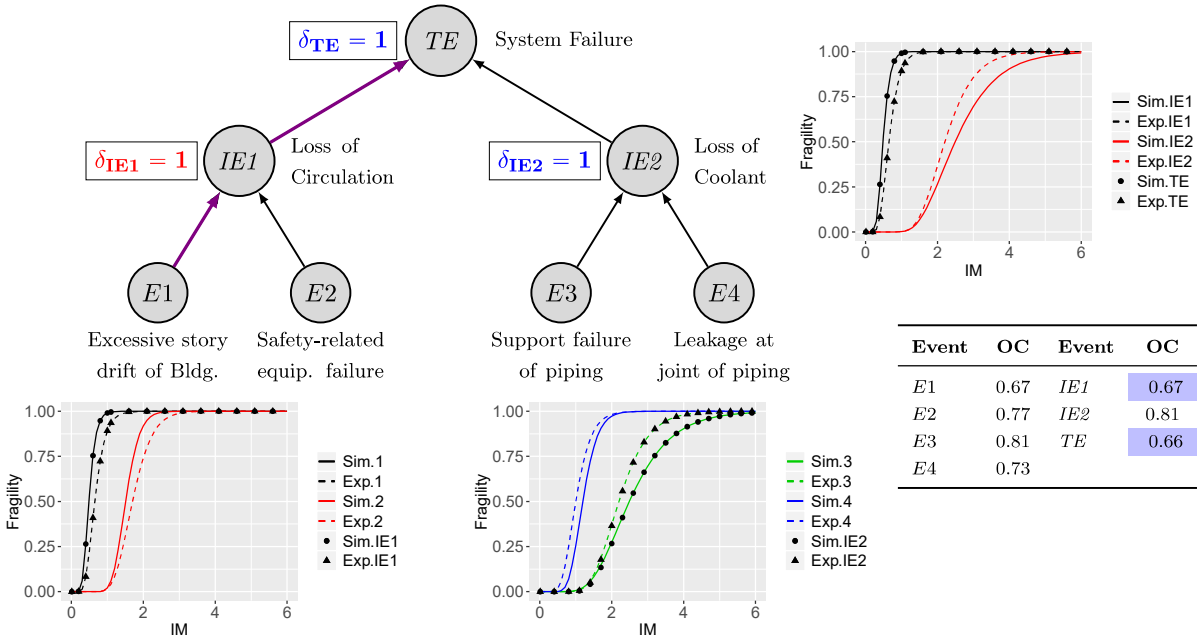

Event	OC	Event	OC
$E1$	0.67	$IE1$	0.67
$E2$	0.77	$IE2$	0.81
$E3$	0.81	TE	0.66
$E4$	0.73		

Figure III.10: Case 3 Updated

III.6 Code Applicability

Maturity levels provide a quantitative assessment to predict the accuracy for all important quantities of interest (QoI) under large uncertainties. Existing validation frameworks such as Predictive Capability Maturity Model (PCMM) [11] and Predictive Capability Maturity Quantification (PCMQ) [12] express the degree of validation on the basis of four increasing levels of maturity. The maturity levels are labeled as very low (1), low (2), medium (3), and high (4). The proposed risk informed validation methodology by Kwag et al. [13] and Bodda et al. [14] do not represent the confidence in adequacy of system-level validation in terms of different maturity levels. Therefore, in this study we enhance the existing risk informed validation framework by incorporating the concept of maturity levels from PCMQ. Then, the assessment of decision regarding the adequacy of a simulation code for an intended application is represented by maturity level. In the risk informed validation framework, we first

evaluate the code adequacy for the system-level failure event. If the system-level code adequacy does not meet the desired acceptance criterion, then we look at the code adequacy of those events with high importance measures. Also, if multiple simulation codes are used, the code adequacy for each code can be evaluated.

Similar to Lin's [27] and Athe's [12] studies, the adequacy of code in the proposed risk informed framework depends on two attributes: Validation Result and Data Applicability. These attributes are connected to each other using a Bayesian network as shown in Figure III.11 and the attributes are described below.

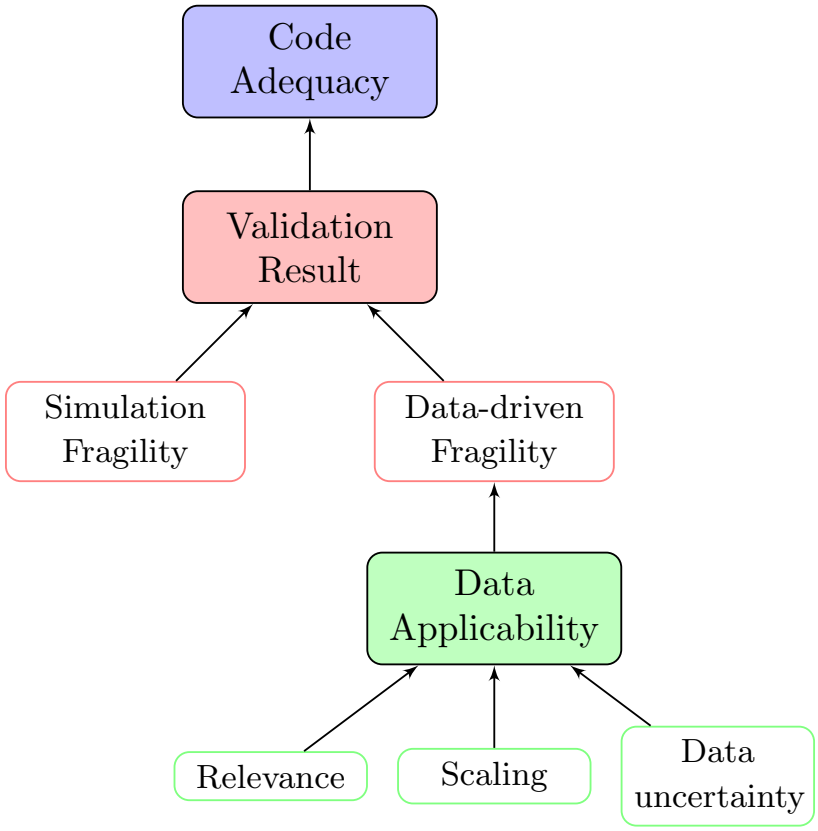

Figure III.11: Bayesian network for Code Adequacy

- **Data Applicability:** It represents the epistemic uncertainty in the experimental data which is used for generating experimental or data-driven fragility curve. The

quality of experimental data is given in terms of three sub-attributes: Relevance, Scaling, and Data Uncertainty (R/S/U). Relevance reflects the degree of applicability of experimental data from a historic or an independent study to the current application. Scaling uncertainty incorporates both geometric and physics scaling uncertainties. Data uncertainty reflects the uncertainty in the measured data. Four grades ranging from 1 to 4 (increasing order of value) are assigned to the R/S/U attributes based on their VUQ quality as shown in Table III.8 [21]. Bodda et al. [14] quantifies R/S/U sub-attributes using a data-driven approach and incorporates the attributes in data-driven fragility curves.

Table III.8: Description of VUQ Quality grade for different Data Applicability attributes

Attributes	**VUQ Quality – Grade**			
	4	**3**	**2**	**1**
Relevance [R]	Very High (direct)	High	Medium	Low
Scaling [S]	Prototypic (full-scale)	Adequately scaled	Medium	Inadequately scaled
Uncertainty [U]	Well-Characterized	Characterized	Medium	Poorly-Characterized

- **Validation Result:** It gives the accuracy of the simulation model compared to experimental model. Different types of validation metric can be adopted for evaluating the validation result [41]. In this study, we use two type of validation metric for comparing the probability density function (PDF) responses between simulation ($P_{sim}(y)$) and experiment ($P_{exp}(y)$) data: Overlapping Coefficient (OC) and Kullback-Leibler (KL) Divergence. OC is calculated by evaluating the percentage of overlapping area between two probability density curves and is

given by Eq (III.1).

KL divergence is a metric developed from information theory. It is based on the concept of entropy and is defined as a quantitative measure of uncertainty in a random variable. KL divergence of $P_{exp}(y)$ from $P_{sim}(y)$, denoted $D_{KL}(P_{sim}||P_{exp})$ and given by Eq (III.4), is a measure of the information lost by assuming that the distribution is $P_{exp}(y)$ when the true distribution is $P_{sim}(y)$. KL divergence is an asymmetric measure of the difference between two PDFs, i.e. $D_{KL}(P_{sim}||P_{exp}) \neq D_{KL}(P_{exp}||P_{sim})$.

Numerically, $D_{KL}(P_{sim}||P_{exp}) \geq 0$ and $D_{KL}(P_{sim}||P_{exp}) = 0$ if and only if $P_{sim} = P_{exp}$.

$$D_{KL}(P_{sim}||P_{exp}) = \int_{-\infty}^{\infty} P_{sim}(y) \ln \frac{P_{sim}(y)}{P_{exp}(y)} dy \tag{III.4}$$

In this study, we use a standardized symmetrize measure of KL divergence called J-divergence [12, 42] (see Eq. (III.5)), so that it can be compared with standardized measure of OC.

$$J = e^{-\lambda \times (D_{KL}(P_{sim}||P_{exp}) + D_{KL}(P_{exp}||P_{sim}))} \tag{III.5}$$

where, $\lambda > 0$. If $J = 0$, then there is no similarity between two PDFs and if $J = 1$, then the distributions are similar.

- **Code Adequacy:** Based on the validation result, code applicability evaluates the maturity of the simulation tool. The histogram of the validation metric is divided into 4 regions based on the maturity range given in Table III.9 and the percentage of the area in each region is computed.

Table III.9: Maturity levels for Code Adequacy

Maturity Level	**% of Area in Histogram of Validation metric**
Very Low (VL)	[0.0 0.1)
Low (L)	[0.1 0.4)
Medium (M)	[0.4 0.7)
High (H)	[0.7 1.0]

III.7 Illustrative Application Example for Code Applicability

In this section, we present a simple example of flooding risk assessment that illustrates the application of risk informed validation framework for assessment of adequacy of the simulation code. The synthetic example considered in this study is failure of diesel generator (DG) due to an external flooding event caused by a storm surge [14]. A failure of the DG occurs when the water level in the DG room due to vent overflow exceeds the height of the DG as shown in Figure III.12. In this study, we assume the fragility information for simulation model and data-driven model is directly available. Next, the code adequacy is evaluated by establishing data applicability and validation result for the given scenario.

Figure III.12: Diesel generator failure

Data Applicability: In this study, we assume two cases for maturity levels of R/S/U sub-attributes: (1) all the sub-attributes have high maturity, and (2) all the sub-attributes have very low maturity. High maturity corresponds to an experimental setup that is directly relevant to the given scenario, the setup is completely scaled, and the data is well characterized. Similarly, very low maturity indicates that the experimental data has very low relevance, inadequately scaled, and the data is poorly characterized.

Validation Result: The simulation-based and data-driven lognormal median fragility curves (i.e. without any epistemic uncertainty) for the DG failure event are shown in Figure III.13. For obtaining the validation metrics, the cumulative distribution function (CDF) fragility curves are converted into probability density function (PDF) curves. Then, OC is calculated using Eq. (III.1) and J-divergence, J is calculated using Eq. (III.5) with $\lambda = 1$ [12]. The values of obtained validation metrics are $OC = 0.61$ and $J = 0.21$. As J-divergence is standardized from symmetric KL divergence using an exponential function, it depends on value of λ chosen.

In order to evaluate the sensitivity of λ on J-divergence, we considered two Gaussian distributions with varying levels of overlapping area from 0% to 100%. For each of these cases, we obtained its corresponding J-divergence value. As there is no

guidance on choosing the λ value, the J-divergence is obtained based on different values of $\lambda = 0.2, 1, 5$. As seen in Figure III.14, the curves vary considerably with the λ value. If J-divergence is used, then the validation becomes very sensitive to the value of λ itself whereas the overlapping coefficient is much more stable and unique. J-divergence gives non-unique values when the validation is very good or very bad (extreme cases). Therefore, OC is used as the validation metric for rest of this study.

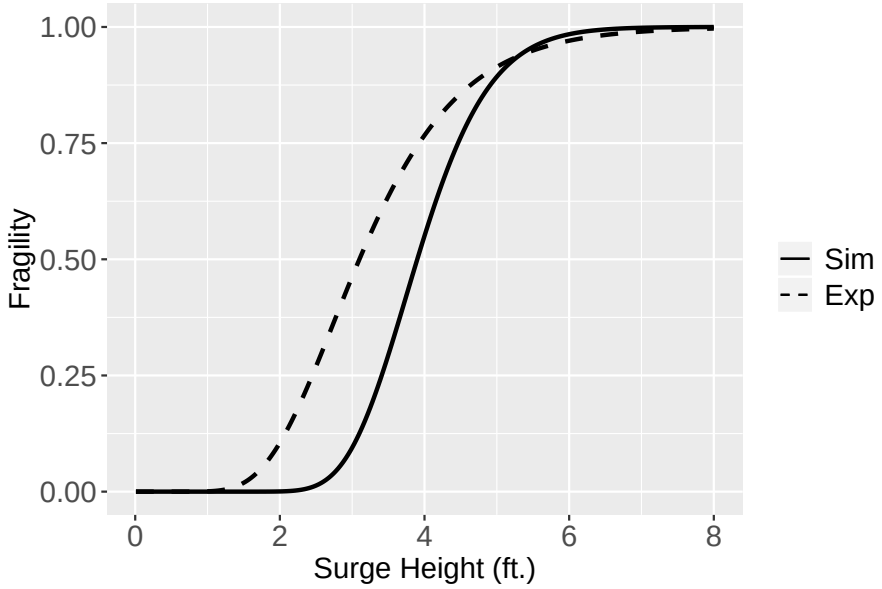

Figure III.13: Simulation and Data-driven (median) fragility curves

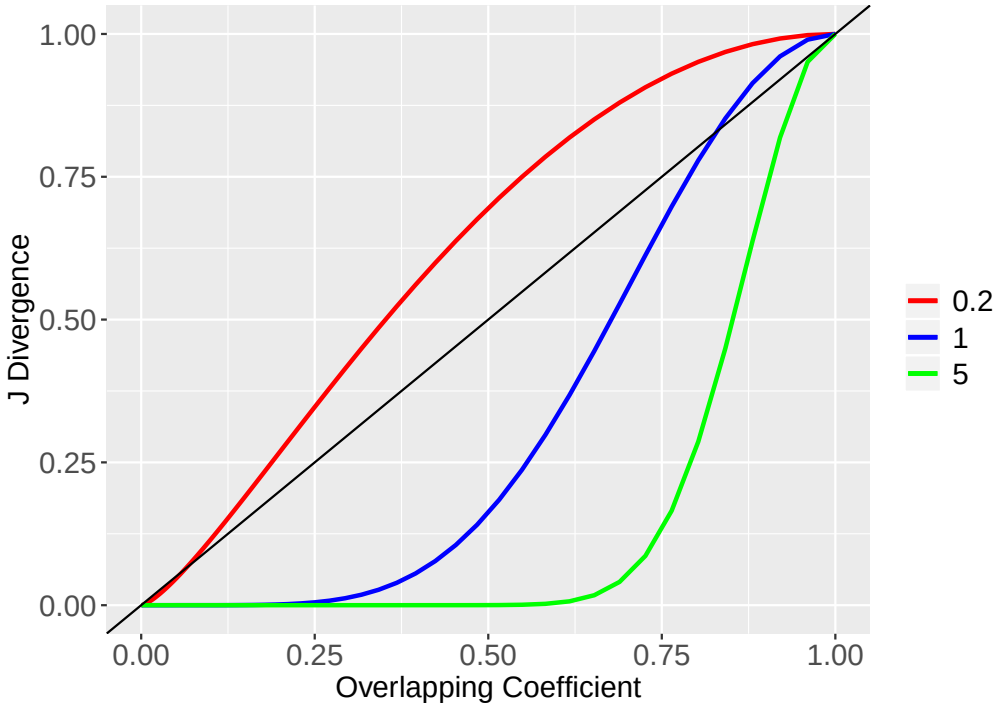

Figure III.14: Overlapping Coefficient vs J-Divergence

Next, epistemic uncertainty is included in simulation-based fragility by assuming a coefficient of variation of 0.1 for the simulation median capacity. Similarly, data-driven fragility curves are generated based on the maturity level of R/S/U attributes [14]. The simulation-based fragility curves by including epistemic uncertainty are shown in Figure III.15 and the data-driven fragility curves with high and very low maturity of data applicability are shown in Figure III.16. Then, OC is computed by taking multiple combinations of simulation and data-driven fragility curves. The histogram of obtained OCs for high and very low data applicability are shown in Figure III.17.

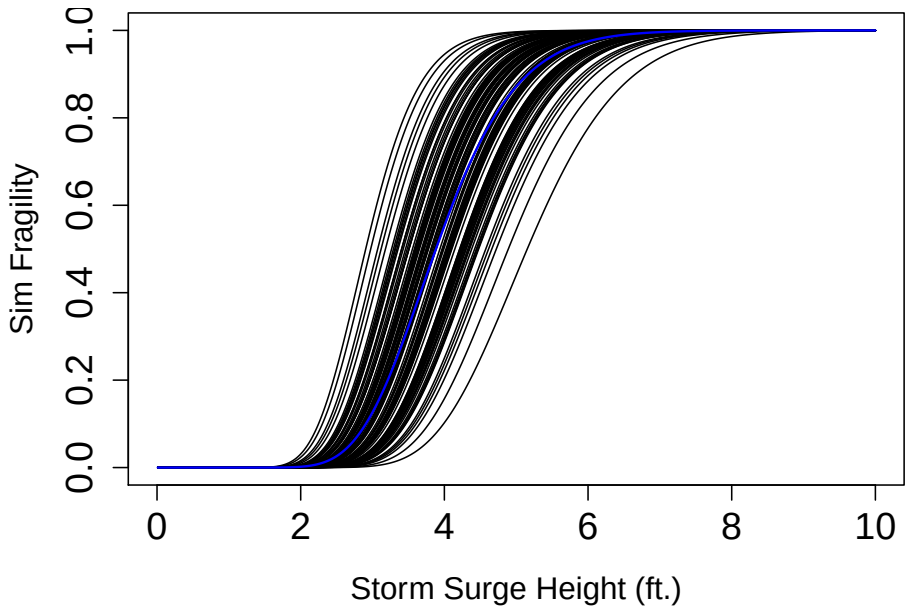

Figure III.15: Simulation-based fragility curves with epistemic uncertainty

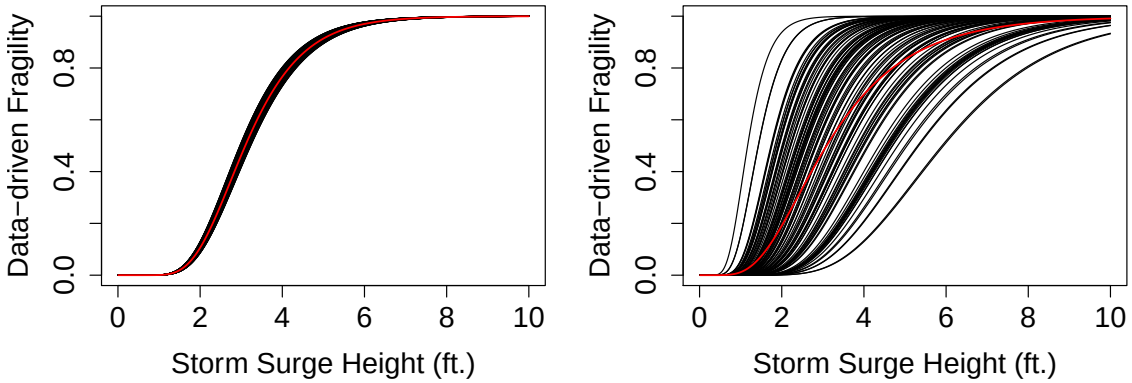

Figure III.16: Data-driven fragility curves with high (left) and very low (right) maturity of Data Applicability

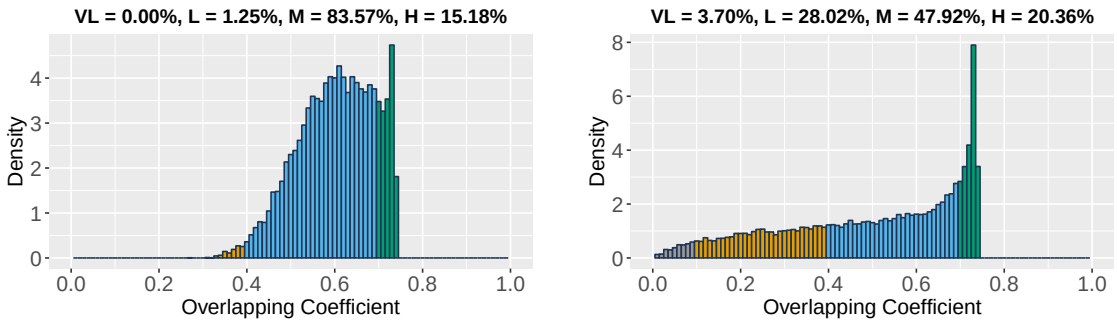

Figure III.17: Histogram of DG failure event Overlapping Coefficients with high (left) and very low (right) maturity of Data Applicability

Code Adequacy: For code adequacy, the histogram of OCs shown in Figure 16 is divided into 4 regions based on the maturity table given in Table III.8. Then, the percentage of overlapping area in the region corresponding to the maturity level is computed and assigned to the maturity level given in Table III.10. These values can be further used for decision making by assigning utilities to maturity levels [12, 27].

As seen in Figure III.17 and Table III.10, when the maturity of data applicability is high the uncertainty in the estimated OC is very low and has a standard deviation of 0.09. In this case, the code adequacy has a medium maturity of 83.57% because the mean value of the OC is 0.60 and the uncertainty in the data-driven fragility curves is very less.

Table III.10: Percentage of Maturity Levels for Code Adequacy

Code Adequacy *Maturity Level*	**Data Applicability**	
	High Maturity	*Low Maturity*
Very Low (VL)	0 %	3.70 %
Low (L)	1.25 %	28.02 %
Medium (M)	83.57 %	47.92 %
High (H)	15.18 %	20.36 %

For the case with very low maturity of data applicability and the uncertainty in simulation fragility being unchanged, the uncertainty in the estimated OC is high. In this case, the code adequacy has a high maturity of 20.36% and a low maturity of 28.02% which is greater than the case with high maturity of data applicability (15.18% and 1.25%). This is because we are uncertain about the estimated median capacity of data-driven fragility when the maturity of data applicability is very low. Therefore, in the enhanced risk informed validation framework, code adequacy reflects the maturity of data applicability in the maturity of the overall validation which gives confidence in the decision making.

III.8 Summary and Conclusions

This study focuses on the enhancement of existing risk informed validation framework to assess the system-level validation. In this methodology, we propose two major enhancements to the framework by developing a new set of validation metric (consistency index) and an additional attribute (Code adequacy) for making the

framework more robust. In this study, the methodology to identify the critical path that leads to system-level failure is illustrated using a seismic case study. The overall validation is assessed for completeness and consistency by comparing the critical path for both the system-level simulation and data-driven models. The interpretation of consistency index in the risk informed framework is illustrated for various cases of building piping system failure. For obtaining an accurate estimate of overlapping coefficient for the system-level failure, all the events on the critical path have to be consistent. The adequacy of the simulation code for an intended application depends on two attributes: validation result and data applicability. The code applicability evaluates the maturity of simulation tool based on the validation result and helps in the process of decision making. The key conclusions of this study are summarized as follows:

- The critical path in a Bayesian network is identified by using extended definition of Fussell-Vesely (FV) Importance measure for Bayesian networks.
- The risk informed validation framework by Kwag et al. [13] and Bodda et al. [14] can give inconsistent results if the identified critical events are not consistent.
- Introduces the concept of consistency index (δ) in the validation metric which ensures that the simulation and data-driven fragilities correspond to the same set of critical events.
- Overlapping coefficient is used as the standardized validation metric.
- The existing risk informed validation framework is enhanced by incorporating the concept of maturity levels to assess the decision regarding the adequacy of a simulation code for an intended application.

PART IV

Assessment of Risk Informed Validation Framework to a Real Life Like Application – Sunny Day Dam Failure

IV.1 Introduction

External hazards act as initiators of severe accidents in nuclear plants and as experienced in Fukushima-Daiichi nuclear disaster, it is necessary to improve our understanding of the accident sequence of events to appropriately assist decision makers. In this context, studies [12, 13, 14, 27] have shown that significant uncertainties exist in the predictive capability of advanced simulation codes to evaluate the risk assessments. The range of applicability of a simulation code is assessed by the physics and the models it contains. Verification, Validation, and Uncertainty Quantification (VVUQ) are the three ongoing active research areas in which these processes help to assess the adequacy of simulation models in predicting the risk assessments over the range of an intended application and the uncertainty associated with those predictions. One of the major challenges in validation is related to lack of relevant experimental data and lack of confidence in the applicability of simulation models. This leads to excessive reliance on human judgment and conservative assumptions in the safety assessment of nuclear plants. The motivation of this study is to develop a robust risk informed framework for validation of advanced simulation codes with a probabilistic criterion for adequate level of validation.

The proposed risk informed validation framework in this study aims to build upon the USNRC's regulatory guide 1.203 [10] on "Transient and Accident Analysis Methods," also known as Evaluation Model Development and Assessment Process (EMDAP). As a result, the existing risk informed validation framework presented in Part II and Part III is mapped into the four elements of EMDAP framework. The integrated risk informed EMDAP framework is used for estimating the degree of

validation (or credibility) in simulation-based risk estimates for the given external hazard scenario. As the experimental data is expensive and usually not available for an intended application, we have to make use of the data that we have or can obtain from existing and related studies. The quality of experimental data that is based on expert knowledge is incorporated in the quantification process using a data-driven methodology [14]. Then, the integrated risk informed EMDAP framework is used as the basis for validation data planning and to identify the events that require new experiments in the context of safety assessment.

In this manuscript, we evaluate the applicability of risk informed validation framework to a more complex flooding scenario that corresponds to real life like application of sunny day dam failure [43]. This paper combines the risk informed methodologies by Kwag et al. [13], Part II and Part III of this dissertation. In addition, such an application would require integration of the performance-based risk informed methodology into EMDAP framework. In the risk informed validation framework, the system-level validation is evaluated based on fragility estimates of structures, systems and components (SSCs). However, in a complex flooding scenario there are a few non-physical events such as "warning time upon protective dike failure" and "random failure of boron system" that are not sensitive to details of hydrodynamics and fragility modeling but are required for the probabilistic risk assessment (PRA). Therefore, in the risk-informed validation framework we propose a new methodology to handle the events that are not physics based. As the event tree resulting from the realistic flooding scenario contains many SSCs, we evaluate the importance rankings of SSCs to determine the set of events which are critical from a perspective of system-level safety or performance. For the identified critical events, we develop the assessment base for

the performance-based Quantities of Interest (QoI) and generate data-driven fragility curves. For the non-critical events, we assume the data-driven fragility estimates are same as the simulation-based fragility estimates. The framework uses Bayesian inference to identify the evaluation models that needs to be enhanced so that the reduction in uncertainties will help improve the overall confidence in risk-estimates.

IV.2 Summary of Performance-Based Risk Informed Validation Frameworks

The recent frameworks that are based on a risk consistent approach for validation particularly in the context of external hazard PRA are Kwag et al. [13], Bodda et al. [14], and Part III. Kwag et al. [13] uses a seismic case study and Bodda et al. [14] a flooding case study to illustrate the application of the methodology. Kwag et al.'s [13] methodology employs Bayesian network for propagation of fragilities from component-level to system-level and assess the degree of validation using overlapping coefficient and point estimate. Overlapping coefficient is simply defined as the percentage of overlapping area between two probability density curves. However, Kwag et al.'s [13] approach to flooding PRA is restricted due to a lack of relevant experimental data for flooding failures. Bodda et al. [14] developed a data-driven approach to quantify the quality of experimental data used for generating data-driven (or experimental) fragility curves in terms of three attributes: Relevance, Scaling, and Data uncertainty (R/S/U). Relevance reflects the degree of applicability of experimental data from existing studies to the current application. Scaling uncertainty incorporates both geometric and physics scaling uncertainties. Data uncertainty reflects the uncertainty in the measured data. Also, Bodda et al. [14] expressed the credibility of overall validation by using a probabilistic distribution rather than a point estimate.

Part III enhanced the risk informed methodology by considering an additional validation index called consistency index that ensures the system-level validation is complete and consistent. In the enhanced methodology, the assessment of decision regarding the adequacy of a simulation code is represented by four maturity levels (very low, low, medium, and high).

The key steps involved in the existing risk informed methodology are listed below:

- Construct an event tree/fault trees corresponding to an initiating external hazard such as flooding or seismic.
- Develop component-level simulation-based fragility curves and map event tree/fault tree into a Bayesian network.
- Evaluate system-level and intermediate-level simulation-based fragilities by propagating fragilities from basic events through the Bayesian network.
- Identify experimental data at component-level and establish maturity level for R/S/U attributes. Obtain system-level data-driven fragility curves by propagating data-driven fragilities from basic events through the Bayesian network.
- Identify critical path for both the simulation and data-driven models. If the critical path is same ($\delta = 1$), then compute the validation metric for the system-level validation.
- If the critical path is different or validation metric does not satisfy the desired acceptance criterion, then conduct high-fidelity simulations or collect additional experimental data for the critical events.
- Represent the adequacy of overall validation in terms of various maturity levels.

IV.3 Integration of Risk Informed Validation Methodology with EMDAP

In 2005, USNRC Regulatory Guide 1.203 [10] introduced Evaluation Model Development and Assessment Process (EMDAP) which is a systematic process to confirm the adequacy of a particular code for analyzing transient and accident behavior that is within the design basis of a nuclear power plant. The complete EMDAP framework is illustrated through the flowchart shown in Figure IV.1. The key steps involved in the EMDAP process are listed below:

- Identification of analysis purpose, figures of merit (FOM), mathematical modeling methods, components, phenomena, and physical processes.
- Hierarchical breakdown of systems, phenomena and process.
- Development of an experimental database comprising of Separate Effect Test (SETs) and Integral Effect Test (IETs). Scaling and applicability analysis of test facilities and models.
- Development of evaluation model (EM) with state-of-the-art modeling tools and algorithms.
- Assessment of EM models adequacy using a two-tier review process (top-down and bottom-up). The bottom-up approach focuses on the fundamental building blocks of the code in which closure and correlation models are evaluated by considering their fidelity to fundamental or SET data, and scalability. The top-down approach focuses on capabilities and performance of the EM in which field equations and numeric solutions are evaluated by considering their fidelity to component or IET data, and scalability.
- Characterization of EM bases and uncertainties.

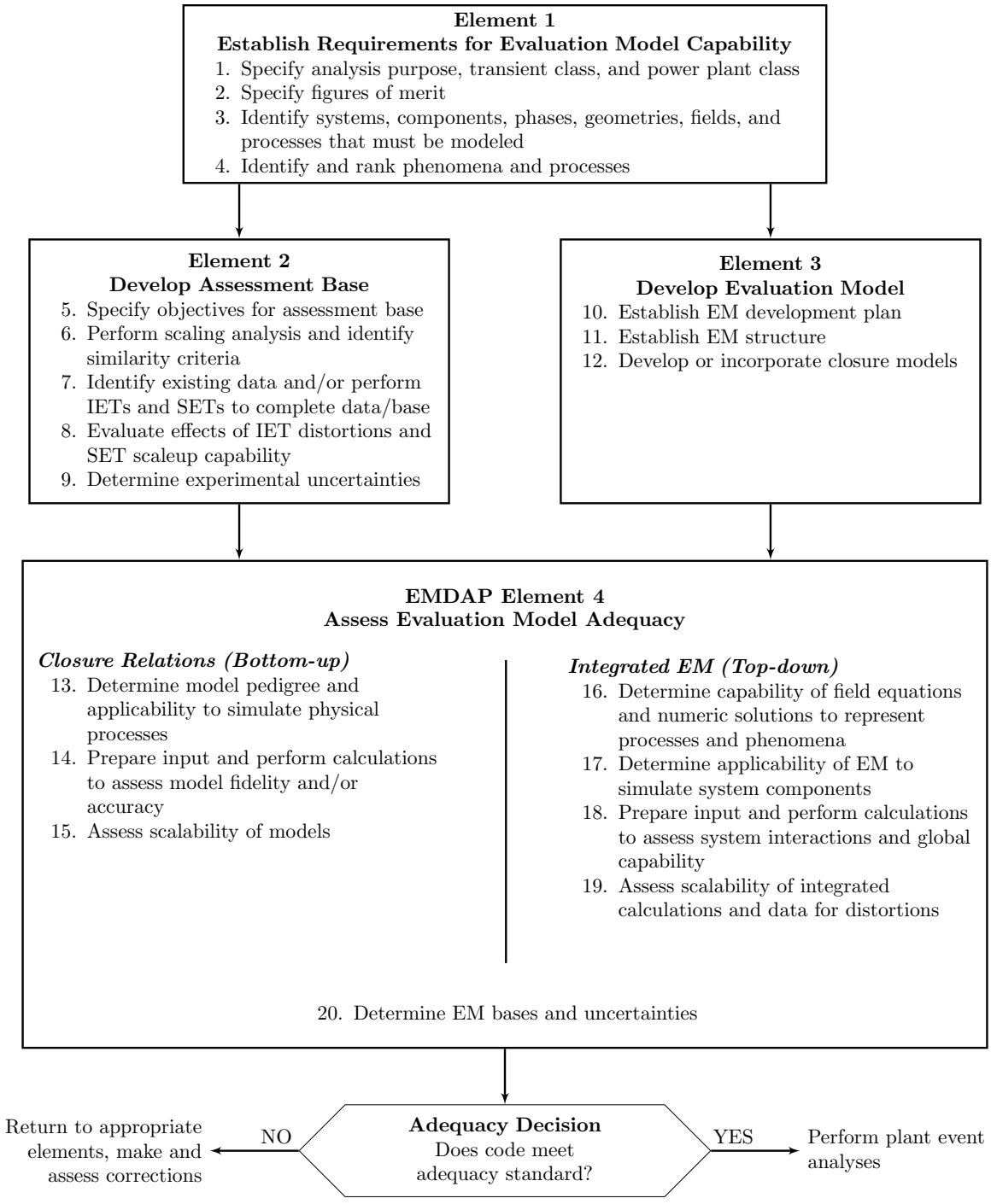

Figure IV.1: EMDAP Framework [10]

Though EMDAP is a quite powerful framework with a comprehensive structure, the decision process for the validation of simulation codes is not formalized and the epistemic uncertainty can be easily overlooked [27]. Therefore, in this study, we integrate the risk informed validation framework with EMDAP to quantify all the information and formalize the process, which turns to be much less heuristic. The integrated risk informed EMDAP framework is illustrated through the flowchart shown in Figure IV.2. The integrated framework employs four key elements that are described below:

Element 1: Establish Requirements for Evaluation Model Capability

- Develop an event tree to represent all possible accident scenarios resulting from an initiating external hazard.
- Construct the corresponding fault trees for the top events in the event tree.
- Map the fault trees and the event tree into a Bayesian network using a mapping algorithm.
- Characterize failure in terms of performance function.
- Identify critical events with respect to system vulnerability using importance measures.

Element 2: Develop Assessment Base

- Collect experimental data at component level (SETs) and sub-system level (IETs) for the identified critical events.
- Establish the quality of experimental data based on Relevance, Scaling, and Data uncertainty (R/S/U) attributes.

Element 3: Develop Evaluation Model

- Develop performance-based simulation fragility curves for all the basic events and data-driven fragility curves for the identified critical events. In general, fragility assessment requires use of a Monte Carlo approach to include uncertainties from various sources. However, if sufficient knowledge base has been developed then one can make use of the standard lognormal fragility parameters.

Element 4: Assess Evaluation Model Adequacy

- For bottom-up approach, propagate fragility information from basic events to intermediate-level and system-level through the Bayesian network. Then, calculate overlapping coefficient and consistency index based on simulation and data-driven fragility curves for the events along the critical path.
- For top-down approach, the evaluation models that needs to be improved are identified by specifying the acceptance criterion of overall validation to be 100% of high maturity. If additional data becomes available at higher levels, then update the fragility curves and the subsequent OCs using Bayesian inference.

Decision

- If all the events on the critical path are consistent then compare system-level overlapping coefficient with a predefined acceptance criterion.
- If the adequacy of system-level validation is not satisfied collect more experimental data or improve evaluation (simulation or data-driven) models of the identified critical events.

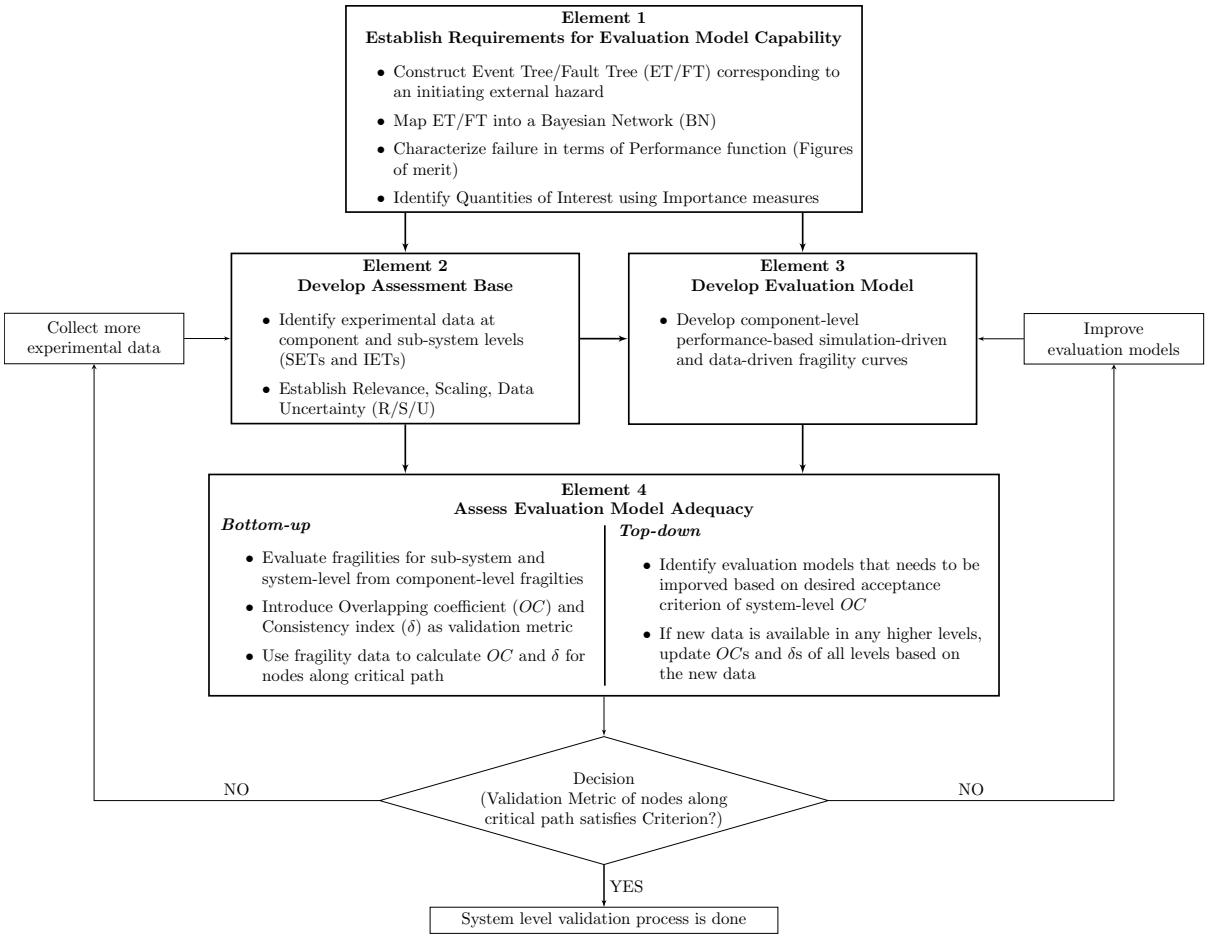

Figure IV.2: Integrated Risk informed EMDAP framework

IV.4 Realistic Scenario – Sunny Day Dam Failure

The realistic scenario we considered in this study is based in part of the NRC Working Example Template [43]. The layout of the plant is shown in Figure IV.3. The scenario begins with a sunny day dam break upstream of a Pressurized water reactor (PWR) nuclear plant situated in a typical riverine environment. The release of water due to dam break acts as an external flooding at the plant. The plant has a dike along the riverbank for basic flood protection. If the plant has at least 8 hours notification time

prior to flood arrival, it is assumed that the plant will be successful in achieving hot shutdown; otherwise, the plant must contend with external flooding (EF) site conditions of the plant during shutdown. During the flood event, all the key safety functions such as maintaining onsite power, reactivity control, reactor cooling, and reactor pressure should be in a safe stable state. If the safety functions are working properly and there is a sufficient warning time before the landscape flooding occurs, the operators will test and align the severe flood management system (SFMS) for the external flooding. Then, the atmospheric dump valves (ADVs) are opened to reject steam to the atmosphere. If the ADVs are not able to be opened or prevented from reclosing, the main steam safety valves (MSSVs) will be opened to create an alternate path for steam rejection and secondary side heat removal. The SFMS will be placed into service by providing power and water to the plant. If the normal plant equipment is lost due to flooding, then the decay heat removal (DHR) will need to be transferred to the steam generator (SG) from the DHR system. If the SFMS continues to remove decay heat, the plant will be in a safe stable state and the post flood procedures will be implemented [43].

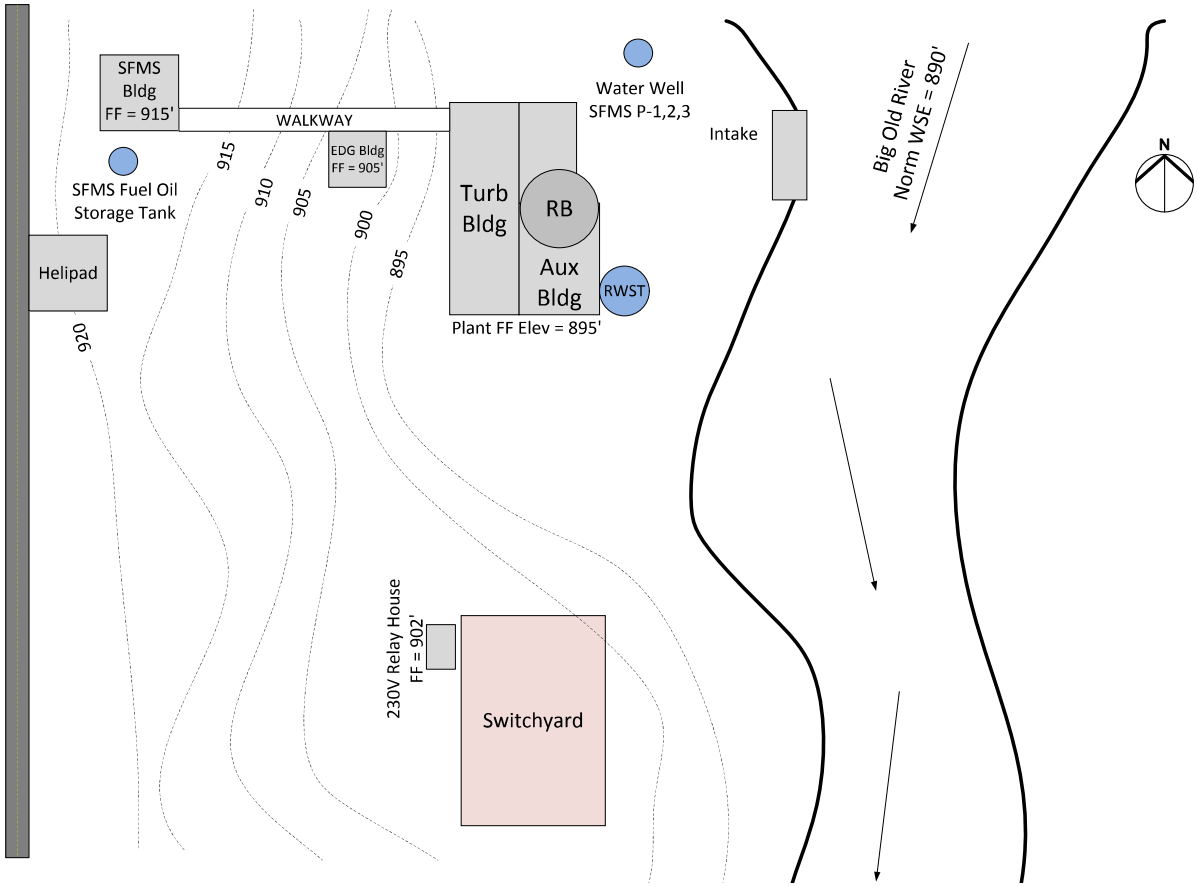

Figure IV.3: Plant Layout [43]

IV.4.1 Event Tree / Fault Tree Logic

The event tree resulting from this realistic example is shown in Figure IV.4 and it includes the following top events:

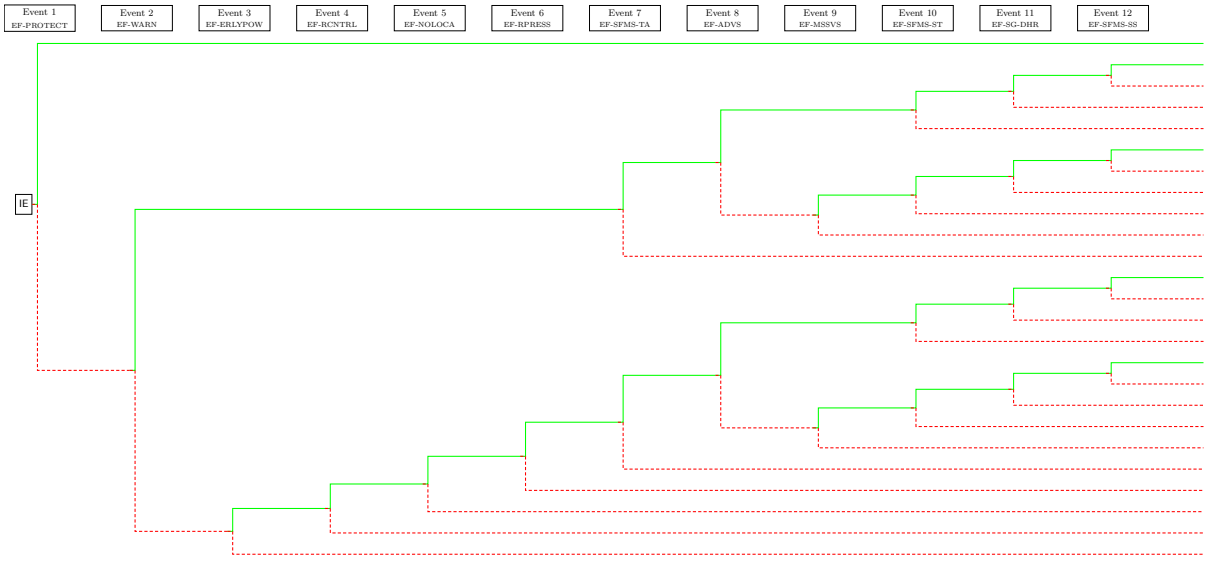

Figure IV.4: Event Tree logic for the Sunny Day Dam failure

Initiating Event: Sunny-Day Dam Break

The initiating event is an external flooding (EF) event due to a sunny day dam break. The failure of the dam is not due to any external event such as an extreme flood or an earthquake but may result from a structural or operational deficiency on a normal sunny day [44].

Event 1: EF-PROTECT

The protective dike is effective in preventing an EF event at the plant and this top event is further decomposed into a fault tree as shown in Figure IV.5. The protective dike is lost if the dike overtops (***E1–B1***) or if the dike collapses due to structural failure

(***E1–B2***).

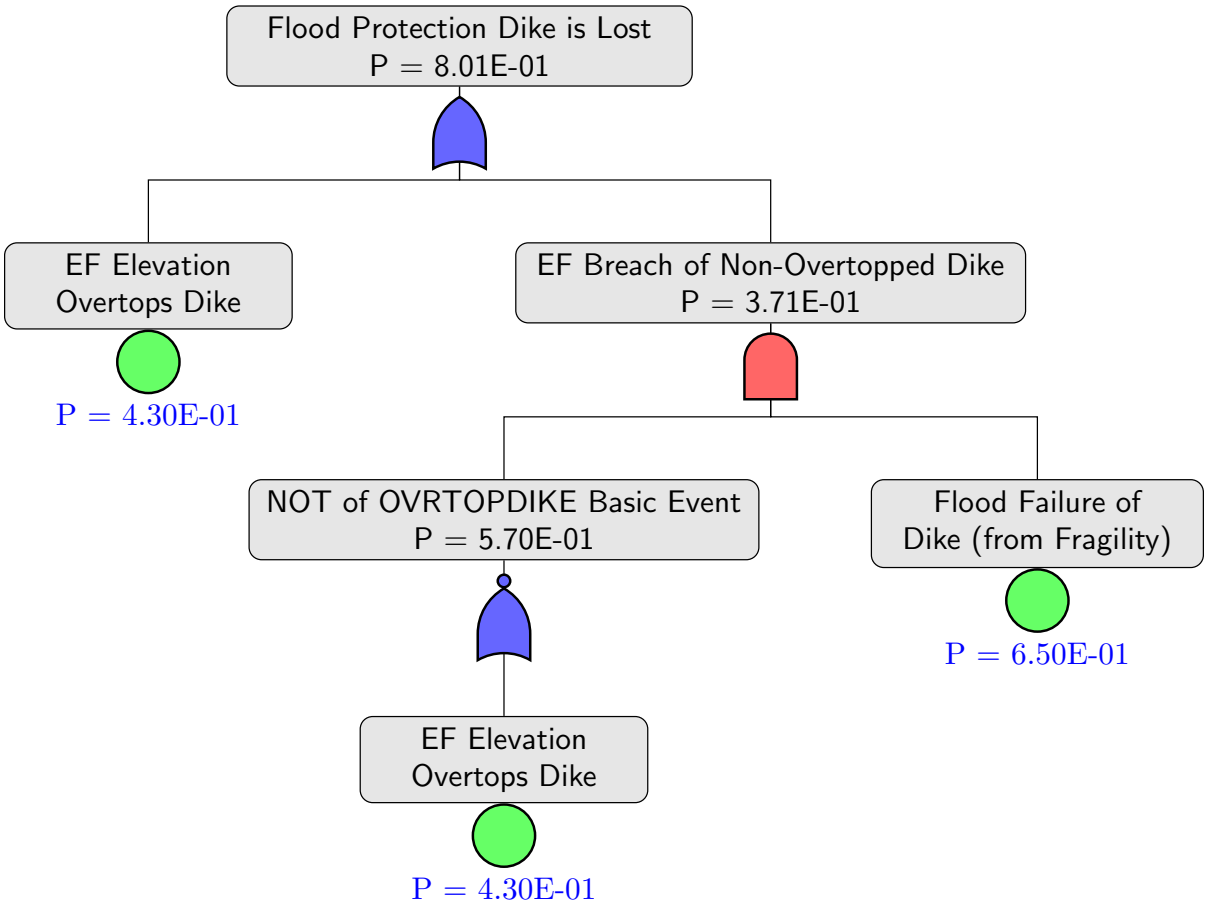

Figure IV.5: Fault Tree of Event 1: EF-PROTECT

Event 2: EF-WARN

EF-WARN describes the event in which at least 8 hours notification time prior to the protective dike being lost has been given. This event determines if the plant hot shutdown occurs prior to the flood arrival or if the plant shutdown process must cope with the landscape flooding.

Event 3: EF-ERLYPOW

This event determines if the onsite power can be maintained until hot shutdown of the plant is achieved. EF-ERLYPOW top event is further decomposed using a fault tree to obtain its failure probability as shown in Figure IV.6 and it includes the following basic events:

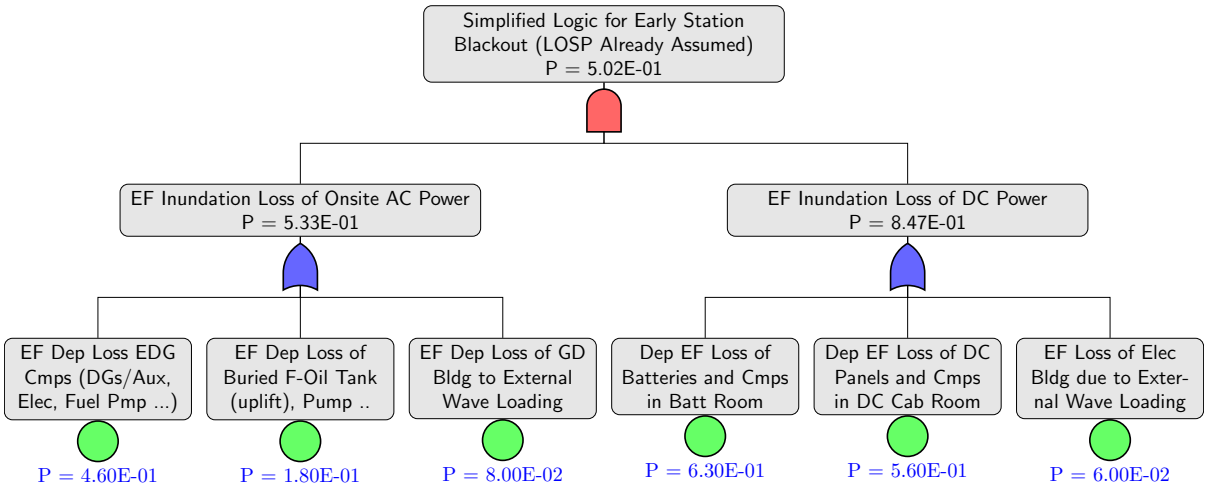

Figure IV.6: Fault Tree of Event 3: EF-ERLYPOW

- ***E3–B1:*** Failure of dependent emergency diesel generators (EDGs) and their auxiliaries, control panels, fuel pumps, etc. due to flooding inundation
- ***E3–B2:*** Failure of buried diesel tanks due to hydrostatic forces (uplift and/or shell wall buckling)
- ***E3–B3:*** Partial or complete failure of EDG building due to external wave loading and related effects
- ***E3–B4:*** Dependent loss of batteries and equipment in battery rooms occur upon flooding inundation
- ***E3–B5:*** Dependent loss of DC cabinets and related components in the DC Panel room occurs upon flooding inundation

- ***E3–B6:*** Partial or complete failure of electrical building due to external wave loading and related effects

Event 4: EF-RCNTRL

This event determines if the reactivity control is established and maintained. EF-RCNTRL top event is further developed into the fault tree as shown in Figure IV.7 and it includes the following basic events:

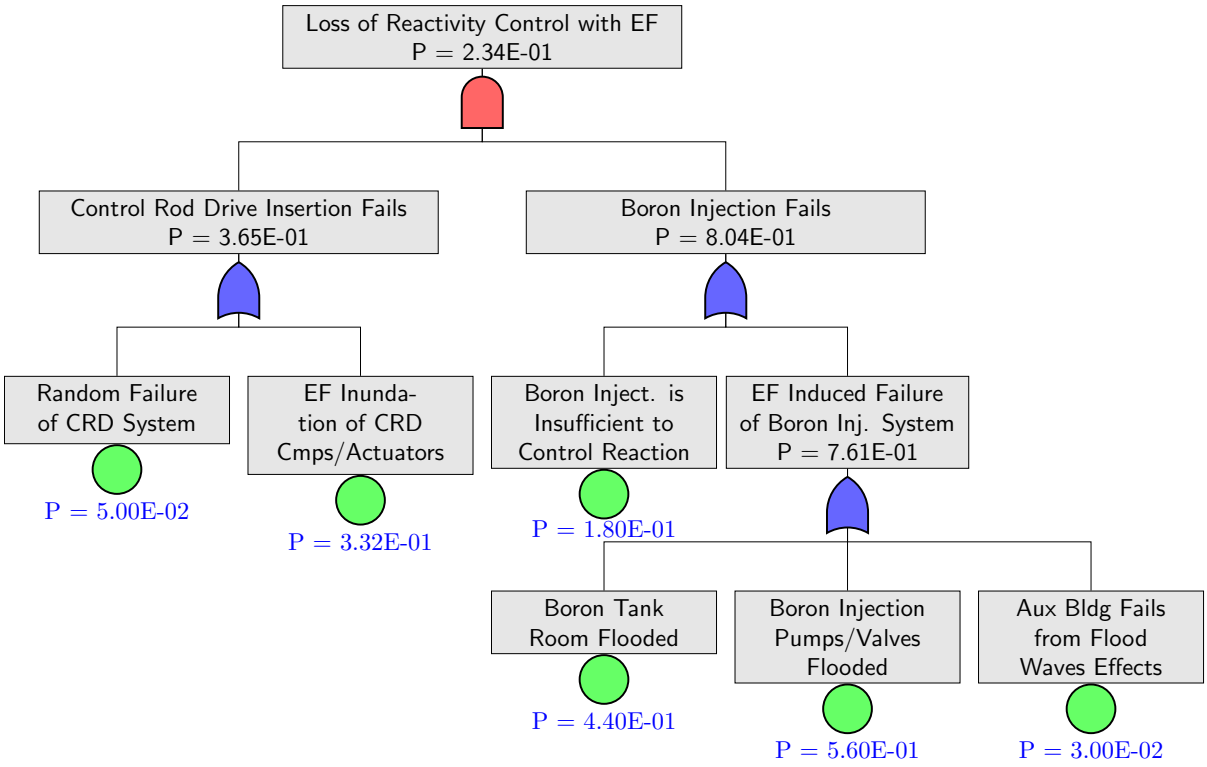

Figure IV.7: Fault Tree of Event 4: EF-RCNTRL

- ***E4–B1:*** Random failure of control rod drive (CRD) insertion
- ***E4–B2:*** Dependent loss of CRD actuators and/or related CRD component auxiliaries fail upon flooding inundation
- ***E4–B3:*** Random failure of boron system

- ***E4–B4:*** Borated water storage tank, related instrumentation and components are disabled with flooding inundation
- ***E4–B5:*** Flooding inundation of pumps/valves of the boron delivery system
- ***E4–B6:*** Partial or complete failure of auxiliary building due to external wave loading and related effects

Event 5: EF-NOLOCA

This event determines that no loss-of-coolant accident (LOCA) occurs and the reactor inventory control is achieved. EF-NOLOCA top event is further developed into the fault tree as shown in Figure IV.8 and it includes the following basic events:

- ***E5–B1:*** Failure of refueling water storage tank (RWST) due to impact from a large or sharp water-born missile
- ***E5–B2:*** Flooding inundation of reactor coolant system (RCS) charging pumps
- ***E5–B3:*** Flooding inundation of motor operated valves of the RCS
- ***E5–B4:*** Flooding inundation of high-pressure (HP) pumps that injects water to the primary system
- ***E5–B5:*** Flooding inundation of motor operated valves of the HP injection system
- ***E4–B6:*** Partial or complete failure of auxiliary building due to external wave loading and related effects
- ***E5–B6:*** Operators fail to recover a stuck-open pressurizer relief valve (PRV)
- ***E5–B7:*** A PRV sticks open

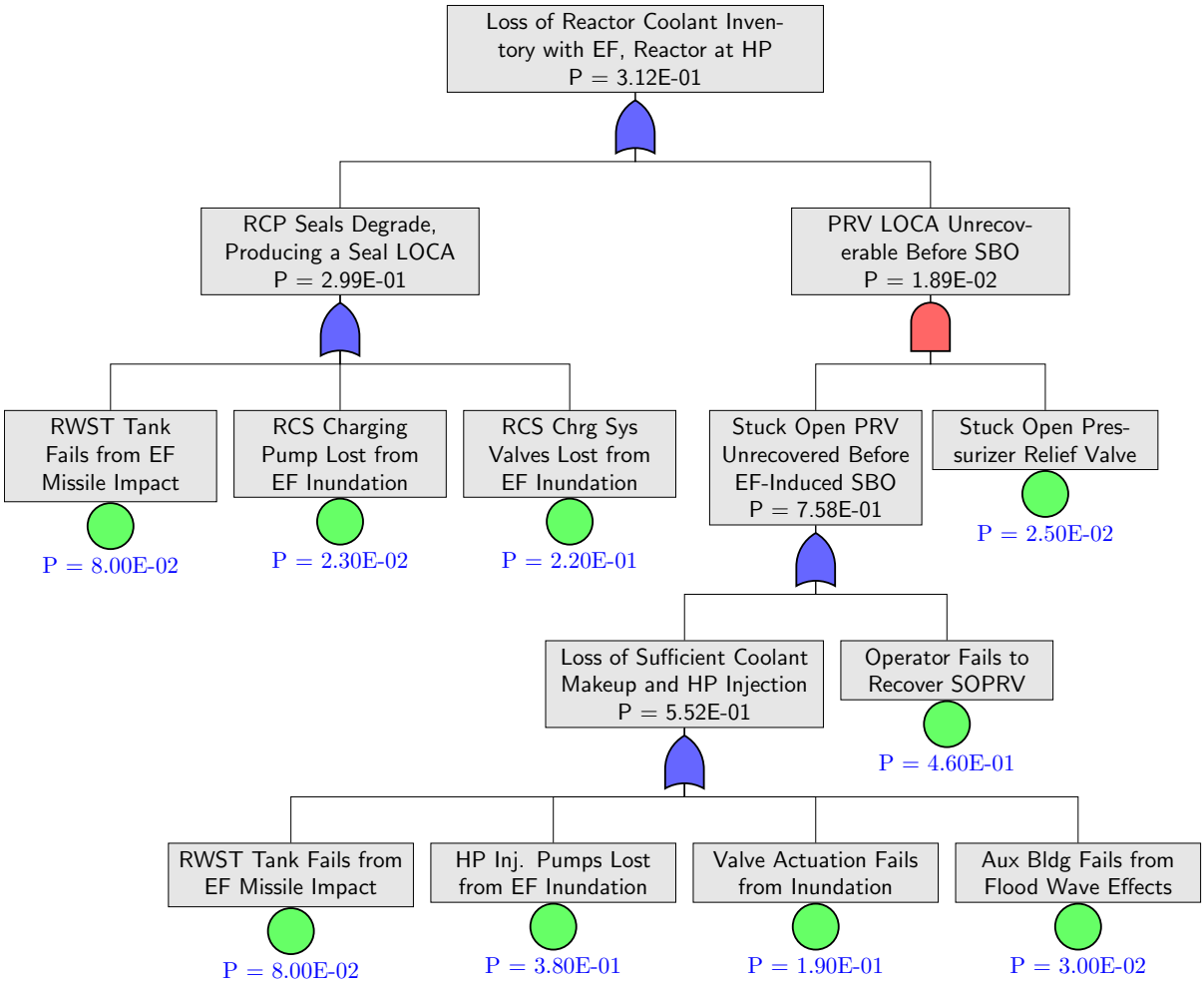

Figure IV.8: Fault Tree of Event 5: EF-NOLOCA

Event 6: EF-RPRESS

This event determines that the reactor pressure control is achieved to depressurize the reactor, supply makeup water, and initiate and maintain the residual heat removal (RHR) function through completion of the hot shutdown process. EF-RPRESS top event is further developed into the fault tree as shown in Figure IV.9 and it includes the following basic events:

- ***E5–B1:*** Failure of refueling water storage tank (RWST) due to impact from a

large or sharp water-born missile

- ***E6–B1:*** Flooding inundation of low-pressure (LP) pumps that injects water to the primary system
- ***E5–B5:*** Flooding inundation of motor operated valves of the LP injection system
- ***E4–B6:*** Partial or complete failure of auxiliary building due to external wave loading and related effects
- ***E6–B2:*** Random malfunction of PRV

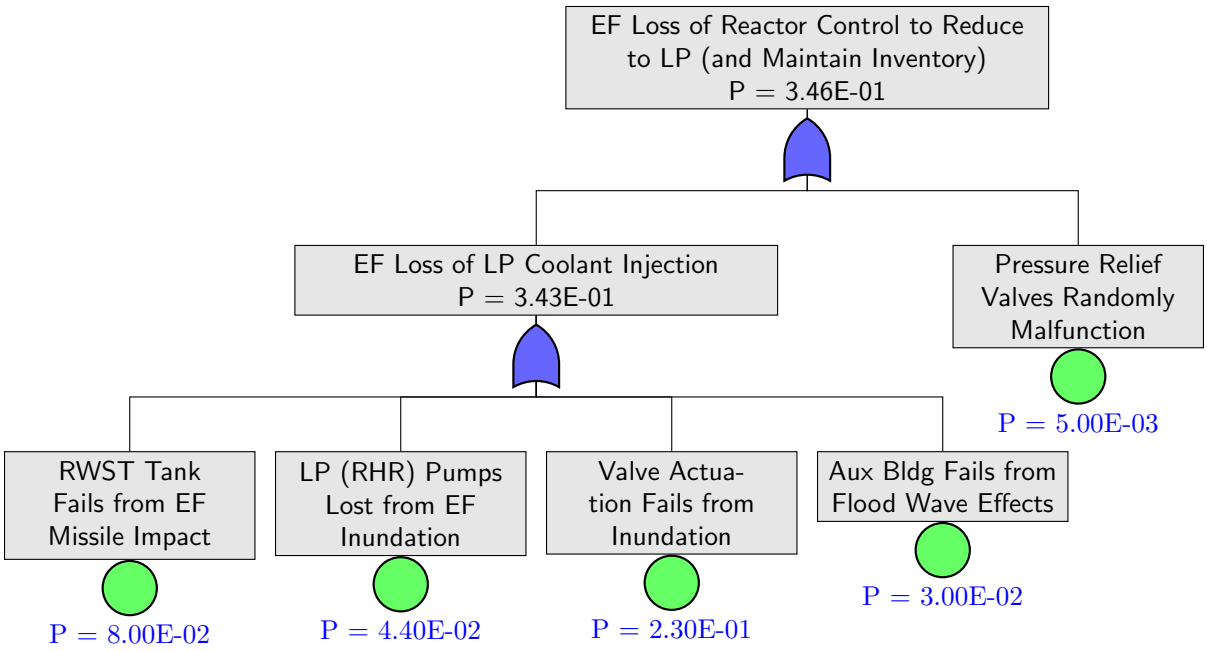

Figure IV.9: Fault Tree of Event 6: EF-RPRESS

Event 7: EF-SFMS-TA

This event determines the testing and aligning of the severe flood management system (SFMS) for the external flooding.

Event 8: EF-ADVS

This event determines that the atmospheric dump valves (ADVs) are opened to reject steam to the atmosphere. EF-ADVS top event is further developed into the fault tree as shown in Figure IV.10 and it includes the following basic events:

- ***E8–B1:*** Random failure of the ADVs and their needed configuration
- ***E8–B2:*** Partial or complete failure of turbine building due to potential adverse flood effects

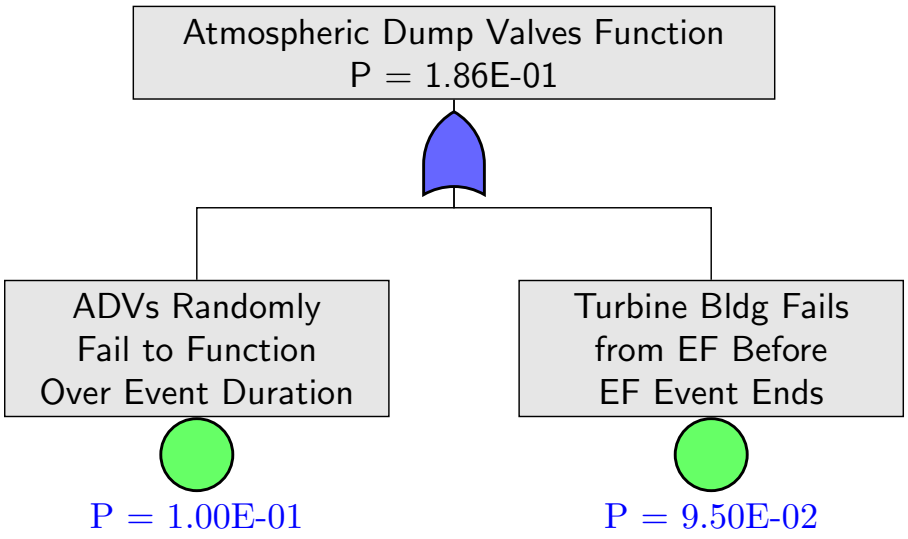

Figure IV.10: Fault Tree of Event 8: EF-ADVS

Event 9: EF-MSSVS

This event determines that the main steam safety valves (MSSVs) will be opened to create an alternate path for steam rejection and secondary side heat removal. EF-MSSVS top event is further developed into the fault tree as shown in Figure IV.11 and it includes the following basic events:

- ***E9–B1:*** Random failure of the main safety steam valves (MSSVs) and their needed

configuration

- ***E8–B2:*** Partial or complete failure of turbine building due to potential adverse flood effects

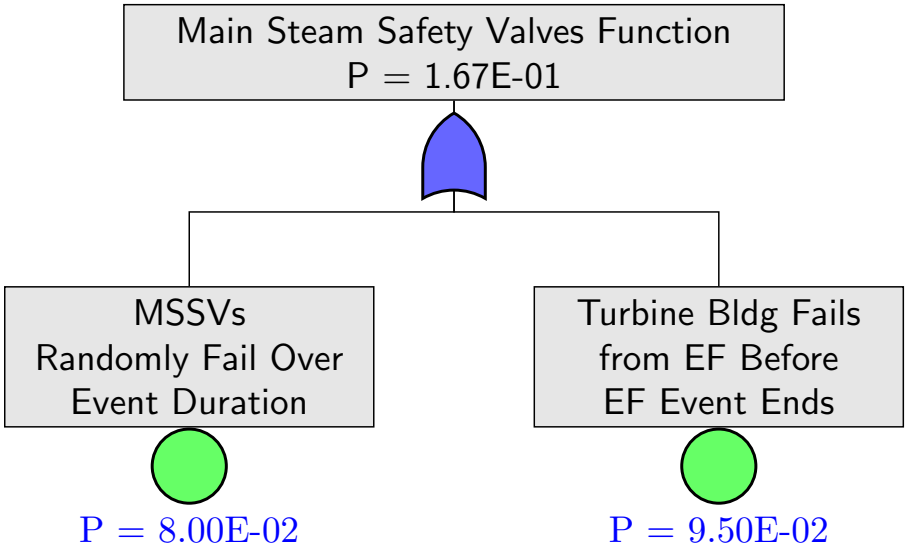

Figure IV.11: Fault Tree of Event 9: EF-MSSVS

Event 10: EF-SFMS-ST

This event determines if the SFMS provides power and water to the plant.

Event 11: EF-SG-DHR

This event determines if the decay heat removal (DHR) system transfers decay heat to the steam generator.

Event 12: EF-SFMS-SS

This event determines if the SFMS continues to remove the decay heat and maintains the plant in a safe stable state.

IV.5 Application of Integrated Risk Informed EMDAP Framework

In this section, we illustrate the application of the integrated framework to the realistic flooding scenario described in section IV.4. The flooding scenario consists a total of 12 top events in the event tree and 26 unique basic events in the fault trees. In this scenario, there are a total of 5 top events and 7 basic events that are due to random or operational failures as shown below:

Top Events

- *Event 2:* Warning Time Upon Dike Failure
- *Event 7:* Severe Flood Management System (SFMS) Test & Alignment
- *Event 10:* SFMS Startup with EF
- *Event 11:* DHR via SG with EF
- *Event 12:* SFMS maintains Plant in a safe, stable state with EF

Basic Events

- *E4–B1:* Random failure of control rod drive insertion
- *E4–B3:* Random failure of boron system
- *E5–B6:* Operators fail to recover a stuck-open pressurizer relief valve (PRV)
- *E5–B7:* A PRV sticks open
- *E6–B2:* Random malfunction of pressurizer relief valve
- *E8–B1:* Random failure of the ADVs and their needed configuration
- *E9–B1:* Random failure of the MSSVs and their needed configuration

In a validation point of view, these non-physical events are not sensitive to the

details of hydrodynamic and fragility modeling. Therefore, in the integrated framework we categorize the non-physical events into the following two cases so that they are not critical in the validation process.

- Case 1: Treating non-physical events as completely safe
- Case 2: Treating non-physical events as completely fail

The failure probability of the non-physical events remains the same for all the intensity measures of flood height. In this study, we assume that the simulation fragility information for all the physics-based basic events is directly available. The critical events are obtained based on the simulation fragility curves. The data-driven fragility parameters are assumed only for the identified critical events. For all the non-critical events, we consider the data-driven fragility parameters to be same as the simulation-based fragility parameters. Table IV.1 gives the lognormal simulation-based fragility parameters for all the events and Table IV.2 gives the lognormal data-driven fragility parameters for all the critical events. In addition to the data-driven fragility parameters, we also assume that the grade quality of experimental data for the critical events is directly available.

Table IV.1: Simulation-based lognormal fragility parameters of basic events ($\hat{\lambda}$ = Median, β_{AU} = Lognormal standard deviation)

BASIC EVENT	$\hat{\lambda}$ $(ft.)$	β_{AU}
E1–B1	8.10	0.15
E1–B2	7.82	0.25
E3–B1	5.08	0.15
E3–B2	6.29	0.25
E3–B3	11.62	0.60
E3–B4	4.84	0.10
E3–B5	4.91	0.12
E3–B6	11.58	0.54
E4–B1	Non-physical event	
E4–B2	5.41	0.18
E4–B3	Non-physical event	
E4–B4	5.15	0.20
E4–B5	4.89	0.15
E4–B6	9.13	0.32
E5–B1	13.37	0.70
E5–B2	8.40	0.26
E5–B3	5.84	0.20
E5–B4	5.32	0.20
E5–B5	5.96	0.20
E5–B6	Non-physical event	

Table IV.1: Continued

BASIC EVENT	$\hat{\lambda}$ $(ft.)$	β_{AU}
E5–B7	Non-physical event	
E6–B1	6.80	0.18
E6–B2	Non-physical event	
E8–B1	Non-physical event	
E8–B2	6.23	0.38
E9–B1	Non-physical event	

Table IV.2: Data-driven lognormal fragility parameters and Epistemic uncertainty (maturity) of critical events

Basic Event	$\hat{\lambda}$ $(ft.)$	β_{AU}	**Data Applicability**	**Simulation Uncertainty**
E1–B1	9.17	0.30	High Maturity	Medium Maturity
E1–B2	7.30	0.40	High Maturity	Medium Maturity
E8–B2	8.50	0.30	Medium Maturity	High Maturity

IV.5.1 Case 1: Treating non-physical events as completely safe

The event tree resulting from case 1 is shown in Figure IV.12. The failure probability of all the non-physical events is equal to 0 for all the intensity measures of flood height. The identified critical event in this case is "partial or complete failure of turbine building due to potential adverse flood effects" that corresponds to the basic event in the fault

trees of *Event 8: EF-ADVS* and *Event 9: EF-MSSVS*. The simulation-based fragility curves for the system-level event and the top events are shown in Figure IV.13. The *OC* for the system-level has a high maturity of 30.36% and medium maturity of 69.53% as shown in Figure IV.14. The adequacy of the code for the overall validation would be unacceptable if an acceptance criterion of 100% of high maturity is adopted. Therefore, we have to improve the system-level validation by either enhancing the simulation model or collecting additional experimental data for the identified critical event.

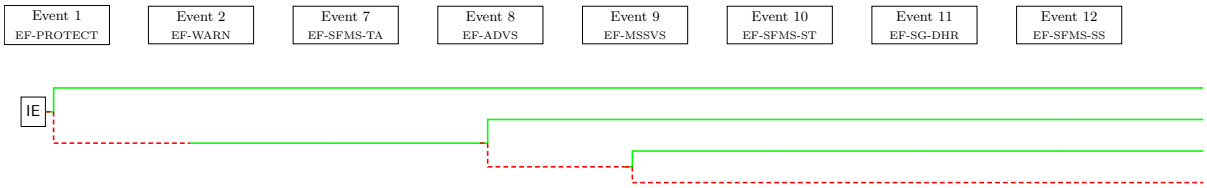

Figure IV.12: Event Tree for Case 1

In the integrated risk informed EMDAP methodology, we identify which evaluation models to be improved by specifying the *OC* of system-level event as 0.8 that corresponds to high maturity of code adequacy. Then, Bayesian inference is used to update the evaluation models. The updated simulation and data-driven fragility curves of the critical event are shown in Figure IV.15. As seen in Figure IV.15, the data-driven evaluation model has to be improved in order to achieve high maturity of the code adequacy. Therefore, the resources can be utilized efficiently by planning additional experiments for the critical event rather than conducting high-fidelity simulations.

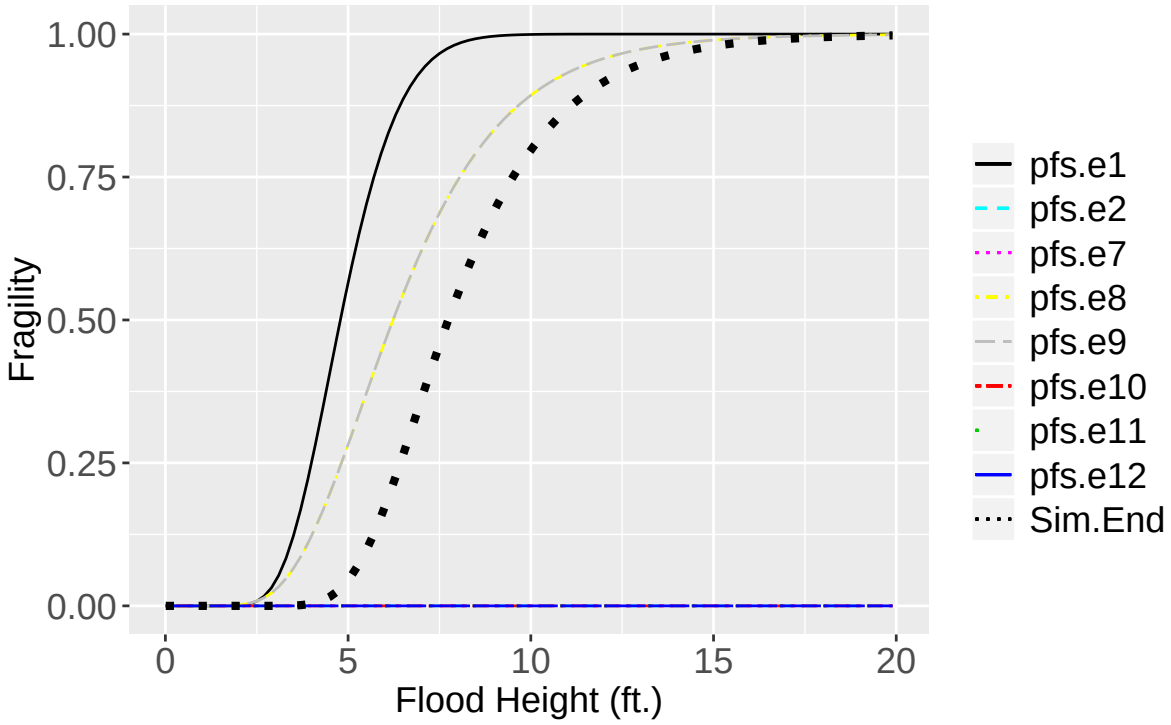

Figure IV.13: Simulation (median) fragility curves for TOP events (Case 1)

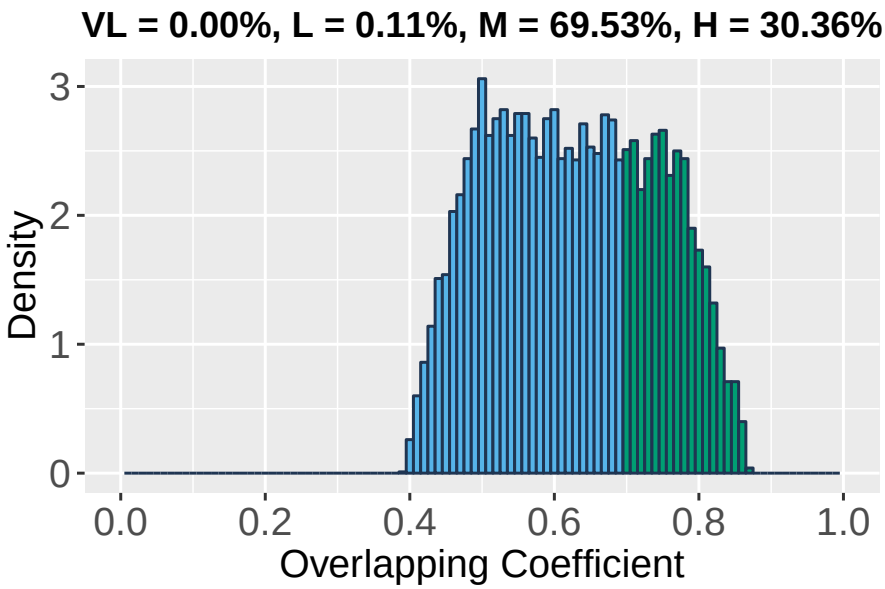

Figure IV.14: Code Adequacy of system-level event (Case 1)

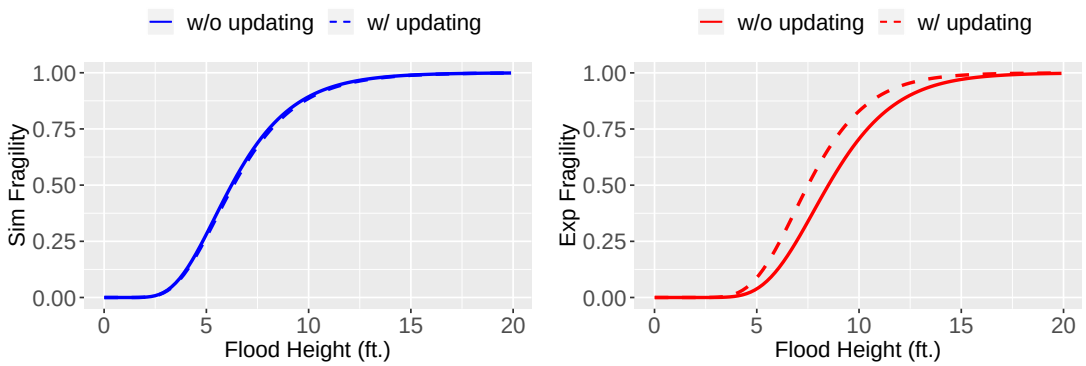

Figure IV.15: Simulation and Data-driven fragility curves of critical event (Case 1)

IV.5.2 Case 2: Treating non-physical events as completely fail

The event tree resulting from by treating non-physical events as completely fail is shown in Figure IV.16. In this case, the failure probability of all the non-physical events is equal to 1 for all the intensity measures of flood height. The identified multiple critical events in this case are "B2: dike collapses due to structural failure" and "B1: Overtopping of dike". These critical events corresponds to the basic events in the fault tree of *Event 1: EF-Protect*. The simulation-based fragility curves for the system-level event and the critical events $(B1, B2)$ are shown in Figure IV.17. As seen in Figure IV.17, the event $B2$ governs until a flood height of 8 ft. and the event $B1$ governs after the food height of 8 ft. This is because *Event 1: EF-Protect* is connected to basic events $B1$ and $B2$ by OR logic. Therefore, the fragility of *Event 1: EF-Protect* is governed by the event which has the highest failure probability.

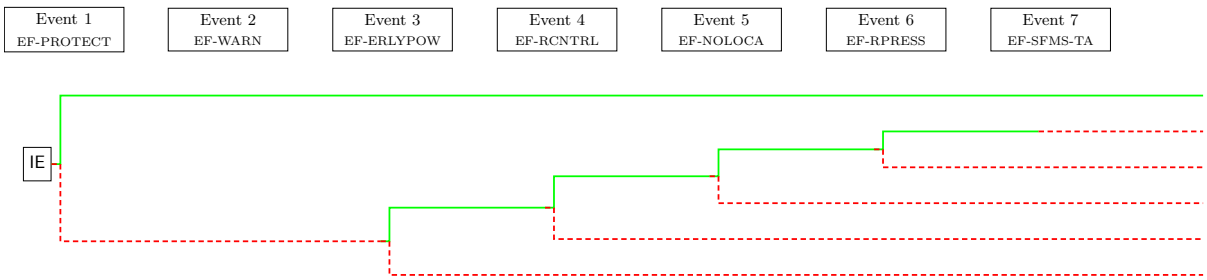

Figure IV.16: Event Tree for Case 2

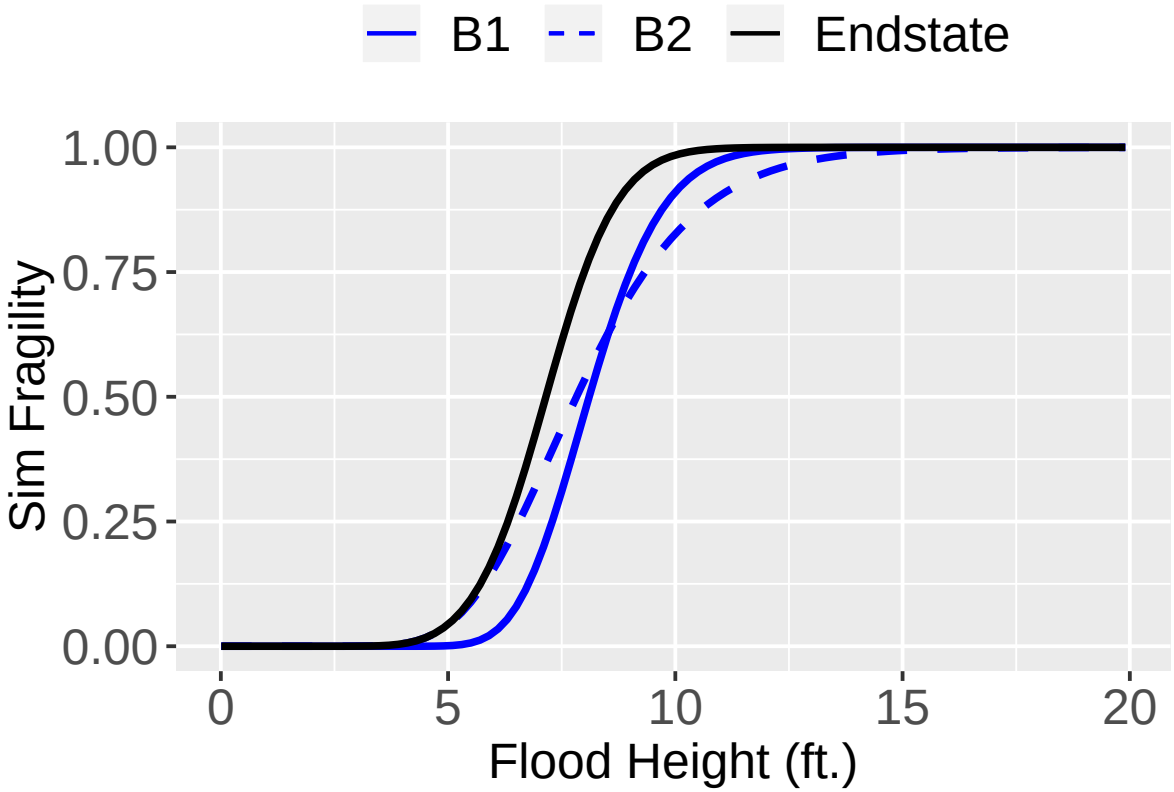

Figure IV.17: Simulation fragility curves for system-level and critical events (Case 2)

The code adequacy is obtained for the system-level and critical events as shown in Figure IV.18. The mean value of OC for system-level, $B1$, and $B2$ events are 0.71, 0.63, and 0.75 respectively. As the system-level fragility is dependent on multiple critical events, the OC for the system-level event lies in between the OC for the critical events.

For an acceptance criterion of 100% of high maturity, the adequacy of the code for the overall validation is unacceptable. Therefore, we use Bayesian inference to identify the evaluation models that needs to be improved. The updated simulation and data-driven fragility curves of the critical events are shown in Figure IV.19. In this case, the simulation-based evaluation model for both the critical events has to be improved.

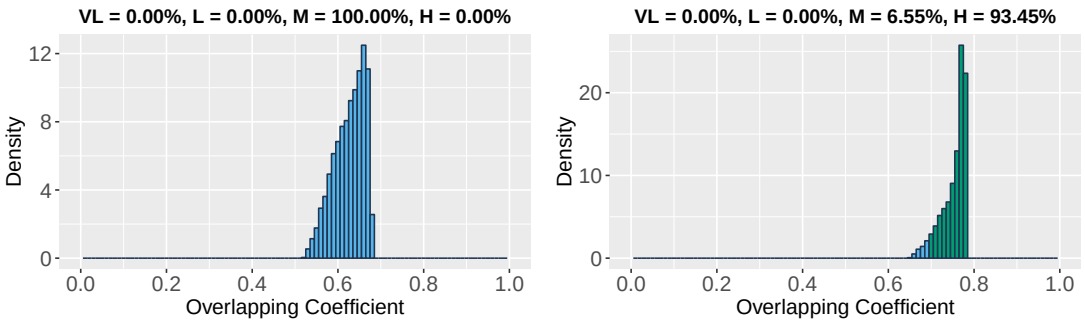

(a) Event: $B1$

(b) Event: $B2$

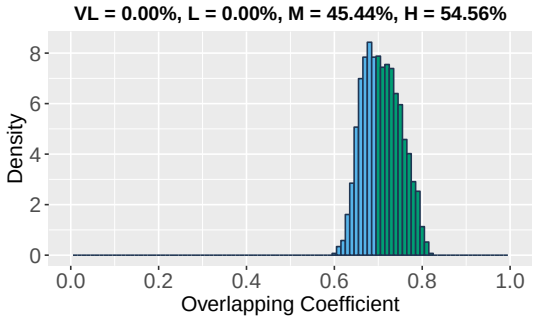

(c) System-level

Figure IV.18: Code Adequacy of system-level and critical events (Case 2)

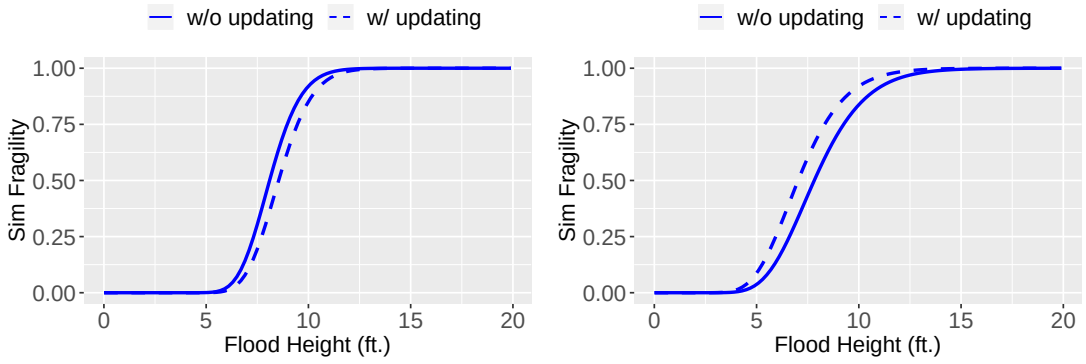

(a) Event: $B1$

(b) Event: $B2$

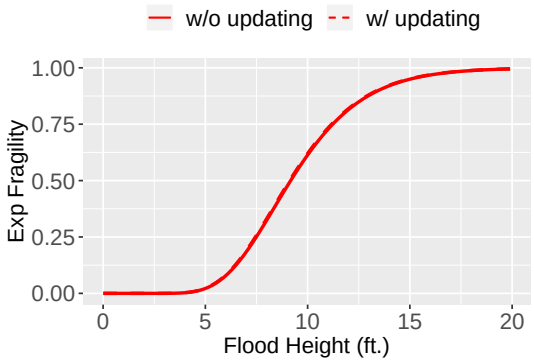

(c) *Event 1: EF-Protect*

Figure IV.19: Simulation and Data-driven fragility curves of critical events (Case 2)

IV.6 Summary and Conclusions

This study integrates the risk informed validation methodology with EMDAP framework to formalize the validation process for an external hazard scenario. The integrated framework serves as a basis for validation data planning by identifying the critical events that require experimental data in the context of system-level failure. In this study, a realistic and complex external flooding scenario is considered to evaluate the applicability of integrated risk informed EMDAP framework.

The primary conclusions of this study can be summarized as follows. The risk informed methodology is mapped into four elements of the EMDAP framework to enable consistency and completeness in the validation process. The integrated framework formalizes the validation process by quantifying the expert knowledge and making it less heuristic. The non-physical events in the PRA model are identified and treated as either completely safe or fail in the validation process. The data-driven fragilities are generated only for critical events. For non-critical events, the data-driven fragilities are considered to be same as simulation-based fragilities. The evaluation models that needs to be improved are identified by specifying the overall validation as 100% of high maturity.

PART V

Summary, Conclusions, and Recommendations for Future Research

V.1 Summary and Conclusions

This dissertation presents a risk informed based approach for effectively and efficiently evaluating the validation of advanced simulation codes for external hazards. This dissertation includes three main manuscripts that focus on describing the following key topics:

- Risk Informed Validation Framework for External Flooding Scenario
- Enhancement of Existing Risk Informed Validation Framework
- Assessment of Risk Informed Validation Framework to a Real Life Like Application – Sunny Day Dam Failure

The summary and conclusions for each of these topics are given below:

V.1.1 Risk Informed Validation Framework for External Flooding Scenario

This study presents a novel approach to quantitatively assess the system level validation by connecting individual validation events through a PRA informed validation framework. In this methodology, we include uncertainty in both simulation and data-driven models which gets reflected in the confidence levels of the overall validation. Event tree and fault trees are constructed for the system level performance, and they are mapped into a Bayesian network that allows propagation of fragility information from component level to system level. The uncertainty in the experimental data is represented in terms of three attributes: Relevance, Scaling, and Data Uncertainty. These attributes are graded based on their VUQ quality and are incorporated in the data-driven fragility analysis. In this study, the system level validation and the identification of critical events are evaluated based on fragility

estimates. To improve the overall validation, we either enhance the simulation models of events along the critical path or collect additional field data until the adequacy of the system level validation is satisfied. This process helps in allocating the resources efficiently thereby reducing the effort to conduct high fidelity simulations and large-scale experiments. The proposed framework based on risk informed approach for system-level validation can be adopted by advanced flooding simulation codes such as Neutrino. The credibility of the Neutrino code for the intended application can be quantified similar to the synthetic example described in this manuscript.

The key conclusions of this study are summarized as follows:

- The quality of experimental data used in the validation study is quantified and incorporated in the data-driven fragility curves.
- The basic events that are critical in the perspective of system level validation are identified.
- Multiple fragility curves are evaluated using different confidence levels instead of just the mean fragility curves.
- The credibility of the overall validation is estimated which gives confidence in the decision making.
- The robustness of the modified framework is illustrated by enabling clarity, consistency, and completeness for a synthetic example of a simplistic flooding scenario.

V.1.2 Enhancement of Existing Risk Informed Validation Framework

This study focuses on the enhancement of existing risk informed validation framework to assess the system-level validation. In this methodology, we propose two major enhancements to the framework by developing a new set of validation metric (consistency index) and an additional attribute (Code adequacy) for making the framework more robust. In this study, the methodology to identify the critical path that leads to system-level failure is illustrated using a seismic case study. The overall validation is assessed for completeness and consistency by comparing the critical path for both the system-level simulation and data-driven models. The interpretation of consistency index in the risk informed framework is illustrated for various cases of building piping system failure. For obtaining an accurate estimate of overlapping coefficient for the system-level failure, all the events on the critical path have to be consistent. The adequacy of the simulation code for an intended application depends on two attributes: validation result and data applicability. The code applicability evaluates the maturity of simulation tool based on the validation result and helps in the process of decision making. The key conclusions of this study are summarized as follows:

- The critical path in a Bayesian network is identified by using extended definition of Fussell-Vesely (FV) Importance measure for Bayesian networks.
- The risk informed validation framework by Kwag et al. (2018) can give inconsistent results if the identified critical events are not consistent.
- Introduces the concept of consistency index (δ) in the validation metric which ensures that the simulation and data-driven fragilities correspond to the same set of critical events.

- Overlapping coefficient is used as the standardized validation metric.
- The existing risk informed validation framework is enhanced by incorporating the concept of maturity levels to assess the decision regarding the adequacy of a simulation code for an intended application.

V.1.3 Assessment of Risk Informed Validation Framework to a Real Life Like Application – Sunny Day Dam Failure

This study integrates the risk informed validation methodology with EMDAP framework to formalize the validation process for an external hazard scenario. The integrated framework serves as a basis for validation data planning by identifying the critical events that require experimental data in the context of system-level failure. In this study, a realistic and complex external flooding scenario is considered to evaluate the applicability of integrated risk informed EMDAP framework.

The primary conclusions of this study can be summarized as follows:

- The risk informed methodology is mapped into four elements of the EMDAP framework to enable consistency and completeness in the validation process.
- The integrated framework formalizes the validation process by quantifying the expert knowledge and making it less heuristic.
- The non-physical events in the PRA model are identified and treated as either completely safe or fail in the validation process.
- The data-driven fragilities are generated only for critical events. For non-critical events, the data-driven fragilities are considered to be same as simulation-based fragilities.
- The evaluation models that needs to be improved are identified by specifying the

overall validation as 100% of high maturity.

V.2 Recommendations for Future Research

Based on the experience gained in conducting this research, it is suggested that further research should consider the following aspects:

- The proposed framework can be used to plan experiments by quantifying the uncertainty in the R/S/U attributes of Data Applicability. If there is more uncertainty in Relevance, then new experiments directly related to the current phenomenon can to be conducted. If there is more uncertainty in Scaling, then the validation can be improved by conducting large-scale experiments. Similarly, if the data uncertainty is large, the experimental data can be collected using high resolution instruments.
- The temporal effect of the accident scenario can be evaluated by employing Dynamic Bayesian network in the risk informed methodology.
- Evaluation of multiple fragility curves through the use of advanced simulation codes such as Neutrino [45] can pose computational challenges due to a large number of simulations that might be needed particularly if uncertainties are accounted for through Monte Carlo. This can be addressed by employing statistical inference concepts for fragility estimates while minimizing the required number of SPH analysis [46].
- When multiple evidence with varying maturity levels is available for R/S/U attributes, a cost-benefit analysis can be carried out to identify the evidence with the most value.
- The efficiency of the risk informed validation methodology for a very large scenario

can be improved by limiting the validation to critical path only.

REFERENCES

[1] IAEA, *The Fukushima Daiichi Accident*, Non-serial Publications, International Atomic Energy Agency, Vienna (2015).

[2] J. Queally, "As Historic Flooding Grips Texas, Groups Demand Nuclear Plant Be Shut Down," CommonDreams (2017).

[3] S. Mufson, "3 nuclear power reactors shut down during Hurricane Sandy," The Washington Post (2012).

[4] M. Bensi and J. Kanney, "Development of a Framework for Probabilistic Storm Surge Hazard Assessment for United States Nuclear Power Plants," *Transactions of the 23rd International Conference on Structural Mechanics in Reactor Technology* (2015).

[5] AIAA, *Guide: Guide for the Verification and Validation of Computational Fluid Dynamics Simulations (AIAA G-077-1998(2002))*; 10.2514/4.472855.001., URL https://arc.aiaa.org/doi/abs/10.2514/4.472855.001.

[6] ASME, *Guide for Verification and Validation in Computational Solid Mechanics*, ASME V&V, American Society of Mechanical Engineers (2006).

[7] DoD Instruction 5000.61, "DoD Modeling and Simulation (M&S) Verification, Validation, and Accreditation (VV&A)," Office of the Director of Defense Research and Engineering (2003).

[8] D. Kuzmin, "Lecture 1: Introduction to Computational Fluid Dynamics," University of Dortmund.

[9] B. Boyack, R. Duffey, P. Griffith, K. Katsma, G. Lellouche, S. Levy, U. Rohatgi, G. Wilson, W. Wulff, and N. Zuber, "Quantifying reactor safety margins part 1: An overview of the code scaling, applicability, and uncertainty evaluation methodology," *Nuclear Engineering and Design*, **119**, *1*, 1 (1990); https://doi.org/10.1016/0029-5493(90)90071-5.

[10] USNRC, "Transient and Accident Analysis Methods - Regulatory Guide 1.203," (2005).

[11] W. L. Oberkampf, M. Pilch, and T. Guy Trucano, "Predictive Capability Maturity Model for Computational Modeling and Simulation," SAND2007-5948, Sandia National Laboratories (2007); 10.2172/976951.

[12] P. Athe, "A Framework for Predictive Capability Maturity Assessment of Computer Simulation Codes," PhD Thesis, North Carolina State University (2018).

[13] S. Kwag, A. Gupta, and N. Dinh, "Probabilistic risk assessment based model validation method using Bayesian network," *Reliability Engineering & System Safety*, **169**, 380 (2018); https://doi.org/10.1016/j.ress.2017.09.013., URL http://www.sciencedirect.com/science/article/pii/S0951832016305907.

[14] S. S. Bodda, A. Gupta, and N. Dinh, "Risk informed validation framework for external flooding scenario," *Nuclear Engineering and Design*, **356**, 110377 (2020); https://doi.org/10.1016/j.nucengdes.2019.110377., URL http://www.sciencedirect.com/science/article/pii/S002954931930408X.

[15] S. Kwag and A. Gupta, "Probabilistic risk assessment framework for structural systems under multiple hazards using Bayesian statistics," *Nuclear Engineering and*

Design, **315**, 20 (2017); 10.1016/j.nucengdes.2017.02.009., URL http://dx.doi.org/10.1016/j.nucengdes.2017.02.009.

[16] G. Unnikrishnan, Shrihari, and N. A. Siddiqui, "Application of Bayesian methods to event trees with case studies," *Reliability: Theory & Applications*, **9**, 32 (2014).

[17] W. L. Oberkampf and C. J. Roy, *Verification and Validation in Scientific Computing*, Cambridge University Press, New York, NY, USA (2010).

[18] D. Vose, *Risk analysis a quantitative guide*, Hoboken, NJ Wiley (2008)URL http://openlibrary.org/books/OL18498451M.

[19] R. Kennedy and M. Ravindra, "Seismic fragilities for nuclear power plant risk studies," *Nuclear Engineering and Design*, **79**, *1*, 47 (1984); https://doi.org/10.1016/0029-5493(84)90188-2.

[20] C. K. LO, N. PEDRONI, and E. ZIO, "Treating Uncertainties in a Nuclear Seismic Probabilistic Risk Assessment by Means of the Dempster-Shafer Theory of Evidence," *Nuclear Engineering and Technology*, **46**, *1*, 11 (2014); https://doi.org/10.5516/NET.03.2014.701.

[21] N. Dinh, "CIPS Validation Data Plan," INL/EXT-12-25347, Idaho National Laboratory (2012); https://doi.org/10.2172/1044197.

[22] S. Nair, N. Walkinshaw, and T. Kelly, "Quantifying Uncertainty in Safety Cases Using Evidential Reasoning," *Computer Safety, Reliability, and Security*, 413–418, Springer International Publishing, Cham (2014).

[23] R. Ferdous, F. Khan, R. Sadiq, P. Amyotte, and B. Veitch, "Fault and Event Tree Analyses for Process Systems Risk Analysis: Uncertainty Handling Formulations," *Risk Analysis*, **31**, *1*, 86 (2011); https://doi.org/10.1111/j.1539-6924.2010.01475.x.

[24] A. J. Dababneh and J. E. Weglian, "Probabilistic Flood Hazard Assessment – Storm Surge," 2016 DOE Natural Phenomena Hazards (2016).

[25] S. Bodda, "Multi-Hazard Risk Assessment of a Flood Defense Structure," Master's Thesis, North Carolina State University (2018).

[26] M. J. Reader-Harris and J. M. McNaught, "Best Practice Guide Impulse Lines for Differential Pressure Flowmeters," NEL No.: 2005/224 (2005).

[27] L. Lin, "Development and Assessment of Smoothed Particle Hydrodynamics Method for Analysis of External Hazards," PhD Thesis, North Carolina State University (2019).

[28] N. Dinh, H. Abdel-Khalik, A. Gupta, X. Sun, I. Bolotnov, J. Baugh, M. Avramova, P. Bardet, R. Youngblood, C. Rabiti, S. Prescott, and W. Ren, "Development and Application of a Data-Driven Methodology for Validation of Risk-Informed Safety Margin Characterization Models," North Carolina State University (2015).

[29] S. Prescott, D. Mandelli, R. Sampath, C. Smith, and L. Lin, "3D Simulation of External Flooding Events for the RISMC Pathway," INL/EXT-15-36773 - Light Water Reactor Sustainability Program, Idaho National Laboratory (2015).

[30] C. Smith, D. Mandelli, S. Prescott, A. Alfonsi, C. Rabiti, J. Cogliati, and R. Kinoshita, "Analysis of pressurized water reactor station blackout caused by external flooding using the RISMC toolkit," INL/EXT-14-32906, Idaho National Laboratory (2014).

[31] NIMBLE Development Team, "NIMBLE: MCMC, Particle Filtering, and Programmable Hierarchical Modeling," (2019).

[32] USNRC, "Natural Hazards could be more Risk-Informed," Report submitted to U.S. Government Accountability Office, GAO-12-465 (2012).

[33] IAEA, "A Methodology to Assess the Safety Vulnerabilities of Nuclear Power Plants against Site Specific Extreme Natural Hazards," (2011).

[34] USNRC, "An Approach for Determining the Technical Adequacy of Probabilistic Risk Assessment Results for Risk-Informed Activities," Regulatory Guide 1.2, Revision 2 (2009).

[35] W. Kuo and X. Zhu, *Importance measures in reliability, risk, and optimization: principles and applications*, John Wiley & Sons (2012).

[36] T. Aven and T. Nøkland, "On the use of uncertainty importance measures in reliability and risk analysis," *Reliability Engineering & System Safety*, **95**, *2*, 127 (2010).

[37] W. Kuo and X. Zhu, "Some recent advances on importance measures in reliability," *IEEE Transactions on Reliability*, **61**, *2*, 344 (2012).

[38] A. Noroozian, R. B. Kazemzadeh, S. T. A. Niaki, and E. Zio, "System risk

importance analysis using Bayesian networks," *International journal of reliability, quality and safety engineering*, **25**, *01*, 1850004 (2018).

[39] J. C. Salazar, F. Nejjari, R. Sarrate, P. Weber, and D. Theilliol, "Reliability importance measures for a health-aware control of drinking water networks," *2016 3rd Conference on Control and Fault-Tolerant Systems (SysTol)*, 572–578, IEEE (2016).

[40] D. Codetta-Raiteri, "Applying generalized continuous time bayesian networks to a reliability case study," *IFAC-PapersOnLine*, **48**, *21*, 676 (2015).

[41] K. A. Maupin, L. P. Swiler, and N. W. Porter, "Validation metrics for deterministic and probabilistic data," *Journal of Verification, Validation and Uncertainty Quantification*, **3**, *3*, 031002 (2018).

[42] F. Nielsen, "On the Jensen–Shannon Symmetrization of Distances Relying on Abstract Means," *Entropy*, **21**, *5*, 485 (2019).

[43] NRC, "Working Example Template: Scenario Based Integrated Assessment Evaluation of a Sunny Day Dam Failure with Advance Warning of an External Flood and Severe Site Flooding," (2014).

[44] USNRC, "NEI White Paper (Draft) On Supplemental Guidance For The Evaluation Of Dam Failures," ML12254A813 (2012).

[45] "NEUTRINO," URL http://www.neutrinodynamics.com.

[46] J. W. Baker, "Efficient Analytical Fragility Function Fitting Using Dynamic Structural Analysis," *Earthquake Spectra*, **31**, *1*, 579 (2015); 10.1193/021113EQS025M.